Renal Drug Transporters – Clinical Significance and Role in Drug-Drug Interactions

Jia Yin

A dissertation

submitted in partial fulfillment of the

requirements for the degree of

Doctor of Philosophy

2016

Reading Committee:

Joanne Wang, Chair

Nina Isoherranen

Kenneth Thummel

Program Authorized to Offer Degree:

Pharmaceutics

University of Washington

Abstract

Renal Drug Transporters – Clinical Significance and Role in Drug-Drug Interactions

Jia Yin

Chair of the Supervisory Committee:

Professor Joanne Wang

Department of Pharmaceutics

Drug transporters play an important role in drug disposition and can be major determinants of drug pharmacokinetics, pharmacodynamics and toxicity. In contrast to drug metabolizing enzymes, which mainly concentrate in the liver and small intestine, drug transporters are expressed ubiquitously throughout human body. In human kidney, drug transporters are primarily expressed in the basolateral and apical membranes of proximal tubule cells and often work in tandem to secrete therapeutic drugs and their metabolites into tubular lumen. Furthermore, transporter-mediated drug-drug interactions (DDIs) have become a significant clinical concern as they can adversely impact drug disposition, efficacy, and toxicity. The overall goal of my research project is to understand the clinical significance of renal drug transporters and their role in drug-drug interactions.

An analysis of the top 200 prescribed drugs in U.S. and their DDI studies suggests that there is considerable potential for clinically significant renal DDI to occur among commonly used drugs. Potent drug transport inhibitors elicit significant interactions in vivo that approach maximums predicted from in vitro-derived inhibition kinetics. However, high-magnitude renal DDIs in the clinical setting appear to be rare, which may partly be due to a lack of potent in vivo inhibitors, low fraction of net secretion of victim drugs, and compensating transport pathways for the victim drug.

Our analysis also identified two widely used antihypertensive drugs, atenolol and hydrochlorothiazide that are cleared predominantly by the kidney but the molecular mechanisms involved in its renal secretion are virtually unknown. Using a panel of HEK cell lines stably expressing major renal drug transporters and absolute quantification of membrane transporter proteins by LC-MS/MS, we found that atenolol is an excellent substrate for the renal organic cation transporter 2 (hOCT2), multidrug and toxin extrusion proteins 1 and 2-K (hMATE1 and 2-K). It can inhibit but not be transported by renal organic anion transporters 1 and 3 (hOAT1 and hOAT3). We also demonstrate unidirectional transepithelial transport of atenolol in an hOCT2/hMATE1 double-transfected MDCK cell culture model. Our data suggest that renal secretion of atenolol is mediated by hOCT2/hMATEs pathway. On the other hand, hydrochlorothiazide was identified to be a substrate of both organic cation transporters hOAT1 and hOAT3 and organic anion transporters hOCT2 and hMATE2-K. However, hOCT2 and hMATE2-K showed much lower affinity and transport efficiency for hydrochlorothiazide than hOAT1 and hOAT3. Combined with findings from other investigators, we propose that renal tubular secretion of hydrochlorothiazide is mediated by two parallel pathways, with hOATs/multidrug resistance-associated protein 4 (hMRP4) being the major one and

hOCT2/hMATE2-K being a minor pathway. Our in vitro inhibition studies using potent hOAT1/3 inhibitors also suggest that caution should be taken when hydrochlorothiazide is co-prescribed with potent hOAT1/3 inhibitors, as renal secretion is not only important for its elimination, it may also play a role in its efficacy.

Emerging evidence suggests that renal hOCT2 and hMATE1/2-K exhibit substrate-dependent inhibition but the impact on renal drug secretion and intracellular accumulation is unknown. Regulatory agencies recently developed guidelines for transporter-mediated DDI risk assessment but the potential influence of probe substrate choice on prediction is not clear. Using drug substrates, we showed that inhibition of the renal basolateral organic cation transporter 2 by classic clinical inhibitors is highly substrate-dependent, leading to strikingly different DDI predictions. In contrast, inhibition of the apical multidrug and toxin extrusion proteins is less affected by substrate choice. Using a cell culture model simulating tubular secretion, we further demonstrate that substrate-dependent inhibition can shift the major substrate-inhibitor interacting site between apical and basolateral transporters, leading to different effects on intracellular drug accumulation. These findings revealed the complex and dynamic nature of substrate-inhibitor interactions in multispecific drug transporters.

In summary, this dissertation research has evaluated the clinical significance of renal DDIs, demonstrated the important role of renal transporters in the clearance and efficacy of two widely used antihypertensive drugs and highlighted the necessity of considering substrate-dependent inhibition in predicting transporter-mediated DDIs

Table of Contents

List of Figures……vi

List of Tables……...viii

Chapter 1. Introduction……1

1.1 Background……1

1.1.1 Role of Transporters in Renal Clearance and Renal DDIs…….1

1.1.2 Major Drug Transporters in Human Kidney……...2

1.1.3 Renal Transporter-mediated Drug Interactions……12

1.2 Specific Aims……...13

1.3 Research Focus and Overall Significance……14

Chapter 2. Clinical Significance of Renal Transporter Mediated Drug-Drug Interactions: Analysis of Substrate Sensitivity and Magnitude of Interactions among Commonly Prescribed Drugs ……19

2.1 Introduction……..19

2.2 Methods……20

2.2.1 Theory…….....20

2.2.2 Literature Search Strategy……21

2.2.3 Collection and Evaluation of *in vivo* and *in vitro* Data of Drugs Susceptible to Renal DDIs ……...22

2.2.4 Prediction of *in vivo* Inhibition of Renal Transporters and Subsequent DDIs……..…….23

2.2.5 Simulation of AUC and CL_R Change under Inhibition of Renal Transporters…….....24

2.3 Results……..24

2.3.1 Identification of Drugs Susceptible to Renal Transporter mediated DDIs……...24

2.3.2 Evaluation of Observed *in vivo* DDIs of Drugs Susceptible to Renal DDIs……...25

2.3.3 Prediction of *in vivo* Inhibition of Renal Transporters and Subsequent DDIs……...26

2.4 Discussion……27

Chapter 3. Atenolol Renal Secretion Is Mediated by Human Organic Cation Transporter 2 and Multidrug and Toxin Extrusion Proteins……...44

3.1 Introduction……..44

3.2 Materials and Methods……46

3.2.1 Materials……...46

3.2.2 Cell Culture……..47

3.2.3 Generation of HEK293 Cell Lines Stably Expressing Transporters……47

3.2.4 Generation of hOCT2/hMATE1 Double-transfected MDCK cells…….48

3.2.5 Uptake and Inhibition Assays in HEK293 Cells……..49

3.2.6 Atenolol Inhibition Study Using A Fluorescent Substrate……...49

3.2.7 Transport Study in hOCT2/hMATE1 Double-transfected MDCK Cells….50

3.2.8 Membrane Protein Preparation and LC-MS/MS Quantification of Transporter Protein……51

3.2.9 Data Analysis……52

3.3 Results……..53

3.3.1 Functional Validation of Transporter-expressing Cell Lines……53

3.3.2 Inhibitory Effect of Atenolol on Selected Drug Transporters……..54

3.3.3 Uptake of Atenolol by Selected Drug Transporters……..54

3.3.4 Atenolol Uptake Kinetics by hOCT1 and hOCT2……54

3.3.5 Atenolol Uptake Kinetics by hMATE1 and hMATE2-K…….55

3.3.6 Transporter Quantification and Turnover Number (k_{cat}) Determination…..55

3.3.7 Inhibition of hOCT1, hOCT2, hMATE1 and hMATE2-K by R- and S-Atenolol…….56

3.3.8 Establishment of A hOCT2/hMATE1 Double-transfected MDCK Cell Line……56

3.3.9 Transcellular Transport of Atenolol in hOCT2/hMATE1 Double-transfected MDCK Cells……..57

3.4 Discussion……58

Chapter 4. Renal Secretion of Hydrochlorothiazide Involves both Organic Anion and Organic Cation Transporters…….78

4.1 Introduction……..78

4.2 Materials and Methods…….81

4.2.1 Materials……...81

4.2.2 Cell Lines and Cell Culture……...81

4.2.3 Uptake and Inhibition Assays in HEK293 Cells……...81

4.2.4 Quantification of Hydrochlorothiazide by LC-MS/MS……82

4.2.5 Membrane Protein Preparation and LC-MS/MS Quantification of Transporter Proteins……...83

4.2.6 Data Analysis……84

4.3 Results……..85

4.3.1 Inhibitory Effect of HCTZ on Renal Drug Transporters……..85

4.3.2 Uptake of HCTZ by Renal Drug Transporters…….....85

4.3.3 HCTZ Uptake Kinetics by hOAT1 and hOAT3……...85

4.3.4 HCTZ Uptake Kinetics by hOCT2 and hMATE2-K……86

4.3.5 Transporter Quantification and Turnover Number Determination……...86

4.3.6 Inhibitory Potential of HCTZ towards hOAT1 and hOAT3…….....87

4.3.7 Probenecid and Valsartan Inhibition of hOAT1 and hOAT3 Mediated Hydrochlorothiazide Transport……..87

4.4 Discussion……88

Chapter 5. Impact of Substrate-dependent Inhibition on Predicting Transporter-mediated Renal Drug Interaction and Accumulation……106

5.1 Introduction……106

5.2 Materials and Methods……...108

5.2.1 Materials…….108

5.2.2 Cell Lines and Cell Culture…….108

5.2.3 Uptake and Inhibition Assays in HEK293 Cells…….109

5.2.4 Transwell Studies in MDCK-hOCT2/hMATE1 Cells……110

5.2.5 Data Analysis……..111

5.3 Results……111

5.3.1 Inhibition of hOCT2 by Classic Inhibitors Is Highly Dependent on Substrate……...111

5.3.2 Substrate-dependent Inhibition Results in Different Prediction of DDI Potential……...113

5.3.3 Cimetidine Applied in the Basal Chamber Inhibited B-to-A Flux of Atenolol and Metformin in MDCK-hOCT2/hMATE1 Monolayer……113

5.3.4 Cimetidine Differentially Impacted Intracellular Drug Accumulation in A Substrate-dependent Manner……...114

5.3.5 Basally Applied Cimetidine Accumulated in MDCK-hOCT2/hMATE1 Cells…….115

5.4 Discussion……..116

Chapter 6. Conclusions and Future Directions……...130

Bibliography……...133

List of Figures

Figure 1.1 Major drug transporters expressed in human renal proximal tubule cells……16

Figure 1.2 Hypothesized effects of transporter inhibition on tubular drug secretion and intracellular accumulation …….17

Figure 2.1 The relationship between f_e, f_{ns} and f_{ns}' and theoretical maximum AUC and CL_R change for the drugs in Table 2.2……..35

Figure 2.2 Comparison of observed DDIs with theoretical maximum DDIs for victim drugs in Table 2.3……36

Figure 2.3 Simulation of impact of inhibitor potency and net secretion fractions of substrate on the magnitude of renal DDIs……..37

Figure 3.1 Functional characterization of HEK293 cells stably expressing selected drug transporters…….63

Figure 3.2 Inhibitory effect of atenolol on the uptake of probe substrates by selected drug transporters…….64

Figure 3.3 Uptake of atenolol by selected drug transporters…….65

Figure 3.4 Atenolol uptake kinetics by hOCT1 and hOCT2…….66

Figure 3.5 Atenolol uptake kinetics by hMATE1 and hMATE2-K……..67

Figure 3.6 Inhibition of hOCT1, hOCT2, hMATE1, and hMATE2-K by R- and S- atenolol…..68

Figure 3.7 Transcelluar flux of mannitol and metformin in hOCT2/hMATE1 double-transfected and control MDCK cells……69

Figure 3.8 Transcelluar flux and permeability and intracelluar accumulation of atenolol in hOCT2/hMATE1 double-transfected and control MDCK cells……70

Figure 3.9 Proposed scheme of atenolol transport in human renal proximal tubule cells…….71

Figure 4.1 Inhibitory effect of hydrochlorothiazide on the uptake of probe substrates by renal transporters……94

Figure 4.2 Uptake of hydrochlorothiazide by renal transporters……...95

Figure 4.3 Hydrochlorothiazide uptake kinetics by hOAT1 and hOAT3……..96

Figure 4.4 Hydrochlorothiazide uptake kinetics by hOCT2 and hMATE2-K……...97

Figure 4.5 Inhibition of hOAT1 and hOAT3 by hydrochlorothiazide……...98

Figure 4.6 Inhibition of hOAT1- and hOAT3-mediated hydrochlorothiazide uptake by probenecid and valsartan……99

Figure 4.7 Proposed scheme of hydrochlorothiazide (HCT) transport in human renal proximal tubule cells……...100

Figure 4.8 Hydrochlorothiazide uptake by hMATE1……..101

Figure 5.1 Inhibition of hOCT2, hMATE1 and hMATE2-K-by cimetidine, pyrimethamine and carvedilol using atenolol or metformin as the probe substrate……121

Figure 5.2 Effect of cimetidine inhibition on atenolol or metformin transport kinetics of hOCT2, hMATE1 and 2-K……122

Figure 5.3 Effects of cimetidine on B-to-A flux of atenolol and metformin in MDCK-hOCT2/hMATE1 cells……123

Figure 5.4 Effect of cimetidine inhibition on permeability and intracellular accumulation of atenolol and metformin in MDCK-hOCT2/hMATE1 cells……124

Figure 5.5 Cimetidine permeability and intracellular accumulation in MDCK-hOCT2/hMATE1 cells……..125

Figure 5.6. Hypothesized effects and sites of interaction for cimetidine on renal tubular secretion and intracellular accumulation of atenolol and metformin……..126

List of Tables

Table 1.1 Examples of clinically observed DDIs involving renal drug transporters…….18

Table 2.1 Pharmacokinetic parameters of drugs with f_e > 25% among top 200 prescribed drugs in U.S. 2010. (total 30 drugs)…….38

Table 2.2 Calculated maximum AUCR for top 200 drugs with f_e > 25% and net secretion. (24 drugs) ……40

Table 2.3 Clinical DDI studies with AUC, CL or CL_R change > 25% and renal transporters identified for drugs with f_{ns}' > 33%……..41

Table 2.4 Prediction of the %inhibition of renal transporters in DDI studies of 4 selected drugs and their AUC and CL_R change by inhibition of renal transporters……..43

Table 3.1 Surrogate peptides of hOCT1, hOCT2, hMATE1 and hMATE2-K and their MS/MS parameters for protein quantification…….72

Table 3.2 Kinetic parameters of atenolol uptake by hOCT1, hOCT2, hMATE1 and hMATE2-K…….73

Table 3.3 Comparison of K_m and V_{max} values derived from Michaelis-Menten (MM) equation and MM with a diffusional component……..74

Table 3.4 Turnover number and transport efficiency of atenolol uptake by hOCT1, hOCT2, hMATE1 and hMATE2-K…….75

Table 3.5 IC_{50} of R- and S- atenolol inhibition of ASP+ uptake by hOCT1, hOCT2, hMATE1 and hMATE2-K…….76

Table 3.6 A comparison of physiochemical properties and human pharmacokinetic parameters for atenolol and metformin……77

Table 4.1 Surrogate peptides of hOAT1, hOAT3, hOCT2 and hMATE2-K and their MS/MS parameters for protein quantification……...102

Table 4.2 Kinetic parameters of hydrochlorothiazide uptake by hOAT1, hOAT3, hOCT2 and hMATE2-K……..103

Table 4.3 Turnover number and transport efficiency of hydrochlorothiazide uptake by hOAT1, hOAT3, hOCT2 and hMATE2-K……104

Table 4.4 Prediction of % inhibition of hOAT1- and hOAT3-mediated hydrochlorothiazide transport in vivo by probenecid and valsartan……105

Table 5.1 Cimetidine IC_{50} values for atenolol and metformin……127

Table 5.2 Comparison of cimetidine IC_{50} and K_i values……128

Table 5.3 Prediction of hOCT2 DDIs following FDA decision tree……...129

Acknowledgement

This dissertation is a heavy chapter in my academic career. I am fortunate to have people around me who helped me and supported me through this long journey. This work cannot be accomplished without them.

I first want to express my sincere gratitude to my thesis advisor Dr. Joanne Wang for her guidance, advice and tremendous efforts spent on helping me with all my writings. She has been a dedicated mentor both in science and career. She guided me through my projects and gave advice on how to be successful as a scientist. Without her, I could not come this far.

I want to offer my sincere appreciation to my thesis committee: Dr. Isoherranen, Dr. Thummel, Dr. Unadkat, and Dr. Anderson for their insights and guidance on my dissertation research. I am deeply grateful for their stimulating questions, thoughtful comments and suggestions that help me to drive my research forward.

I want to thank my lab members, both former and present, who are always willing to help and have discussions about research and conversations about life.

Lastly, I want to thank the faculty and staff in the Department of Pharmaceutics, Department of Medicinal Chemistry and Mass Spectrometry Center for their support over the years.

Dedication

I dedicate my dissertation work to my family, for their continuous love and caring through the years.

Chapter 1. Introduction

Part of the chapter was used in a manuscript and accepted by Acta Pharamceutica Sinica B.

1.1 Background

1.1.1 Role of Transporters in Renal Clearance and Renal DDIs

Renal clearance is a major pathway of drug elimination. About 32% of the top 200 prescribed drugs in the U.S. in 2010 are renally eliminated with more than 25% of the absorbed dose excreted unchanged in urine (Morrissey et al., 2012). Renal elimination is the result of three concurrent processes occurring in the nephron, which include glomerular filtration, tubular secretion, and tubular reabsorption. Glomerular filtration is a passive process while tubular secretion, and sometimes reabsorption, involves a variety of transporters located on the basolateral and luminal membranes of the tubular epithelium. These transporters are predominantly expressed in the proximal tubule and they work in tandem to eliminate drugs from the blood circulation to the urine (Li et al., 2006b; Giacomini et al., 2010; Morrissey et al., 2012). Both basolateral and apical transporters tend to be charge selective for anionic and cationic drugs, although recent study suggests that there is some degree of overlap (Ahn et al., 2009; Giacomini et al., 2010). In humans, major transporters involved in tubular secretion of cationic drugs include organic cation transporter 2 (hOCT2) on the basolateral membrane and the multidrug and toxin extrusion protein 1 and 2-K (hMATE1, hMATE2-K) on the apical membrane (Giacomini et al., 2010; Morrissey et al., 2012). P-glycoprotein (P-gp) is also expressed in the apical member to facilitate the excretion of larger and more hydrophobic cations. The major transporters engaged in secretion of anionic drugs include organic anion transporters 1 and 3 (hOAT1, hOAT3) on the basolateral membrane and multidrug resistance-associated protein 2 and 4 (hMRP2, hMRP4) on the apical membrane (Giacomini et al., 2010;

Morrissey et al., 2012). In addition, several closely related transporters are present in the proximal tubules and they may also contribute to renal handling of drugs and metabolic wastes.

Transporter-mediated DDIs are increasingly recognized as an important modifier of the pharmacokinetics and pharmacodynamics of drugs (Masereeuw and Russel, 2001; Li et al., 2006b; Giacomini et al., 2010). Drugs inhibiting renal drug transporters may cause marked changes in the pharmacokinetics of the affected drug, resulting in clinically significant DDIs (Masereeuw and Russel, 2001; Li et al., 2006b; Morrissey et al., 2012). Furthermore, expression and inhibition of renal drug transporters may result in abnormal drug accumulation in renal tubular cells, leading to drug-induced nephrotoxicity. This review focuses on renal drug transporters and their significance in DDIs and drug-induced nephrotoxicity. We first briefly summarize the current knowledge on major renal drug transporters including their expression, cellular localization, transport mechanisms, and substrate specificities. We then review the basic principles underlying renal DDIs and highlight the importance of renal drug transporters in clinically significant DDIs. The relevant consequences on pharmacokinetics, pharmacodynamics, and drug-induced nephrotoxicity are illustrated using several well-studied clinical DDI examples. Lastly, a brief summary along with current challenges in the field is presented.

1.1.2 Major Drug Transporters in Human Kidney

More than 400 membrane transporters are encoded by the human genome, and generally fall into two superfamilies: the adenosine triphosphate (ATP)--binding cassette (ABC) and the solute carrier (SLC) (Giacomini et al., 2010; Morrissey et al., 2012). ABC transporters are primary active transporters that can transport substrates against their electrochemical gradients, utilizing energy generated from ATP hydrolysis. SLC transporters have diverse modes of

transport. Facilitative SLC transporters transport substrates down their electrochemical gradients without direct energy input. On the other hand, active SLC transporters can mediate uphill transport of a substrate against its electrochemical gradient by coupling to a co-transported ion (e.g. Na^+, H^+) or solute (Morrissey et al., 2012). The major drug transporters involved in OC and OA transport in the human kidney are shown in Figure 1.1. The molecular and functional characteristics of these transporters are described below.

1.1.2.1 hOCTs (*SLC22A*)

hOCTs belong to the SLC22 family (Koepsell et al., 2007). Following the first cloning of rat OCT1 (rOct1) in 1994 (Grundemann et al., 1994), 16 additional OCTs were cloned from different species (Koepsell et al., 2007). In human, three OCT isoforms (hOCT1, 2, 3) have been identified. hOCT2 is about 70% identical to hOCT1 (Gorboulev et al., 1997), and hOCT3 is about 50% identical to hOCT1 and 2 (Grundemann et al., 1998). hOCTs are membrane proteins with 553-556 amino acid residues (Gorboulev et al., 1997; Grundemann et al., 1998) and are predicted to have 12 transmembrane domains (TMDs) (Koepsell et al., 2007). In humans, hOCT2 is the major OCT isoform expressed in the kidney (Gorboulev et al., 1997; Koepsell et al., 2007). hOCT1, on the other hand, is predominantly expressed in the liver; and hOCT3 is broadly expressed in many tissues including the skeletal muscle, heart, placenta, and salivary glands (Grundemann et al., 1998; Koepsell et al., 2007; Lee et al., 2014). hOCT1-3 are polyspecific transporters with a large overlap in substrate specificity (Koepsell et al., 2007). They typically translocate relatively small, hydrophilic, and structurally diverse organic cations (Li et al., 2006b; Koepsell et al., 2007). In the kidney, hOCT2 is located in the basolateral membrane of renal proximal tubule cells (Morrissey et al., 2012). It mediates the first step in OC secretion in the kidney by translocating drug molecules from systemic circulation into the renal

tubule cells (Fujita et al., 2006; Li et al., 2006b; Koepsell et al., 2007). Transport by hOCT2 is electrogenic and Na^+-independent, and facilitated by the inside-negative membrane potential existing in the kidney tubular cells (Gorboulev et al., 1997). Common substrates for hOCT2 include model cations tetraethylammonium (TEA) and 1-methyl-4-phenylpyridimium (MPP+), endogenous monoamines, the antidiabetic drug metformin, the antihypertensive drug atenolol, the antiviral drug lamivudine, and the cytostatic drug oxaliplatin (Li et al., 2006b; Nies et al., 2011; Morrissey et al., 2012; Yin et al., 2015a) Most hOCT2 inhibitors are larger, more hydrophobic cations that may or may not be transported by the transporter (Li et al., 2006b; Koepsell et al., 2007; Morrissey et al., 2012). Several clinically used drugs, including cimetidine, quinidine and dolutegravir, are known hOCT2 inhibitors (Li et al., 2006b; Song et al., 2016). The mRNA of hOCT3 is also detectable in the kidney but at a much lower level (Motohashi et al., 2002; Wright and Dantzler, 2004). The membrane localization of hOCT3 in human kidney is unclear. Further investigation is needed to elucidate the role of hOCT3 in renal excretion of drug molecules.

1.1.2.2 hMATEs (*SLC47A*)

hMATEs belong to SLC47 family. Two human orthologues of the bacterial MATE proteins, MATE1 and MATE2 were first cloned in 2005 (Otsuka et al., 2005). Soon after, two splice variants of hMATE2 were isolated from kidney and brain separately and were designated as hMATE2-K and hMATE2-B, respectively (Masuda et al., 2006). hMATE1 and hMATE2 are 47.5% identical (Otsuka et al., 2005). hMATE1, hMATE2 and hMATE2-K are proteins of 570, 602 and 566 amino acids(Otsuka et al., 2005; Masuda et al., 2006), respectively, and are currently predicted to have 13 TMDs (Zhang et al., 2007; Zhang and Wright, 2009). hMATE2-B is a truncated protein of 220 amino acids and is not functional with respect to transport (Masuda

et al., 2006). hMATE1 has the highest expression level in the kidney and is also strongly expressed in other tissues including the liver, skeleton muscle and adrenal gland (Otsuka et al., 2005; Masuda et al., 2006). Immunohistochemistry of human tissue revealed that in the kidney, hMATE1 is localized to the apical membrane of renal proximal tubule cells and distal convoluted tubules; and in the liver, it is expressed in bile canaliculi (Otsuka et al., 2005). The full-length hMATE2 and the kidney-specific splice variant hMATE2-K are predominantly expressed in the kidney (Otsuka et al., 2005; Masuda et al., 2006; Komatsu et al., 2011). Immunostaining showed both of them are expressed in the renal proximal tubule and hMATE2-K is localized to the luminal membrane of the tubule cells (Masuda et al., 2006; Komatsu et al., 2011). Different from hMATE1/2-K, hMATE2 was localized in intracellular vesicular structures upon expression in human embryonic kidney (HEK) 293 cells and only showed transport activity when reconstituted into liposomes (Komatsu et al., 2011). hMATE1 and hMATE2-K are OC/proton exchangers and need an oppositely oriented proton gradient to drive the transport (Otsuka et al., 2005; Masuda et al., 2006; Komatsu et al., 2011). In the nephron, the tubular lumen is more acidic (~pH 6.3) than the cytosol, providing an inwardly directed proton gradient across the apical membrane of proximal tubule epithelial cells. hMATE-mediated influx of protons is coupled with the efflux of OCs into the urine. hMATE1/2-K share a broad spectrum of substrates and inhibitors with the hOCT2 (Tanihara et al., 2007). In the kidney, hMATE1/2-K mainly coordinate with hOCT2 to mediate OC secretion. However, hMATE1/2-K can also transport several anionic compounds and zwitterions (Tanihara et al., 2007), which suggests that they may also partner with hOATs for renal excretion of anionic and zwitterionic drugs.

1.1.2.3 hOCTN (*SLC22A*)

Organic zwitterions/cation transporters (OCTNs) belong to the same SLC22 gene subfamily as OCTs. There are three OCTN isomers (OCTN1 ~ 3) in rodents, but humans only have OCTN1 and 2 (Koepsell et al., 2007). The first human OCTN, hOCTN1, was cloned in 1997 from human fetal liver (Tamai et al., 1997). Soon after, hOCTN2 was cloned by screening a human kidney cDNA library (Tamai et al., 1998). hOCTN1 and hOCTN2 have 75.8% identity and both have high expression level in the kidney (Tamai et al., 1997; Tamai et al., 1998), where they are located in the apical membrane of renal proximal tubule cells (Tamai et al., 2001; Tamai et al., 2004; Koepsell et al., 2007). Both hOCTN1 and hOCTN2 can transport OC and zwitterions, but the transport mechanisms are substrate-dependent and quite different for each transporter. hOCTN1 has a high affinity for the zwitterionic antioxidant ergothioneine, the uptake of which is stimulated by extracellular sodium (Grundemann et al., 2005). hOCTN1 also appears to transport OCs such as TEA by an OC/H^+ exchange mechanism (Tamai et al., 1997; Yabuuchi et al., 1999). The exact role of hOCTN1 in the renal proximal tubules is unclear. It may participate in Na^+-dependent reabsorption of ergothioneine from the filtrate; alternatively, it may contribute to tubular secretion by mediating OC efflux at the apical membrane driven by the acidic pH in the lumen (Tamai et al., 1997; Yabuuchi et al., 1999; Grundemann et al., 2005). hOCTN2 has a high affinity for L-carnitine and functions as a Na^+-L-carnitine cotransporter (Tamai et al., 1998). In addition, hOCTN2 can also transport OCs in Na^+-independent manner (Wu et al., 1999). Similar to hOCTN1, hOCTN2 may participate in either renal reabsorption of zwitterions (e.g. L-carnitine) or secretion of xenobiotic OCs depending on its mode of transport. While the proton/OC antiporters hMATE1/2-K are apparently the most important extrusion transporters for OC efflux at the luminal membrane (Terada and Inui, 2008), hOCTN1/2 have different substrate selectivity and may contribute to the secretion of certain OC or zwitterion

drugs. Interestingly, a recent pharmacogenomics study suggested that hOCTN1 is involved in active tubular secretion of gabapentin, an anticonvulsant widely prescribed for epilepsy and other neuropathic disorders (Urban et al., 2008).

1.1.2.4 P-gp (*ABCB1*)

P-glycoprotein (P-gp) is probably the most well studied ABC transporter to date. It was first identified in 1976 as a cell surface glycoprotein from Chinese hamster ovary (CHO) cells resistant to colchicine (Juliano and Ling, 1976). Overexpressed in many cancer cells, P-gp decreases drug accumulation in multidrug-resistant cells and mediates the development of resistance to anticancer drugs (Juliano and Ling, 1976). As a typical ABC transporter, it has two membrane-spanning domains (MSDs) and two cytoplasmic nucleotide-binding domains (NBDs). Using energy generated from ATP hydrolysis, P-gp actively transports its substrates out of cells against their concentration gradients. A vast number of therapeutic drugs, such as anticancer drugs, HIV protease inhibitors, immunosuppressants, cardioactive drugs and antifungals, interact with P-gp (Cummins et al., 2002; Schinkel and Jonker, 2003; Yu et al., 2016). Typical P-gp substrates are lipophilic or amphipathic large molecules (molecular weight > 400 Dalton) carrying a positive charge at pH 7.4. However, neutral drugs with bulky ring structures (steroids and cyclic peptides) are also transported by P-gp. Interestingly, many of drugs transported by P-gp are also substrate of drug-metabolizing cytochrome P450 (CYP) enzymes, especially CYP3A4/5 (Cummins et al., 2002).

Besides cancer cells, P-gp is broadly expressed in many normal tissues including excretory organs and tissue barriers important for drug disposition. The transporter has been localized to the luminal membrane of brain endothelial cells forming the blood-brain barrier (BBB), canalicular membrane of hepatocytes, apical surface of intestinal columnar epithelial

cells, the apical membrane of kidney proximal tubule cells, and the apical membrane of placental syncytiotrophoblast cells (Thiebaut et al., 1987; Schinkel and Jonker, 2003; Li et al., 2006b). The expression of P-gp in organs important for drug elimination and distribution is consistent with a protective role of P-gp in promoting drug elimination from the body and preventing drug entry into critical organs such as the brain and the developing fetus (Gramatte et al., 1996; Cummins et al., 2002; Chen et al., 2003; Chandra and Brouwer, 2004). In the human intestine, P-gp and CYP3A are co-localized to the mucosal epithelial cells (Thiebaut et al., 1987; Kolars et al., 1994). It was suggested that P-gp and CYP3A work together to synergistically limit oral bioavailability of many drugs (Cummins et al., 2002). Both P-gp and CYP3A are inducible by pregnane X receptor ligands (e.g. rifampin) (Kolars et al., 1992; Greiner et al., 1999). In the kidney, P-gp has been identified in the apical membrane of human proximal tubule cells by immunostaining, consistent with a role in facilitating renal drug excretion (Schinkel and Jonker, 2003). There is also evidence that expression of P-gp is increased after ischemic reperfusion injury in kidney (Huls et al., 2006).

1.1.2.5 hOATs (*SLC22A*)

Despite transporting a largely different group of anionic substrates, OATs belong to the same SLC22 family that also encodes the OCTs. OAT was first discovered in 1997 with the cloning of rat and flounder Oat1 (Sekine et al., 1997; Sweet et al., 1997; Wolff et al., 1997). The cloned OAT/Oats are proteins of 536 ~ 556 amino acids and are predicted to have 12 TMDs (Perry et al., 2006; Srimaroeng et al., 2008; Burckhardt, 2012). In human, 10 OAT isoforms have been identified, including hOAT1 ~ 8, hOAT10, and the urate transporter 1 (hURAT1) (Burckhardt, 2012). Among them, hOAT1 ~ 4, hOAT7, hOAT10 and hURAT1 have been functionally characterized (Burckhardt, 2012; Koepsell, 2013). hOAT1, the first cloned human

OAT (Reid et al., 1998), has 4 splice variants, hOAT1-1, hOAT1-2, hOAT1-3 and hOAT1-4 (Bahn et al., 2004). hOAT1-1 and hOAT1-2 are longer and showed similar transport activity while hOAT1-3 and hOAT1-4 are shorter and lack of transport activity (Bahn et al., 2004). Most hOATs have expression in the renal proximal tubule, except hOAT7, for which expression is restricted to the liver (Shin et al., 2007; Burckhardt, 2012). In the kidney, hOAT1 ~ 3 are located on the basolateral membrane of renal tubule cells whereas hOAT4, hOAT10 and hURAT1 are expressed on the luminal membrane (Burckhardt, 2012). Basally-expressed hOAT1 ~ 3 function as organic anion (OA)/dicarboxylate exchangers which mediate the first step of OA renal excretion by transporting OAs into renal tubule cells utilizing the outward dicarboxylate (e.g. α-ketoglutarate for hOAT1/3, succinate for hOAT2) gradient established by the Na+-dicarboxylate cotransporter (Burckhardt, 2012). hOAT1 and hOAT3 have substantial overlap in their substrate specificities, accepting relatively small and hydrophilic OAs (Li et al., 2006b; Koepsell, 2013). hOAT3 appears to be more tolerant in size and charge of its substrates than hOAT1 and can transport bulkier (e.g. estrone sulfate) and even positively charged (e.g. cimetidine) compounds (Li et al., 2006b; Koepsell, 2013). Numerous drugs have been shown to be substrates of hOAT1/3, including antibiotics, antivirals, antihypertensive drugs, diuretics, cytostatics, H_2-antagonists, non-steroidal anti-inflammatory drugs (NSAIDs), statins and uricosurics (Rizwan and Burckhardt, 2007; Morrissey et al., 2012). The role of hOAT2 in renal handling of drugs is less clear. Reported substrates of hOAT2 include some endogenous compounds, such as glutamate, nucleobases, nucleosides and nucleotides, and some drug molecules, such as salicylate, bumetanide and erythromycin (Koepsell, 2013).

Apically-expressed hOATs and hURAT1 may have multiple transport mechanisms. hOAT4 can transport in both influx and efflux modes (Hagos et al., 2007). As an influx

transporter, it can take up estrone sulfate and urate through OA/dicarboxylate or OA/OH^- exchange mode (Ekaratanawong et al., 2004; Hagos et al., 2007). As an efflux transporter, it can release PAH into the tubule lumen via PAH/Cl^- exchange (Hagos et al., 2007). hOAT10 is an antiporter, taking up p-aminohippurate (PAH), urate and nicotinate possibly by OA/OH^- exchange (Bahn et al., 2008). Although hOAT4 and hOAT10 have both been implicated in drug transport in the kidney, their roles in tubular drug secretion and/or reabsorption still need to be clarified. hURAT1 is known to play an important role in urate homeostasis. It reabsorbs urate from the lumen of the renal tubule by exchanging extracellular urate with intracellular OAs such as lactate and nicotinate (Enomoto et al., 2002).

1.1.2.6 hMRPs (*ABCC*)

MRPs are ATP-dependent efflux transporters. They use energy generated from ATP hydrolysis to export molecules out of cells. They are part of the C branch of ABC family, which can be further divided into two subfamilies, "long" (MRP1, 2, 3, 6,7) and "short" (MRP4, 5, 8, 9, 10) (Deeley et al., 2006). The short MRPs have the typical ABC transporter structure with two membrane-spanning domains (MSDs) and two cytoplasmic nucleotide-binding domains (NBDs), while the long MRPs have an additional MSD (Deeley et al., 2006). Among the ten identified hMRPs genes, eight (hMRP1 ~ 8) have been confirmed to encode functional proteins (Deeley et al., 2006). Several hMRP isoforms are expressed in the kidney, including hMRP1, hMRP2, hMRP3, and hMRP4 (Flens et al., 1996; Belinsky et al., 1998; Kiuchi et al., 1998; Schaub et al., 1999; van Aubel et al., 2002). In particular, hMRP2 and hMRP4 are located in the apical membrane domain of renal proximal tubule cells, suggesting their role in efflux of molecules into the tubule lumen (Schaub et al., 1999; van Aubel et al., 2002). In mouse kidney, Mrp1 was found in the basolateral membrane of the distal and collecting tubule cells, but not in proximal

tubule cells (Peng et al., 1999). Similarly, in human kidney, hMRP3 is located in the basolateral membrane of distal convoluted tubules (Scheffer et al., 2002). The role of hMRP1 and hMRP3 in the kidney remains unclear. The typical substrates of hMRPs are the smaller unconjugated organic anions, such as PAH, and the larger conjugated organic anions, including glutathione (GSH) conjugates and glucuronides (Li et al., 2006b). hMRP2/4 have some substrate overlap with hOAT1/3. Accordingly, hMRP2 and hMRP4 may coordinate with hOAT1/3 to mediate renal excretion of certain anionic drugs.

1.1.2.7 hOATPs (*SLCO*)

Organic anion-transporting peptides (OATPs) are SLC carriers predicted to have 12 TMDs (Hagenbuch and Meier, 2003). The first OATP was cloned from rat in 1994 (Jacquemin et al., 1994). One year later, the first human OATP, OATP1A2, was isolated from human liver (Kullak-Ublick et al., 1995). Today, OATP superfamily consists of more than 300 members from over 40 species, which form 6 families, OATP1 ~ 6 (Hagenbuch and Stieger, 2013). In human, 11 members have been identified, which are hOATP1A2, hOATP1B1, hOATP1B3, hOATP1C1, hOATP2A1, hOATP2B1, hOATP3A1, hOATP4A1, hOATP4C1, hOATP5A1 and hOATP6A1 (Hagenbuch and Stieger, 2013). OATPs can transport anionic and amphipathic molecules that are relatively large (> 450) and have a high degree of albumin binding under physiological conditions (Hagenbuch and Meier, 2004). The transport by OATPs is Na+-independent, but the exact transport mechanisms are unclear (Hagenbuch and Stieger, 2013). They are believed to act as an OA/OA exchanger, coupling cellular uptake of organic compounds with efflux of intracellular bicarbonate, GSH and GSH conjugates (Hagenbuch and Stieger, 2013). In addition, uptake by various OATPs is pH-sensitive and appears to have higher uptake at lower extracellular pH (Hagenbuch and Stieger, 2013). Among the 11 hOATPs,

hOATP1B1 and 1B3 are considered to be liver-specific (Roth et al., 2012), while hOATP4C1 was predicted to be kidney-specific(Mikkaichi et al., 2004). hOATP4C1 can transport cardiac glycoside (digoxin and ouabain) and thyroid hormone (tri-iodothyronine) with high affinities(Mikkaichi et al., 2004). Its rat counterpart Oatp4c1 is localized to the basolateral membrane of rat kidney proximal tubule cells, suggesting that hOATP4C1 might mediate the first step of renal excretion digoxin and other compounds (Mikkaichi et al., 2004).

1.1.3. Renal Transporter-mediated Drug Interactions

In the human kidney, elimination of drugs consists of passive glomerular filtration, active tubular secretion and passive or active reabsorption. For xenobiotics, reabsorption is believed to mainly through a passive process (Rowland and Tozer, 2011). DDIs due to inhibition of tubular secretion thus represent the most common type of drug interactions at the renal level. Inhibition at a tubular secretion site decreases renal secretion clearance, which may result in increased drug concentrations in the plasma, altered pharmacological and toxicological responses. Table 1.1 lists several selected DDIs known to be mediated by renal drug transporters. Furthermore, renal DDIs may change drug accumulation in proximal tubule cells, leading to drug-induced nephrotoxicity and kidney injury (Li et al., 2006b; Morrissey et al., 2012). Although renal DDIs may often lead to adverse drug reactions, occasionally, coadministration of an inhibitor (e.g., probenecid) is used deliberately to alter renal clearance or reduce toxicity of another drug (Cundy et al., 1995; Cihlar et al., 1999). Recognizing the important roles of transporters in drug disposition and interactions, the International Transporter Consortium (ITC) and the U.S. Food and Drug Administration (FDA) have recently published a series of papers and recommendations for assessing DDI potentials between a new molecular entity (NME) and clinically important

transporters including the renal hOCT2 and hOAT1/3 (Giacomini et al., 2010; Zhang et al., 2011; FDA, 2012; Brouwer et al., 2013; Hillgren et al., 2013).

Historically, numerous clinically significant DDIs in the kidney have been reported and attributed to the inhibition of renal organic cation and anion secretion systems (Masereeuw and Russel, 2001; Li et al., 2006b; Morrissey et al., 2012). Cimetidine has been historically used as the classic inhibitor for the OC system whereas probenecid is considered as the prototypical inhibitor of the anion system (Masereeuw and Russel, 2001; Li et al., 2006b; Morrissey et al., 2012). Inhibitors of the renal OC and OA secretion systems are often non-specific and interact with both apical and basolateral transporters. While inhibition of a basolateral or an apical transporter both decreases tubular secretion, the impact on intrarenal drug accumulation and toxicity is completely different. As illustrated in Figure 1.2, inhibition of a basolateral uptake transporter reduces drug accumulation within renal tubular cells, thus is generally nephron-protective. In contrast, inhibition of apical efflux transporters diminishes drug exit from renal tubular cells, which can lead to increased drug accumulation and nephrotoxicity. Such scenarios are demonstrated by the fact that co-administration of probenecid with cidofovir is required by FDA to protect patients against cidofovir-induced nephrotoxicity (Morrissey et al., 2012) and exploration of hOCT2 inhibitors as potential therapeutic agents to prevent cisplatin-induced nephrotoxicity. Therefore, knowing the precise site of interaction (i.e. apical vs. basolateral) is critical to predict a nephron-toxic or a nephron-protective effect of the inhibitor.

1.2 Specific Aims

The overall goal of my research project is to understand the clinical significance of renal drug transporters and their role in drug-drug interactions. The specific aims are:

Specific Aim 1: Evaluate the clinical significance of renal transporter-mediated DDIs by predicting the maximum renal DDIs and evaluating the observed renal DDIs for commonly used drugs.

Specific Aim 2: Identify major drug transporters involved in renal secretion of atenolol and demonstrate atenolol renal excretion pathway in an in vitro cell model.

Specific Aim 3: Identify major drug transporters involved in renal secretion of hydrochlorothiazide.

Specific Aim 4: Characterize the effect of substrate-dependent inhibition on hOCT2/hMATE-mediated drug secretion and evaluate its impact on renal DDI and toxicity assessment.

1.3 Research Focus and Overall Significance

The overall goal of my research project is to understand the clinical significance of renal drug transporters and their role in drug-drug interactions. Under this goal, **Specific Aim 1** is designed to assess the clinical significance of renal transporter-mediated DDIs using top 200 prescribed drugs in the US as a sample dataset. Our analysis for top 200 prescribed drugs in the US (Specific Aim 1) revealed antihypertensives and antibiotics as the top two categories of drugs susceptible to renal transporter-mediated DDIs. Two widely used antihypertensives drugs, atenolol and hydrochlorothiazide, are particularly interesting because they are almost entirely cleared by renal excretion but the underlying transport mechanisms are virtually unknown. Atenolol is a selective β1-adrenoceptor antagonist used alone or in combination to treat hypertension. It is primarily eliminated by renal excretion with more than 95% of the absorbed dose excreted unchanged in the urine (Brown et al., 1976; Mason et al., 1979). The reported renal clearance of atenolol is greater than glomerular filtration clearance, suggesting a component of net tubular secretion in atenolol renal clearance (Mason et al., 1979; Goodman et

al., 2011). In **Specific Aim 2**, we aim to identify major drug transporters involved renal secretion of atenolol. Hydrochlorothiazide is the most commonly prescribed thiazide diuretic for the treatment of hypertension (Feldman et al., 2015), which lowers blood pressure by inhibiting the electroneutral Na^+/Cl^- cotransporter located on the apical membrane of early segment of the distal convoluted tubule (Tamargo et al., 2014). Its elimination is mainly through renal excretion and tubular net secretion accounts for more than 80% of its renal clearance (Beermann et al., 1976; Baur et al., 1977; Beermann and Groschinsky-Grind, 1977; Tamargo et al., 2014). Thus for hydrochlorothiazide, renal excretion is not only important for its elimination but also necessary for its efficacy. In **Specific Aim 3**, we will identify major drug transporters involved renal secretion of hydrochlorothiazide. Emerging evidence showed that substrate-dependent inhibition exists for several renal transporters such as hOCT2 and hMATE1 (Belzer et al., 2013; Martinez-Guerrero and Wright, 2013; Thevenod et al., 2013), but the clinical implication is unclear. In **Specific Aim 4**, we will characterize substrate-dependent inhibition on hOCT2/hMATE-mediated drug secretion and evaluate its impact on renal DDI and toxicity assessment using an *in vitro* cell culture model double transfected with hOCT2 and hMATE1.

In summary, this project will 1) identify commonly used drugs that are susceptible to renal transporter-mediated DDIs and analyze their observed renal DDIs; 2) elucidate renal transport for two widely used antihypertensive drugs; 3) evaluate the clinical impact of substrate-dependent inhibition on renal DDI and toxicity assessment. These studies will improve our understanding of the clinical significance of renal transporter-mediated DDIs and pave the way for rational prediction of drug DDIs for existing drugs as well as for new molecular entities under development.

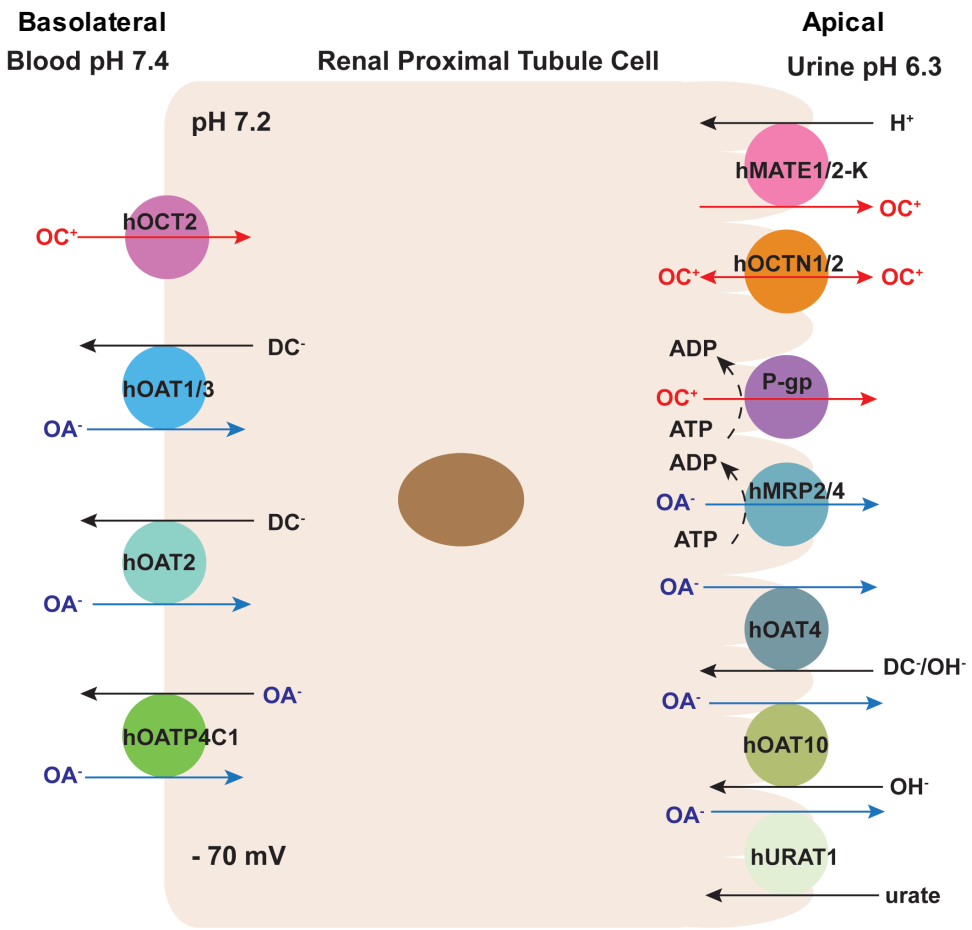

OC: organic cation; **OA**: organic anion; **DC**: dicarboxylate; **ATP**: adenosine triphosphate; **ADP**: adenosine diphosphate

Figure 1.1. Major drug transporters expressed in human renal proximal tubule cells.

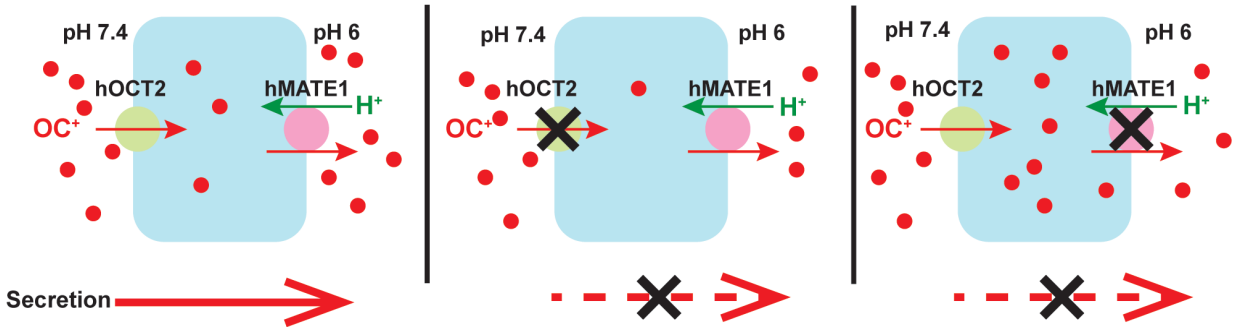

Figure 1.2. Hypothesized effects of transporter inhibition on tubular drug secretion and intracellular accumulation. When a basolateral uptake transporter such as hOCT2 is the main inhibition site, both renal secretion and intracellular drug accumulation are decreased. In contrast, when an apical efflux transporter such as hMATE1 is the primary inhibition site, tubular secretion is decreased but the intracellular drug level is increased.

Table 1.1 Examples of clinically observed DDIs involving renal drug transporters.

Implicated Transporters	Victim Drug	Perpetrator Drug	AUC fold increase	CL_R decrease (%)	Reference
hOCT2 hMATE1 hMATE2-K	Metformin	Cimetidine	1.5	28	(Somogyi et al., 1987)
	Metformin	Cimetidine	1.5	45	(Wang et al., 2008)
	Metformin	Pyrimethamine	1.4	35	(Kusuhara et al., 2011)
	Metformin	Dolutegravir	2.5	N.D.	(Song et al., 2016)
hOAT1 hOAT3	Furosemide	Probenecid	2.7	66	(Vree et al., 1995)
	Furosemide	Probenecid	3.1	80	(Smith et al., 1980)
	Cidofovir	Probenecid	1.8	52	(Cundy et al., 1995)
	Fexofenadine	Probenecid	1.5	73	(Yasui-Furukori et al., 2005)
	Fexofenadine	Probenecid	1.5	70	(Liu et al., 2008)
P-gp	Digoxin	Quinidine	N.D.	56	(Schenck-Gustafsson and Dahlqvist, 1981)
	Digoxin	Quinidine	N.D.	33	(Fenster et al., 1984)
	Digoxin	Quinidine	N.D.	34	(Hager et al., 1979)

N.D.: not determined

Chapter 2. Clinical Significance of Renal Transporter Mediated Drug-Drug Interactions: Analysis of Substrate Sensitivity and Magnitude of Interactions among Commonly Prescribed Drugs

2.1 Introduction

Renal clearance is a major drug elimination pathway (Morrissey et al., 2012). It consists of passive glomerular filtration, active tubular secretion and active and/or passive reabsorption. Many of the transporters involved in renal excretion are expressed in the proximal tubule and work in pairs, one on the basolateral membrane and one on the apical membrane, to actively excrete molecules into the tubule lumen. Both basolateral and apical transporters tend to be charge selective for anionic and cationic drugs, although recent study suggests that the transporters share certain overlap in substrate specificities (Ahn et al., 2009). For excretion of organic cation drugs, the major transporters include Organic Cation Transporter OCT2 on the basolateral membrane and Multidrug and Toxin Extrusion Protein MATE1 and MATE2/2-K on the apical membrane (Morrissey et al., 2012). For excretion of organic anion drugs, the major transporters include Organic Anion Transporters OAT1 and OAT3 on the basolateral membrane, and Multidrug Resistance-associated Protein MRP2 and MRP4 on the apical membrane (Morrissey et al., 2012). P-glycoprotein (P-gp) is also expressed on the apical membrane of kidney tubule cells and appears to contribute to renal secretion of larger, more hydrophobic cationic molecules (Giacomini, 2010).

In recent years, transporter-mediated DDIs have been increasingly recognized as an important factor altering the pharmacokinetics and pharmacodynamics of drugs. The most significant clinical interactions appear to be mediated by Organic Anion-Transporting Polypeptide OATP1B1 in the liver (Giacomini, 2010). For example, cyclosporine increased

pravastatin AUC by 20-fold mainly through inhibition of OATP1B1 (Regazzi et al., 1993). Whether similar magnitude of DDIs can result from renal transporter inhibition is not well established, although generally renal transporter mediated DDIs are considered to be small in magnitude. Known renal transporter mediated DDIs include probenecid decreasing the renal clearance of β-lactam antibiotics, antivirals and diuretics by 19%-75% through inhibiting OAT1/3 (Li et al., 2006b), and cimetidine causing a 1.5-fold increase in metformin AUC by inhibiting OCT2 and MATE1/2K (Wang et al., 2008). These changes are relatively small compared to the maximum DDIs observed with hepatic transporters. However, these observed renal DDIs might not reflect the worst-case scenario of possible clinical DDIs with renal transporters. The aim of this study was to systematically evaluate renal DDI risk for commonly used drugs and to establish the overall clinical significance of inhibition of renal transporters.

2.2 Methods

2.2.1 Theory

Of the renal clearance processes, glomerular filtration is not inhibitable and hence renal drug-drug interactions are expected to be entirely the result of inhibition of active tubular secretion or active reabsorption. Of these processes, inhibition of active tubular secretion is of major concern for inhibitory DDIs. Active reabsorption occurs for many vital endogenous compounds, but for exogenous drugs, reabsorption is thought to occur mainly through a passive process (Rowland and Tozer, 2011). Many drugs that undergo active secretion are very hydrophilic and charged at physiological pH, with relatively low passive reabsorption. Therefore renal net secretion was assumed to approximate active tubular secretion. The basis of the current analysis was that maximum DDI risk is observed when active tubular secretion by all involved transporters is completely inhibited. To establish the overall maximum DDI magnitude, the net

secretion clearance (CL_{ns}) of the drugs of interest was calculated by subtracting filtration clearance (f_u*GFR) from total renal clearance (CL_R). The maximum change in victim drug renal clearance and AUC were calculated for 24 drugs with net secretion among the top 200 prescription drugs in U.S. using equation (1) and (2).

$$\text{Maximum } CL_R \text{ decrease } \% = (1- (CL_R - CL_{ns})/CL_R) * 100\% \quad (1)$$

$$\text{Maximum AUCR} = CL/(CL_{NR} + CL_R - CL_{ns}) = CL/(CL_{NR} + CL_{filtration}) \quad (2)$$

To aid in the risk assessment, the fraction of the total body clearance after i.v. administration that is by net tubular secretion ($f_{ns} = CL_{ns}/CL$) and the fraction of renal clearance that is by net tubular secretion ($f_{ns}' = CL_{ns}/CL_R$) were calculated. To evaluate the role of these fractions and f_e in the magnitude of in vivo DDIs, f_e and f_{ns} were plotted against maximum AUCR, and f_e and f_{ns}' were plotted against maximum CL_R decrease (**Figure 2.1**).

2.2.2 Literature Search Strategy

The clinical importance of potential renal drug-drug interactions was evaluated for the top 200 prescribed drugs in the U.S. The list of top 200 prescribed drugs in U.S. 2010 was obtained from Pharmacytimes.com. Duplicate chemical entities and combination therapies were removed to obtain a list of unique chemical entities. To assess the importance of renal clearance in the elimination of these drugs, the f_e (fraction excreted unchanged in urine after i.v. administration) values were obtained via PubMed searches for each unique entity. For drugs with f_e values greater than 25%, the key pharmacokinetic parameters were collected from publications referenced in PubMed and from product labels available at drugs@fda.gov. The data included f_u (plasma unbound fraction), CL (total body clearance after i.v. administration), and CL_R (renal clearance). A summary of f_e, f_u, CL and CL_R is provided in **Table 2.1**. Using collected f_u values for the compounds with significant renal elimination (f_e > 25%), the glomerular filtration

clearance of these compounds was calculated as $CL_{filtration} = f_u$*GFR, assuming GFR of 120 ml/min. The filtration clearance was compared with total renal clearance to identify drugs with significant net secretion. Drugs with $CL_R > CL_{filtration}$ were considered to have net tubular secretion and were evaluated further.

2.2.3 Collection and Evaluation of *in vivo* and *in vitro* Data of Drugs Susceptible to Renal DDIs

For 19 drugs with theoretical maximum CL_R decrease > 33%, *in vivo* positive DDI studies (> 25% AUC, CL or CL_R change) and *in vitro* transporter studies were collected through the University of Washington Metabolism and Transport Drug Interaction Database (www.druginteractioninfo.org). Specifically, renal transporters of victim drugs identified *in vitro*, dosing regimen of perpetrators, and AUC, CL and CL_R changes of victim drugs observed in positive DDI studies were recorded. As digoxin DDIs have been extensively reviewed previously (Fenner et al., 2009), only two representative DDI studies of digoxin were included. For pravastatin and rosuvastatin, only DDI studies with reported CL_R change were recorded to avoid confounding effect of OATP1B1 inhibition as these drugs are actively taken up into hepatocytes mainly by OATP1B1 and biliary excretion is a major route in their elimination (Singhvi et al., 1990; Martin et al., 2003b; Schachter, 2005; Maeda et al., 2006; Neuvonen et al., 2006; Yamashiro et al., 2006). Indeed, when the *in vivo* DDIs for pravastatin and rosuvastatin were analyzed, all perpetrators, except for itraconazole and fluconazole, were found to be known OATP1B1 inhibitors, with many of them having K_i or IC_{50} < 10μM (Seithel et al., 2007; Gui et al., 2009; Annaert et al., 2010; Bednarczyk, 2010; Takeuchi et al., 2011; Karlgren et al., 2012; Mandery et al., 2012; Sharma et al., 2012; Takashima et al., 2012; Yoshida et al., 2012; Chu et al., 2013a; Izumi et al., 2013; Tamraz et al., 2013). For prediction of *in vivo* inhibition of renal

transporters and subsequent DDIs for 4 selected drugs, the total plasma concentrations of perpetrators ([I]) in DDI studies, the f_u of perpetrators, as well as the IC_{50} or K_i values of perpetrators for each identified renal transporter were collected. The total plasma concentrations were obtained either from the clinical drug-drug interaction study where the inhibitor concentration was measured or from a pharmacokinetic study of the inhibitor where the dose of the inhibitor was the same or similar.

2.2.4 Prediction of *in vivo* Inhibition of Renal Transporters and Subsequent DDIs

Four drugs were selected for prediction based on the spread of f_{ns} values and availability of *in vitro* data. The percent inhibition by the perpetrators for each involved transporter was calculated by equation (3).

$$\text{Inhibition \%} = (1 - 1/ (1 + [I]_u/K_i))*100\% \quad (3)$$

The inhibitor concentrations inside the cells were assumed to be in equilibrium with the unbound concentration in plasma and no active uptake of inhibitor was incorporated in the predictions. In cases where no K_i value was available, the IC_{50} for the inhibitor-transporter pair was used instead, assuming competitive inhibition and substrate concentration $[S] << K_m$. The prediction of DDIs was performed using unbound perpetrator concentrations. Because substrates were known to be transported by multiple renal transporters and which transporter is dominant hasn't been established, the DDIs were predicted for each known renal transporter separately assuming this transporter alone was responsible for all the tubular secretion of the substrate. The resulting magnitude of AUC and CL_R change due to inhibition of specific renal transporter was predicted for cefdinir, furosemide, famotidine and metformin using equations (4) ~ (7).

$$CL_R \text{ decrease \%} = ((CL_R - CL_{R,\,inhibited})/CL_R)*100\% \quad (4)$$

$$CL_{R,inhibited} = GFR*f_u + CL_{ns}/(1 + [I]/K_i \text{ or } [I]_u/K_i) \quad (5)$$

$$\text{AUC increase \%} = (AUC_{inhibited}/AUC - 1)*100\% \quad (6)$$

$$AUC_{inhibited}/AUC = CL/CL_{inhibited} = CL/(CL_{NR} + CL_{R,\ inhibited}) \quad (7)$$

2.2.5 Simulation of AUC and CL_R Change under Inhibition of Renal Transporters

Assuming that only one transporter was responsible for the renal clearance of a drug, the fold AUC change and % CL_R decrease due to inhibition of that transporter was simulated using equations (8) and (9).

$$AUC_i/AUC = 1/[(1-f_{ns}) + f_{ns}/(1 + [I]_u/K_i)] \quad (8)$$

$$CL_R \text{ decrease\%} = (f_{ns}' - f_{ns}'/(1 + [I]_u/K_i))*100\% = (1 - 1/(1 + [I]_u/K_i))*f_{ns}'*100\% \quad (9)$$

Theoretical inhibitors with varying $[I]_u/K_i$ values and theoretical substrates with varying f_{ns} and f_{ns}' were considered. AUC ratio and %CL_R decrease were simulated at $[I]_u/K_i$ equal to 0.1, 1, 2, 5, 8, 15, 90 with f_{ns} and f_{ns}' increasing from 0 to 1.

2.3 Results

2.3.1 Identification of Drugs Susceptible to Renal Transporter mediated DDIs

Among the top 200 prescribed drugs in the U.S. in 2010, representing 98 unique chemical entities, 31% (30 drugs) were found to have significant renal excretion (fraction excreted unchanged f_e > 25%), and 24% (24 drugs) were subject to renal net secretion. A summary of the pharmacokinetic parameters for the 30 drugs identified to have a f_e > 25% is shown in Table 2.1. To determine the maximum DDI risk for the 24 drugs with net secretion, the theoretical maximum AUC change (AUCR) in the event of complete inhibition of renal net secretion was calculated (Table 2.2) and plotted against f_e and fraction of CL by net secretion (f_{ns}) (Figure 2.1 A and B). Weak association between f_e and theoretical maximum AUCR was observed for these drugs (R^2 = 0.23, P = 0.0174), despite the strong correlation between theoretical maximum AUCR and f_{ns} (R^2 = 0.79, P < 0.0001). The theoretical maximum CL_R decrease, which is equal to

fraction of CL_R by net secretion (f_{ns}'), was also plotted against f_e (Figure 2.1 C). Likewise, there was no relationship between theoretical maximum CL_R decrease and f_e.

Among the 24 drugs with f_e > 25%, 83% (20 drugs) had a theoretical maximum AUCR > 1.25-fold, and 25% (6 drugs) had a theoretical maximum AUCR > 2-fold, suggesting that these drugs may be susceptible to clinically significant DDIs. A majority of these drugs (67%, 16 drugs) had theoretical maximum CL_R decrease > 50% (equal to 2-fold CL_R change). Due to the higher sensitivity of CL_R change in comparison to AUCR, a theoretical maximum CL_R decrease > 33%, as suggested by the ITC white paper in 2010 (Giacomini, 2010), was used as the criterion for further risk assessment.

2.3.2 Evaluation of Observed *in vivo* DDIs of Drugs Susceptible to Renal DDIs

The clinical DDI studies and *in vitro* renal transporter studies of the 19 drugs with theoretical maximum CL_R decrease > 33% were collected. Thirteen of these drugs had reported significant DDIs (AUC, CL or CL_R change > 25%). To avoid confounding effect of OATP1B1 inhibition in the liver, for pravastatin and rosuvastatin, only studies reporting CL_R change were considered in our analysis. Based on this criterion, rosuvastatin was eliminated from our analysis because none of the published DDI studies reported a CL_R change. The *in vivo* DDI studies and currently identified *in vitro* renal transporters of 12 drugs with significant renal DDIs are summarized in Table 2.3. Despite the fact that all of these drugs had theoretical maximum CL_R decrease > 33%, only 8 of the 10 drugs with available data showed CL_R decrease > 33% (Figure 2.2A). A comparison of the greatest observed interactions and theoretical maximum DDIs revealed that when the CL_R change was considered, except for famotidine, the observed interactions were weaker than the theoretical maximum interactions by 11% - 55% (Figure 2.2B). When the AUC change was compared, except for digoxin, pravastatin and

hydrochlorothiazide, all other interactions were weaker than theoretical maximum interactions by 4 -317% (Figure 2.2C). The largest CL_R change observed for these 12 drugs was a 66% decrease in furosemide CL_R when co-administered with probenecid.

2.3.3 Prediction of *in vivo* Inhibition of Renal Transporters and Subsequent DDIs

To further characterize what could contribute to the generally weak observed *in vivo* renal DDIs, 4 drugs with perpetrators studied *in vivo* were selected and the percent inhibition of the individual transporters likely contributing to the renal clearance of the 4 drugs were predicted. The predictions (Table 2.4) showed that the maximum predicted *in vivo* % inhibition of any of the renal transporters in the clinical studies was 89% with probenecid. For the other inhibitors, the predicted *in vivo* % inhibition of any given transporter ranged from 5% to 78%, demonstrating that overall complete transporter inhibition is rarely achieved in clinical studies. Due to differential inhibition potency with different transporters, the prediction of AUC and CL_R change was done separately for each identified renal transporter using a static model (Feng et al., 2013). This was translated to the maximum potential *in vivo* DDI, assuming that the inhibited individual renal transporter was solely responsible for the tubular secretion of the victim drug. As shown in Table 2.4, for furosemide and metformin DDIs with documented inhibitors, the predicted risk of *in vivo* DDIs differs considerably depending on which transporter is assumed to be dominant in the secretion of these compounds. When MRP2 was assumed as the dominant transporter for furosemide and OCT2 for metformin, the observed *in vivo* DDI risk was not identified. In contrast, assuming OAT3 as the dominant transporter for furosemide, and MATE1 as the dominant transporter for metformin, both the *in vivo* DDI risk and magnitude of DDIs were generally well predicted (with the exception of the AUC change for the pyrimethamine-

metformin interaction). For famotidine and cefdinir, the *in vivo* DDIs caused by probenecid were also well predicted.

2.4 Discussion

Inhibition of renal transporters has been implicated in numerous DDIs with some of these DDIs having severe clinical consequences (DeGorter et al., 2012). For example, co-administration of nonsteroidal anti-inflammatory drugs (NSAIDs), such as ketoprofen together with methotrexate can result in life-threatening exposure to methotrexate possibly due to inhibition of methotrexate renal clearance through the OATs (Thyss et al., 1986; Takeda et al., 2002a; DeGorter et al., 2012). Therefore, it is critical to determine whether a drug is susceptible to renal transporter-mediated DDIs as a victim drug, and/or whether a drug may impact the exposure to co-administered compounds by inhibiting renal drug transporters (drug as a perpetrator).

In this study, the top 200 prescribed drugs in the U.S. in 2010 were used as a clinically relevant sample dataset. Our result that 31% of the drugs have $f_e > 25\%$ is similar to previous findings (Varma et al., 2009; Morrissey et al., 2012). While this analysis shows that CL_R is an important drug clearance pathway, significant renal DDIs are perceived to be relatively uncommon. In contrast, it is recognized that renal impairment often affects the exposure to drugs cleared by the kidney and may require dosage adjustment (Zhang et al., 2009). A key difference between renal impairment and renal DDI is that the effect of renal impairment on drug disposition mostly depends on the drug f_e, while the magnitude of renal DDIs depends on f_{ns} and f_{ns}' values. The difference in the processes driving clearance changes in renal impairment and in renal DDIs is reflected in the FDA 2010 guidance for renal impairment studies (www.fda.gov/downloads/Drugs/Guidances/UCM204959.pdf) and the DDI decision trees

presented by the International Transporter Consortium (ITC) in 2010 and 2013. According to the guidance, a renal impairment study is recommended for drugs with f_e > 30%, while for DDIs, CL_R > 1.5*f_u*GFR (equal to f_{ns}' > 33%) or (CL_R –f_u*GFR)/CL ≥ 25% (equal to f_{ns} > 25%) should be used to determine if a renal DDI study is necessary.(Giacomini, 2010; Tweedie et al., 2013) As indicated in Figure 2.1, there was no correlation between f_e and f_{ns} or f_{ns}' (R^2 = 0.24 and 0.01 respectively) within the selected group of drugs, which likely explains why many drugs whose disposition is affected by renal impairment are not susceptible to significant renal DDIs. As f_{ns} is always less than f_e, renal DDI's impact on systemic exposure of drugs is predicted to have a lower effect than renal impairment when the worst case scenario is considered. Yet, renal DDIs may have a severe impact on the kidney due to the potential accumulation of nephrotoxic compounds within the kidney tubular cells.

To select drugs at risk of renal DDIs, a theoretical maximum CL_R decrease > 33% (f_{ns}' > 33%) was used as a criterion for the analysis. This criterion was chosen due to the higher sensitivity of CL_R for DDIs when compared to AUC change, and the fact that this parameter can be determined regardless of whether i.v. administration data are available for the victim drug. In contrast, the f_{ns} > 25% criterion in the ITC 2013 decision tree (Tweedie et al., 2013) needs knowledge of the true systemic clearance of the victim drug to accurately assess the risk. f_{ns} after oral administration will underestimate the risk for renal DDIs if bioavailability is < 100%. Because i.v. dosing data are often not available for new drugs in development, it is a challenge to use f_{ns} for risk assessment. In addition, for some renal DDIs, the change in CL_R may be more relevant to consider than the change in systemic CL, due to possible drug accumulation in the kidney and subsequent nephrotoxicity.

Table 2.2 and Figure 2.1 suggest that a major factor contributing to the generally small renal DDIs is the low f_{ns} of the commonly used drugs, even when they are largely renally cleared. In our sample dataset, only 6 drugs had f_{ns} > 50% and only one, cefdinir, had an f_{ns} > 80%, leading to a more than 5-fold theoretical maximum AUC change. As such, only cefdinir could be considered as a sensitive substrate of renal DDIs using the same criteria as used by the FDA for classification of sensitive CYP substrates (FDA, 2012). However, the sensitivity of cefdinir to renal DDIs should be confirmed in appropriate clinical trials. The FDA recommended probe substrates metformin (for OCT2) and ciprofloxacin (for OAT1 and OAT3) (FDA, 2012) have f_{ns} values of 73% and 44%, respectively, indicating that they are not as sensitive as cefdinir for renal DDIs. Similarly, zidovudine, acyclovir, tenofovir and methotrexate, which are less commonly used drugs but recommended probes for OAT1 and OAT3(FDA, 2012), have f_{ns} < 50% (Aherne et al., 1978; Laskin et al., 1982; Chatton et al., 1992; Kiser et al., 2008; 2011). Finally, even the common OAT substrate, furosemide, has an f_{ns} of only 74% and a theoretical maximum AUC increase of 3.8-fold. Therefore, it is likely that the limited sensitivity of the current probe substrates contributes to a large extent to the weak DDIs usually observed when renal transporter inhibition is systematically evaluated during the drug development process.

The low *in vivo* potency of renal transporter inhibitors also seems to contribute to the generally low magnitude of the observed DDIs based on the gap between the theoretical maximum DDI and the clinically observed DDI (Figure 2.2) in our sample dataset. As shown in Table 2.4, probenecid was the most potent *in vivo* inhibitor of the analyzed inhibitors resulting in up to 89% inhibition of OAT1 and OAT3 with the dosing regimens used in these clinical studies. The *in vivo* DDI between valsartan and hydrochlorothiazide was greatest in magnitude (Table 2.3), but this DDI hasn't been evaluated *in vitro* and the AUC increase may include intestinal and

hepatic components. The next greatest interaction was observed with probenecid-furosemide co-administration, and the gap between observed interaction and theoretical maximum can be explained by incomplete inhibition of OATs by probenecid. A higher probenecid dose or a longer duration of probenecid dosing may narrow the gap and allow exploration of maximum clinical DDI risk. Similarly, for metformin, for which a maximum 3.7-fold AUC change was predicted, the observed DDIs were much less (< 2-fold). This is most likely explained by the weak inhibition of OCT2 and MATEs by the inhibitors tested with metformin. It is noteworthy that, while the three inhibitors, cimetidine, pyrimethamine, and trimethoprim inhibit 33-84% of MATE1 and MATE2K activity, none of them is predicted to inhibit OCT2 *in vivo* at the doses used. Cimetidine is the FDA recommended OCT2 and MATE inhibitor (FDA, 2012). At 400mg twice daily (the dosing regimen used in the DDI study with metformin), $[I]_u/K_i$ of cimetidine toward MATE1 is only 2. Assuming doubling the dose (maximum oral dose 800 mg twice daily) in future clinical studies, with an $[I]_u/K_i$ =4, the chance of cimetidine to generate a > 2-fold AUC change for a MATE1 probe is still very low. Similar concerns also exist for pyrimethamine and trimethoprim. Therefore, for OCT2 and MATEs, it is unlikely that the worst case DDI of a victim drug could be observed *in vivo* using currently identified inhibitors.

The data described in Figure 2.2 also show that the extent of the gap between theoretical maximum DDI and the observed DDI can vary greatly between drugs. To further explore these differences between renal transporter substrates, the magnitude of AUC change as a function of $[I]_u/K_i$ and f_{ns}, and $\%CL_R$ decrease as a function of $[I]_u/K_i$ and f_{ns}' were simulated (Figure 2.3). As illustrated in Figure 2.3A, when a victim drug has an f_{ns} < 50%, the change in its AUC when renal transporter is inhibited is always less than 2-fold, regardless of perpetrator's $[I]_u/K_i$. Hence, within clinical variability, it is not possible to differentiate between different inhibitor potencies,

and the gap between the observed and predicted AUC change will always be small. In Figure 2.2C, cephalexin, ciprofloxacin, famotidine and olmesartan fall into this category. When a victim drug has an f_{ns} between 50% and 80%, it has a moderate sensitivity to renal transporter inhibition. For these drugs, the gap between theoretical maximum and observed interactions can be large if the perpetrator's *in vivo* potency is very low, as shown in metformin interactions. When a victim drug's f_{ns} is > 80%, it is highly sensitive to the *in vivo* potency of the perpetrators and large gaps between theoretical maximum and observed DDIs are more likely for these drugs. In our dataset, only cefdinir falls into this category. Based on this analysis, since most clinical transporter substrates in our dataset have f_{ns} values below 0.8, it is very difficult to differentiate between different inhibition potencies and prediction accuracy by assessing AUC change unless a strong inhibitor is identified. Similarly with CL_R change, as shown in Figure 2.3B, regardless of the inhibitor potency the f_{ns}' has to be greater than 33% to observe a change in CL_R, and the substrate must have an f_{ns}' >0.7 to be sensitive enough to detect moderate inhibition ($[I]_u/K_i = 1$). In our dataset, 12 drugs, cefdinir, ciprofloxacin, furosemide hydrochlorothiazide, metformin, olmesartan, penicillin V, pravastatin, ranitidine, rosuvastatin, sitagliptin and tiotropium met this criterion demonstrating the overall sensitivity of CL_R to detect renal interactions. Interestingly the f_{ns}' values of cefdinir, furosemide and olmesartan were all greater than 90%, providing very sensitive measures for evaluating renal transporter mediated DDIs in, and for assessing prediction accuracy as the dynamic range in predictions is large for the different inhibitors and transporters evaluated (Table 2.4).

For inhibition of apical transporters, we assumed that the unbound plasma inhibitor concentration is in equilibrium with intracellular free inhibitor concentration and the inhibition occurs in the intracellular side. However, in vivo, inhibitors can gain access to apical

transporters either through active uptake from the basolateral side of tubule epithelium or from the luminal side from the filtrate. Depending on the binding site of the inhibitor in the transporter, it should be the intracellular free inhibitor concentration or luminal free inhibitor concentration in the proximal tubule that matters. For accurate prediction of in vivo inhibition potency, the most appropriate inhibitor concentration to use is the concentration at the interaction site. However, due to the difficulty of quantifying target site drug concentration in humans and lack of knowledge of the exact binding site of the inhibitor on the transporter, plasma unbound concentration is usually used as a surrogate (Chu et al., 2013b; Dollery, 2013). The assumption that unbound plasma drug concentration mirrors intracellular free drug concentration is based on free-drug hypothesis that at steady state, the free drug concentration is at equilibrium on both sides of the membrane (Smith et al., 2010). For inhibitors that are actively transported, extensively metabolized or have low passive permeability, this assumption no longer holds (Smith et al., 2010; Chu et al., 2013b). On the other hand, the tubular free inhibitor concentration at proximal tubule is theoretically higher than plasma unbound inhibitor concentration due to the reabsorption of water at the tubule. Thus if an inhibitor truly interacts with an apical transporter on the tubular side, our prediction may underestimate the degree of inhibition. With advancement of technology such as imaging mass spectrometry (Dollery, 2013), drug concentrations at the interaction site may be accurately measured, which may significantly improve the accuracy of prediction.

A considerable obstacle for accurate prediction of transporter-based renal DDIs is the lack of knowledge of the relative contribution of the individual transporters to the victim drug's tubular secretion and the significant differences in inhibitor potency toward individual transporters. For example, for furosemide and metformin the predicted interaction ranged from

no DDI to 2.7-fold increase in the AUC depending on which transporter was considered having the predominant role in furosemide renal secretion. This is a major concern, as accurate prospective identification of the dominant transporter(s) for a drug will affect the choice of an optimal *in vivo* inhibitor for clinical studies, and the ability to predict the DDI magnitude with a given inhibitor. As such, this analysis emphasizes the need for more efforts to develop methods to characterize the relative contributions of specific transporters to probe secretion.

Another limiting factor in accurate prediction of transporter-mediated DDIs is substrate-dependent inhibition. In the decision trees presented in FDA guidance and ITC white papers, $[I]_u/IC_{50} > 0.1$ is used as a cutoff for determining whether an in vivo DDI risk evaluation is needed for an in vitro renal transporter inhibitor (Giacomini, 2010; FDA, 2012; Hillgren et al., 2013). The IC_{50} values are typically determined using a probe substrate in transporter-expressing cell lines (Brouwer et al., 2013). The assumption for using this criterion is that the IC_{50} values determined using a probe substrate are applicable to other clinically encountered drug substrates. However, several drug-metabolizing enzymes including CYP3A4 and 2D6 are known to exhibit substrate-dependent inhibition, where the K_i or IC_{50} values of an inhibitor can vary considerably depending on the probe substrate used (Kenworthy et al., 1999; VandenBrink et al., 2012). Emerging evidence also suggests that substrate-dependent inhibition can occur with drug transporters as well (Belzer et al., 2013; Martinez-Guerrero and Wright, 2013; Izumi et al., 2015). Using metformin and several experimental compounds as substrates, Wright and coworkers showed that inhibition of OCT2 and MATE1 is substrate-dependent (Belzer et al., 2013; Martinez-Guerrero and Wright, 2013). In particular, the IC_{50} for OCT2 can vary as high as 88-fold, depending on the substrate used (Belzer et al., 2013). Thus, substrate-dependent inhibition can also alter the predicted magnitude of transporter-mediated DDIs. For accurate

prediction, this problem can be overcome by direct measurement of the in vivo IC_{50} using the victim drug as the substrate. The impact of substrate-dependent inhibition on predicting transporter-mediated renal drug interaction and accumulation will be further investigated in Chapter 5.

In conclusion, the present analysis suggests that although there is a large number of drugs theoretically susceptible to renal DDIs, clinically, it is uncommon to see a renal DDI with a > 2-fold AUC change (3 interactions in our sample dataset) or > 33% CL_R decrease (8 interactions in our sample dataset). This is most probably due to the limited potency of the existing clinical inhibitors of renal transporters. By rigorously designing dedicated clinical studies using perpetrators with high $[I]_u/K_i$ ratios for the target transporters and the most sensitive probe substrates, it should be possible to determine whether the predicted maximum DDIs can be achieved in the clinic.

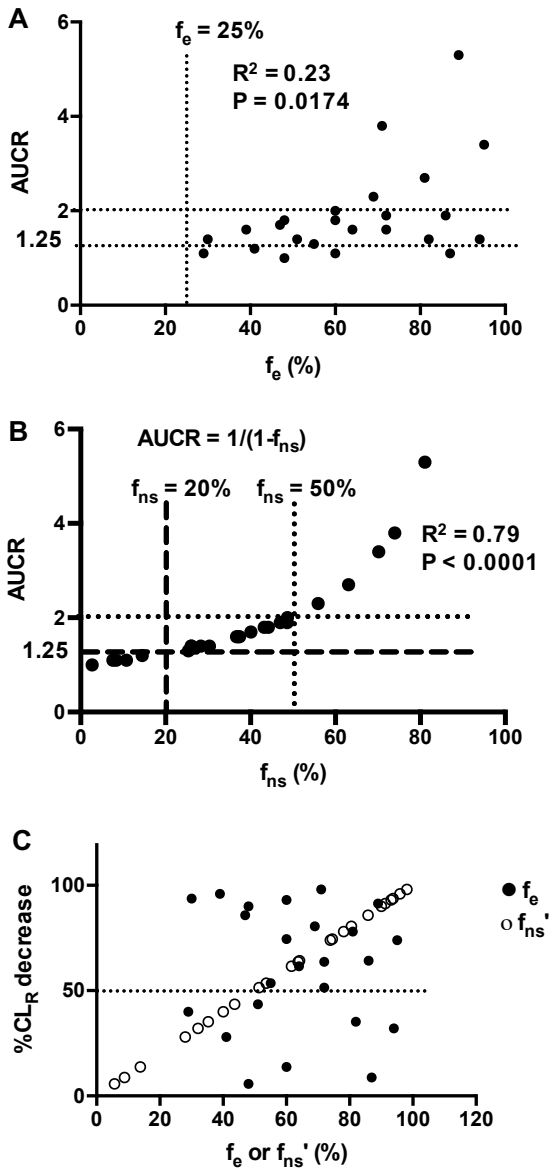

Figure 2.1 The relationship between f_e, f_{ns} and f_{ns}' and theoretical maximum AUC and CL_R change for the drugs in Table 2.2. (A) Relationship between f_e and theoretical maximum AUCR. (B) Relationship between f_{ns} and theoretical maximum AUCR (C) Relationship between f_e and theoretical maximum CL_R decrease. (f_e: fraction excreted unchanged in urine after i.v. dosing; f_{ns}: fraction of total plasma clearance that is net tubular secretion; f_{ns}': fraction of renal clearance that is net tubular secretion)

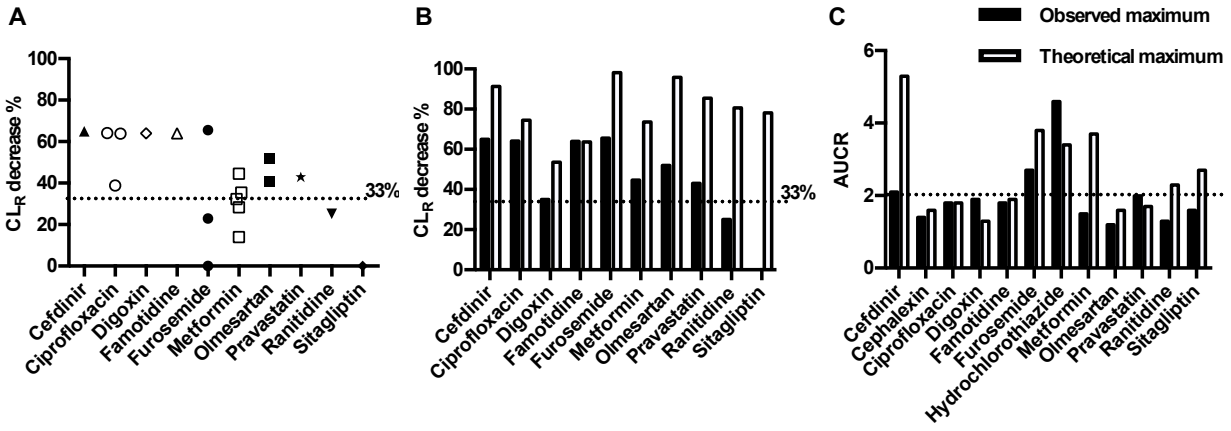

Figure 2.2 Comparison of observed DDIs with theoretical maximum DDIs for victim drugs in Table 2.3. (A) Observed CL_R change in clinical DDI studies for victim drugs. (B) Comparisons of theoretical maximum CL_R change with observed maximum CL_R change. (C) Comparisons of theoretical maximum AUC change with observed maximum AUC change. (Digoxin and pravastatin were excluded for AUC due to confounding factors in systemic CL change.)

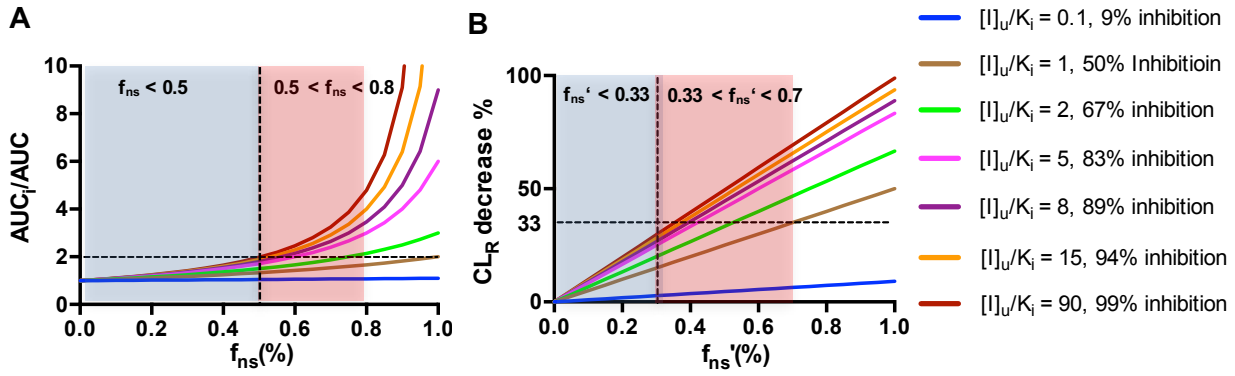

Figure 2.3 Simulation of impact of inhibitor potency and net secretion fractions of substrate on the magnitude of renal DDIs. (A) AUC ratio as a function of f_{ns} at different $[I]_u/K_i$'s. (B) $\%CL_R$ decrease as a function of f_{ns}' at different $[I]_u/K_i$'s. (f_{ns} - fraction of total plasma clearance by net secretion; f_{ns}' - fraction of renal clearance by net secretion; AUC_i - AUC in the presence of inhibitor; $[I]_u$ - unbound inhibitor concentration; K_i - the affinity of an inhibitor to a transporter)

Table 2.1: Pharmacokinetic parameters of drugs with f_e > 25% among top 200 prescribed drugs in U.S. 2010. (total 30 drugs)

Drug	Use	f_e (%)	f_u (%)	CL (ml/min)	CL_R (ml/min)
Alendronic acid	Osteoporosis	40 ~ 60 (Cocquyt et al., 1999)	20 (Cocquyt et al., 1999)	199 (Porras et al., 1999)	71 (Cocquyt et al., 1999)
Amoxicillin	Antibiotic	82 ± 3 (Sjovall et al., 1986)	82 ~ 83 (Sutherland and Rolinson, 1970; Brusch et al., 1974)	192 ± 28 (Sjovall et al., 1986)	154 ± 23 (Sjovall et al., 1986)
Amphetamine	ADHD/Neurologic	> 30 [a]	NA	NA	NA
Atenolol	Antihypertensive	94.1 ± 8 (Mason et al., 1979)	>95 (Wadworth et al., 1991)	178.3 ± 21.2 (Mason et al., 1979)	168.3 ± 24.3 (Mason et al., 1979)
Cefdinir	Antibiotic	88.5 [b]	11.5 (Tomino et al., 1998)	161.5 ~ 213.1 (Richer et al., 1995; Guay, 2000), [b]	137.5 ~ 194.0 (Richer et al., 1995)
Cephalexin	Antibiotic	72 ± 9 (De Maine and Kirby, 1970)	85 (William M. M. Kirby and Regamey, 1973)	291 ± 22 (De Maine and Kirby, 1970)	210 ± 32 (De Maine and Kirby, 1970)
Ciprofloxacin	Antibiotic	60± 9 (Drusano et al., 1986)	60.4 (Hoffken et al., 1985)	475± 78 (Drusano et al., 1986)	281.7± 50 (Drusano et al., 1986)
Clonidine	Cardiovascular	42.3 (MacGregor et al., 1985; Lowenthal et al., 1988)	60~80 (Hulter et al., 1979; Lowenthal et al., 1988)	250 (MacGregor et al., 1985; Lowenthal et al., 1988)	130 ~ 167 (MacGregor et al., 1985; Lowenthal et al., 1988)
Digoxin	Cardiovascular	54.6± 5 (Ding et al., 2004)	70 ~ 80 (Mooradian, 1988)	409 ± 30 (Ding et al., 2004)	194 ± 23 (Ding et al., 2004)
Doxycycline	Antibiotic	40.6 ± 5.28 (Raghuram and Krishnaswamy, 1982)	9.2 ± 3.52 (Raghuram and Krishnaswamy, 1982)	28.9 ± 2.65 (Raghuram and Krishnaswamy, 1982)	14.7 ± 1.44 (Raghuram and Krishnaswamy, 1982)
Famotidine	Antacid	72± 11 (Takabatake et al., 1985)	85 ~ 99 (Kroemer and Klotz, 1987)	412± 125 (Takabatake et al., 1985)	304± 129 (Takabatake et al., 1985)
Fluconazole	Antifungal	73 ± 8 (Shiba et al., 1990; Debruyne and Ryckelynck, 1993)	88 ~ 89 (Humphrey et al., 1985; Debruyne and Ryckelynck, 1993)	19.5 ± 4.7 (Debruyne and Ryckelynck, 1993)	14.7 ± 3.7 (Debruyne and Ryckelynck, 1993)
Furosemide	Antihypertensive	71± 10 (Waller et al., 1982)	1.4± 0.4 (Andreasen et al., 1983)	117.6± 41.3 (Waller et al., 1982)	88.9 ± 44.8 (Waller et al., 1982)
Gabapentin	Anticonvulsant	100 (McLean, 1994; Yagi et al., 2012)	> 95 (Vollmer et al., 1986)	100 ± 28 (Yagi et al., 2012), [b]	100 ± 28 (Yagi et al., 2012)
Hydrochlorothiazide	Antihypertensive	>95 (Beermann et al., 1976)	45 ~ 78 (Baur et al., 1977; Nakano et al., 1979; Niemeyer et al., 1983)	< 300 [b]	285± 30 (Niemeyer et al., 1983)
Levofloxacin	Antibiotic	60 ± 9 (Chien et al., 1997)	62 ~ 76 (Greene et al., 1976)	156.8 ± 32.2 (Chien et al., 1997)	95.5 ± 23 (Chien et al., 1997)

Lisinopril	Antihypertensive	100 [a]	100 [a]	106 ± 13 [b]	106 ± 13 (Ulm et al., 1982)
Memantine	Anti-alzheimer	47.9 ± 14.2 (Periclou et al., 2006)	55 [a]	147.8 ± 28.6 (Periclou et al., 2006)	69.8 ± 22.7 (Periclou et al., 2006)
Metformin	Antidiabetic	99.9 (Pentikainen et al., 1979)	100 (Pentikainen et al., 1979)	459± 6 (Pentikainen et al., 1979)	454± 47 (Pentikainen et al., 1979)
Olmesartan	Antihypertensive	38.7 (9) (von Bergmann et al., 2001)	0.28 (von Bergmann et al., 2001)	23.2 (18) (von Bergmann et al., 2001)	8.8 (18) (von Bergmann et al., 2001)
Penicillin V	Antibiotic	48 [b]	22 (Overbosch et al., 1985)	548.1 (Overbosch et al., 1985), [b]	263± 67 (Heikkila and Erkkola, 1993)
Pravastatin	Antihyperlipidemic	47 (Singhvi et al., 1990)	52 ~ 57 (Singhvi et al., 1990)	996.3 ± 177.1 (Singhvi et al., 1990)	464.9 ± 73.8 (Singhvi et al., 1990)
Pregbalin	Anticonvulsant	> 90 (Randinitis et al., 2003), [a]	100 (Randinitis et al., 2003), [a]	74.4 ~ 89.9 [b]	67 ~ 80.9 [a]
Ranitidine	Antacid	69.4 ± 6.1 (Garg et al., 1983)	85 ± 3 (Roberts, 1984)	759.2 (10.6) (Garg et al., 1983)	525.6 (13.8) (Garg et al., 1983)
Risedronate	Osteoprosis	87 (Mitchell et al., 2001)	76 [a]	115.5 (Mitchell et al., 2001)	100.4 (Mitchell et al., 2001)
Rosuvastatin	Antihyperlipidemic	29.5 ± 7.32 (Martin et al., 2003a)	12 (Martin et al., 2003a)	815± 361.7 (Martin et al., 2003a)	226.7± 651.7 (Martin et al., 2003a)
Salbutamol	Asthma and COPD	64.2 ± 7.1 (Morgan et al., 1986)	93 ± 1 (Morgan et al., 1986)	480 ± 123 (Morgan et al., 1986)	291 ± 70 (Morgan et al., 1986)
Sitagliptin	Antidiabetic	81± 21 (Bergman et al., 2007a)	57 ~ 66 (Bergman et al., 2007b)	421± 50 (Bergman et al., 2007a)	340± 124 (Bergman et al., 2007a)
Tiotropium	Respiratory	60.1 (17.7) (Turck et al., 2004)	21 ~ 29 (Turck et al., 2004)	831 (24.5) (Turck et al., 2004)	435 (12.7) (Turck et al., 2004)
Valsartan	Antihypertensive	28.95 ± 5.82 (Flesch et al., 1997)	3 ~ 6 (Flesch et al., 1997)	36.5 ± 6.5 (Flesch et al., 1997)	10.33 ± 2 (Flesch et al., 1997)

a. value from drug label; b. calculated value

Table 2.2 Calculated maximum AUCR for top 200 drugs with f_e > 25% and net secretion. (24 drugs)

Drug	**f_e (%) ***	**f_{ns} (%)**	**f_{ns}' (%) = Max CL_R decrease (%)**	**AUCR**
Amoxicillin	82	28.3	35.3	1.4
Atenolol	94	30.3	32.1	1.4
Cefdinir	89	81.1	91.3	5.3
Cephalexin	72	37.1	51.4	1.6
Ciprofloxacin	60	44.2	74.5	1.8
Clonidine	42	26.0	43.6	1.4
Digoxin	55	25.4	53.6	1.3
Doxycycline	41	14.5	28.0	1.2
Famotidine	72	47.0	63.7	1.9
Furosemide	71	74.0	98.1	3.8
Hydrochlorothiazide	95	70.2	73.9	3.4
Levofloxacin	60	8.4	13.8	1.1
Memantine	48	2.7	5.7	1.0
Metformin	99.9	72.8	73.6	3.7
Olmesartan	39	36.7	95.9	1.6
Penicillin V	48	43.2	90.0	1.8
Pravastatin	47	40.1	85.8	1.7
Ranitidine	69	55.9	80.6	2.3
Risedronate	87	7.6	8.8	1.1
Rosuvastatin	30	26.1	93.7	1.4
Salbutamol	64	37.4	61.6	1.6
Sitagliptin	81	63.1	78.1	2.7
Tiotropium	60	48.7	93.1	2.0
Valsartan	29	10.8	40.0	1.1

* f_e is fraction excreted unchanged in urine after i.v. administration; f_{ns} is the fraction of total body clearance that is by net tubular secretion; f_{ns}' is the fraction of renal clearance that is by net tubular secretion.

Table 2.3: Clinical DDI studies with AUC, CL or CL_R change > 25% and renal transporters identified for drugs with f_{ns}' > 33%.

Drug	Renal Transporters	Perpetrator	Perpetrator Dosing	AUC ↑ (%)	CL ↓ (%)	CL_R ↓ (%)
Cefdinir	OAT1 (Ueo et al., 2005), OAT3 (Ueo et al., 2005), MRP4 (Akanuma et al., 2011)	Probenecid	p.o. 1g single	113 [b, e]		-65 [b, e]
Cephalexin	MATE1 (Tanihara et al., 2007), MRP4 (Akanuma et al., 2011)	Amlodipine	p.o. 5mg single	38 (Ding et al., 2013), a		
Ciprofloxacin	P-gp (Lin et al., 2011; Park et al., 2011), MRP4 (Haslam et al., 2011)	Azlocillin	i.v. 60mg/kg		-35 (Barriere et al., 1990), a	-39 (Barriere et al., 1990), a
		Probenecid	p.o. 1500mg before, 1500mg after	74 (Landersdorfer et al., 2010), a	-41 (Landersdorfer et al., 2010), a	-64 (Landersdorfer et al., 2010), a
		Probenecid	p.o. 1500mg before, 1500mg after	76 (Jaehde et al., 1995), a	-41 (Jaehde et al., 1995), a	-64 (Jaehde et al., 1995), a
		Diclofenac	p.o. 50mg concurrent	46 (Iqbal et al., 2009), a	-28 (Iqbal et al., 2009), a, d	
		Phenazopyridine	p.o. 200mg concurrent	29 (Marcelin-Jimenez et al., 2006), a		
Digoxin[f]	OATP4C1 (Mikkaichi et al., 2004), P-gp (Ohashi et al., 2006; Bentz et al., 2013)	Ritonavir	p.o. 300mg	86 (Ding et al., 2004), a	-42 (Ding et al., 2004), a	-35 (Ding et al., 2004), a
		Quinidine	p.o. 200mg qid		-64 (Ochs et al., 1981), a	
Famotidine	OAT3 (Motohashi et al., 2004; Tahara et al., 2005), OCT2 (Tahara et al., 2005), P-gp (Dahan and Amidon, 2009)	Probenecid	p.o. 1250mg before, 250mg concurrent	81 (Inotsume et al., 1990), a		-64 (Inotsume et al., 1990), a
Furosemide	OAT1 (Hasannejad et al., 2004), OAT3 (Hasannejad et al., 2004), MRP2 (Berginc et al., 2010; Lin et al., 2011)	Ibuprofen	p.o. 800mg tid, 3 days	36 (Paterson et al., 2011), a	-26 (Paterson et al., 2011), a	-23 (Paterson et al., 2011), a
		Probenecid	p.o. 1g single	168 (Vree et al., 1995), a	-65 (Vree et al., 1995), a, d	-66 (Vree et al., 1995), a
Hydrochlorothiazide	MRP4 (Hasegawa et al., 2007)	Valsartan	p.o. 160mg concurrent	355[h]	-78 (Jiang et al., 2011), b, d	
Metformin	OCT2 (Kimura et al., 2005a; Kimura et al., 2005b; Choi et al., 2007; Song et al., 2008a; Song et al., 2008b; Bachmakov et al., 2009; Zolk et al., 2009a; Zolk et al., 2009b; Chen et al., 2010; Meyer zu Schwabedissen et al., 2010; Konig et al., 2011; Kusuhara et al., 2011; Choi and Song, 2012), MATE1 (Tanihara et al., 2007; Ito et al., 2010; Meyer	Cimetidine	p.o. 400mg bid, 5 days	46 (Somogyi et al., 1987), a		-28 (Somogyi et al., 1987), a
		Cimetidine	p.o. 400mg bid, 6 days	54 (Wang et al., 2008), a	-51 (Wang et al., 2008), a, d	-45 (Wang et al., 2008), a
		Pyrimethamine	p.o. 50mg single	35 (Kusuhara et al., 2011), a		-35 (Kusuhara et al., 2011), a
		Trimethoprim	p.o. 200mg, bid, 6 days	37 (Grun et al., 2013), a	-27 (Grun et al., 2013), a, d	-32 (Grun et al., 2013), a

	zu Schwabedissen et al., 2010; Konig et al., 2011; Kusuhara et al., 2011), MATE2-K (Masuda et al., 2006; Tanihara et al., 2007; Ito et al., 2010; Kusuhara et al., 2011), P-gp (Hemauer et al., 2010)					
Olmesartan	OAT1 (Yamada et al., 2007), OAT3 (Yamada et al., 2007), MRP2 (Nakagomi-Hagihara et al., 2006), MRP4 (Yamada et al., 2007)	Pravastatin	p.o. 10mg concurrent	21 (Suwannakul et al., 2008), b	-20 (Suwannakul et al., 2008), b, d	-41 ~ -52 (Suwannakul et al., 2008), b
Pravastatin[g]	OAT3 (Takeda et al., 2004; Nakagomi-Hagihara et al., 2007a), OAT4 (Nakagomi-Hagihara et al., 2007a), MRP2 (Nakagomi-Hagihara et al., 2007b; Elsby et al., 2011)	Gemfibrozil	p.o. 1200mg for 3 days	102 (Kyrklund et al., 2003), a		-43 (Kyrklund et al., 2003), a
		Rifampicin	p.o. 600mg concurrent	364 (Maeda et al., 2011), a		-15 (Maeda et al., 2011), c
Ranitidine	OAT1 (Tahara et al., 2005), OAT3 (Tahara et al., 2005), OCT2 (Bourdet et al., 2005; Tahara et al., 2005), P-gp (Hellinger et al., 2012)	Cimetidine	p.o. 400mg opd, > 5 days	27 (van Crugten et al., 1986), a		- 25 (van Crugten et al., 1986), a
		Ketoconazole	p.o. 200mg qd, 5 days	74 (Machavaram et al., 2006), a		19 (Machavaram et al., 2006), c
Sitagliptin	OAT3 (Chu et al., 2007), OATP4C1 (Chu et al., 2007), P-gp (Chu et al., 2007)	Cyclosporine	p.o. 600mg single	29 (Krishna et al., 2007), b		No Change (Krishna et al., 2007)
		Gemfibrozil	p.o. 600mg bid, 3 days	60 (K et al., 2012), a	-40 (K et al., 2012), a, d	

[a.] $P < 0.05$; [b.] significance not provided; [c.] not significant; [d.] CL/F change; [e.] NDA 50-739; [f.] Only two representative studies were included; [g.] Only studies with CL_R change were included; [h.] calculated

* Studies with statistically insignificant changes in AUC, CL or CL_R were excluded. Drugs with no positive studies (AUC, CL or CL_R change > 25%) were excluded.

Table 2.4: Prediction of the %inhibition of renal transporters in DDI studies of 4 selected drugs and their AUC and CL_R change by inhibition of renal transporters.

Victim	Perpetrator	[I] (μM)	f_u (%)	$[I]_u$ (μM)	IC_{50} or K_i (μM)		$[I]_u/K_i$ or $[I]_u/IC_{50}$	Predicted % of Inhibition [b] (%)	Prediction using $[I]_u$		Observed	
									AUC ↑(%)	CL_R ↓(%)	AUC ↑ (%)	CL_R ↓(%)
Cefdinir	Probenecid	240 (Selen et al., 1982)	7.5 (Dayton et al., 1963; Vree et al., 1993)	18	OAT1	4.3 (Hill et al., 2002)	4.2	81	190.4	-74.1	113	-65
					OAT3	3.4 (Tahara et al., 2005)	5.3	84	215.3	-77.1		
Furosemide	Ibuprofen	320 (Paterson et al., 2011)	0.8 (Lockwood et al., 1983)	2.56	OAT1	1.38 (Nozaki et al., 2007)	1.9	66	93.1	-63.9	35.8	-22.9
					OAT3	5.11 (Nozaki et al., 2007)	0.5	33	32.9	-32.7		
					MRP2	930 ± 20 (El-Sheikh et al., 2007)	0.0027	0.27	1.6	-2.2		
	Probenecid	240 (Selen et al., 1982)	7.5 (Dayton et al., 1963; Vree et al., 1993)	18	OAT1	4.3 (Hill et al., 2002)	4.2	81	149.2	-79.2	167.9	-65.6
					OAT3	3.4 (Tahara et al., 2005)	5.3	84	166.1	-82.6		
					MRP2	42.2 (Horikawa et al., 2002)	0.43	30	28.7	-29.5		
Famotidine	Probenecid	360 (Selen et al., 1982)	7.5 (Dayton et al., 1963; Vree et al., 1993)	27	OAT3	3.4 (Tahara et al., 2005)	7.9	89	71.5	-56.5	81.1	-64.0
Metformin	Cimetidine	9.4 (Somogyi et al., 1987)	81 (Somogyi et al., 1980)	7.6	OCT2	147.1 ± 11.0 (Tsuda et al., 2009)	0.05	5	3.6	-3.5	46.2, 54.2	-28.3, -44.6
					MATE1	3.8 ± 0.8 (Ito et al., 2012)	2.0	71	94.2	-49		
					MATE2K	6.9 ± 2.3 (Ito et al., 2012)	1.1	52	61.6	-38.5		
	Pyrimethamine	3.5 ± 0.4 (Minzi et al., 2007)	6 (Rudy and Poynor, 1990)	0.21	OCT2	10 ± 2 (Kusuhara et al., 2011)	0.021	2	1.5	-1.5	35.3	-35.4
					MATE1	0.093 ± 0.011 (Kusuhara et al., 2011)	2.3	70	102.9	-51.3		
					MATE2K	0.059 ± 0.008 (Kusuhara et al., 2011)	3.6	78	132.3	-57.6		
	Trimethoprim	9.3 (Sturgill et al., 1999)	37 ± 5 (Goodman et al., 2011)	3.44	OCT2	60.0 ± 19.0 (Kimura et al., 2005b)	0.057	5	4.1	-4.0	36.8	-32.3
					MATE1	6.9 (Muller et al., 2013)	0.50	33	32.0	-24.5		
					MATE2K	0.66 (Muller et al., 2013)	5.21	84	156.7	-61.7		

Chapter 3. Atenolol Renal Secretion Is Mediated by Human Organic Cation Transporter 2 and Multidrug and Toxin Extrusion Proteins

Content of this chapter was published in Drug Metabolism and Disposition 43, 1872-81 (2015).

3.1 Introduction

Hypertension is a global health issue and a leading cause of cardiovascular disease, which contributes to 17 million deaths per year (WHO, 2011). In addition to lifestyle changes, drug therapy is indispensable in the management of hypertension. There are several classes of antihypertensive drugs and most patients need combination antihypertensive therapy in order to achieve blood pressure control (Melin, 2014). Furthermore, patients with comorbidities may take multiple medications, which could lead to potentially adverse drug-drug interactions (DDIs).

Atenolol is an important β blocker used alone or in combination to treat hypertension. It is also used to prevent angina and improve survival after a heart attack (Hernandez-Canero et al., 1972; Poirier and Lacourciere, 2012). Atenolol selectively blocks β1-adrenoceptors and reduces blood pressure mainly by decreasing cardiac output (Wadworth et al., 1991; Tabacova and Kimmel, 2002). Due to its hydrophilicity, atenolol does not pass through the blood–brain barrier thus avoiding various CNS side effects (Agon et al., 1991). Less than 5% of the absorbed atenolol dose is bound to plasma protein and it is almost exclusively eliminated by the kidney, with more than 95% of the absorbed dose excreted unchanged in the urine (Brown et al., 1976; Mason et al., 1979). The total body clearance of atenolol correlates well with renal function; and a dosage reduction is required in patients with impaired renal function (Agrawal et al., 2015). The reported renal clearance (~168 to mL/min) is larger than its glomerular filtration clearance

(GFR) (Mason et al., 1979; Goodman et al., 2011), suggesting that in addition to glomerular filtration, atenolol undergoes net tubular secretion. In the human kidney, tubular secretion of drugs is mediated by the coordinated function of a number of drug transporters located in the basolateral and apical membranes of renal proximal tubular cells (Morrissey et al., 2012). Two major secretion systems exist for organic cation and organ anion drugs. In human kidneys, circulating organic cations are first transported into renal tubular cells by the electrogenic basolateral organic cation transporter 2 (hOCT2) driven by the inside negative membrane potential. Once inside cells, organic cations are further secreted into the urine by the apical multidrug and toxin extrusion proteins 1-2 (hMATE1 and 2-K), which are proton/organic cation exchangers that use the inwardly-directed proton gradient in the nephron to drive efflux (Motohashi and Inui, 2013). Organic anion drugs, on the other hand, are first transported into tubular cells by the basolateral organic anion transporters 1 and 3 (hOAT1 and 3) (You, 2004; Burckhardt, 2012). Although hOAT1 and 3 are generally selective for negatively charged molecules, hOAT3 is also able to transport certain positively charged drugs such as cimetidine (Giacomini et al., 2010). Mechanisms of organic anion efflux at the apical membrane are less clear, and may involve multiple transporters including the multidrug resistance proteins 2 and 4.

Like many other β-blocker agents, atenolol has an oxypropanolamine group that is protonized at the secondary amine moiety. With a pKa of 9.6, atenolol primarily exists in the positively charged form at physiological pH (Martinez et al., 2000). Atenolol was previously shown to be a substrate of the organic anion transporting polypeptide 1A2 (hOATP1A2) (Kato et al., 2009). Intestinal OATPs are thought to play a role in atenolol oral absorption; and inhibition of intestinal OATPs by fruit juices has been proposed as the underlying mechanism of atenolol-fruit juice interactions in humans (Lilja et al., 2005; Jeon et al., 2013). In addition, there is also

evidence that atenolol may be transported by the drug efflux transporter P-glycoprotein (P-gp) (Augustijns and Mols, 2004; Wang et al., 2005).

Little is currently known regarding the involvement of drug transporters in renal handling of atenolol. Recently, Ciarimboli et al showed that hOCTs interact with several β-blockers and may also accept some β-blockers as substrates (Ciarimboli et al., 2013). Based on the physiochemical property of atenolol and known renal elimination mechanism of organ cations, we hypothesized that renal secretion of atenolol is mediated by the hOCT2/hMATEs pathway. The goal of this study is to elucidate the roles of hOCT2 and hMATE1/2-K in renal transport of atenolol. To this end, we first characterized the interaction of atenolol with major renal transporters hOCT2, hMATE1, hMATE2-K, hOAT1, and hOAT3 to identify transporters involved in renal handling of atenolol. Second, the detailed transport kinetics of atenolol was analyzed with identified transporters in conjunction with transporter protein quantification using a targeted LC-MS/MS proteomic approach. Finally, transporter-mediated unidirectional transport of atenolol was demonstrated in an *in vitro* model of organic cation renal secretion, hOCT2/hMATE1 double-transfected MDCK cells.

3.2 Materials and Methods

3.2.1 Materials.

[^{3}H]atenolol (3.3 Ci/mmol) and [^{14}C]metformin (98 mCi/mmol) were purchased from Moravek Biochemicals, Inc. (Brea, CA). [^{3}H]Estrone sulfate (ES) (50 Ci/mmol), [^{3}H]para-aminohippurate (PAH) (3 Ci/mmol) and [^{3}H]mannitol (20 Ci/mmol) were purchased from American Radiolabeled Chemicals, Inc. (St. Louis, MO). Nonradiolabeled compounds were purchased from Sigma-Aldrich (St. Louis, MO) and were of analytical grade. Synthetic signature peptides (Supplementary Table 1) for protein quantification were obtained from New

England Peptides (Boston, MA). The corresponding stable isotope labeled (SIL) internal standards, were obtained from Thermo Fisher Scientific (Rockford, IL). Cell culture media and reagents were purchased from Invitrogen (Carlsbad, CA).

3.2.2 Cell Culture.

Flp-In HEK293 cells stably transfected with transporters and pcDNA5/FRT vector were maintained in Dulbecco's modified Eagle's medium (high glucose) supplemented with 10% FBS, 2 mM L-glutamine, 100 U/ml penicillin, 100 μg/ml streptomycin, and 150 μg/ml hygromycin B. For better attachment of Flp-In 293 cells, cell culture plastic surfaces were coated with 0.01% poly-D-lysine in PBS. MDCK cells transfected with empty vectors or double-transfected with hOCT2 and hMATE1 were maintained in minimum essential medium supplemented with 10% FBS, 500 μg/ml G418, and 200 μg/ml hygromycin B. Cells were cultured in a 37 °C humidified incubator with 5% CO_2.

3.2.3 Generation of HEK293 Cell Lines Stably Expressing Transporters.

To generate HEK293 cell lines stably expressing various transporters at isogenic locations, the Flp-in system from Invitrogen was used as we previous described for hOCT3 (Duan and Wang, 2010). The same procedure was used to generate HEK293 cell lines stably expressing hOCT1, hOCT2, hMATE1, hMATE2-K, hOAT1 and hOAT3. The cDNAs encoding hOCT1 (*SLC22A1*) and hOCT2 (*SLC22A2*) were amplified from human liver and kidney mRNA by RT-PCR as previously described (Duan and Wang, 2010). The cDNAs encoding hOAT1 (*SLC26A6*) and hOAT3 (*SLC26A8*) were previously developed in our laboratory (Li et al., 2006a). The hMATE1 (*SLC47A1*) plasmid was purchased from GE Dharmacon (Lafayette, CO); and hMATE2-K plasmid was kindly provided to us by Dr. Kazuo Matsubara at Kyoto University, Japan (Masuda et al., 2006). The insert encoding a transporter was then subcloned

into the pcDNA5/FRT vector by PCR amplification, restriction enzyme digestion and ligation. The cDNA sequences of all inserts were verified by DNA sequencing and compared with National Center for Biotechnology Information reference genes (BC126364.1 for hOCT1, BC039899.1 for hOCT2, NM_153276.2 for hOAT1, NM_004254.3 for hOAT3, NM_018242.2 for hMATE1, and NM_001099646.1 for hMATE2-K) to ensure fidelity. The constructs were then co-transfected with pOG44 Flp-Recombinase Expression Vector (Invitrogen, Carlsbad, CA) into the Flp-In HEK293 cells. Transfected cells were selected by hygromycin B (150 μg/ml) and expanded. The pcDNA5/FRT empty vector was also co-transfected with pOG44 into the Flp-In HEK293 cells to serve as control cells.

3.2.4 Generation of hOCT2/hMATE1 Double-transfected MDCK Cells.

hOCT2/hMATE1 MDCK cells were generated through double-transfection, followed by antibiotic selection and activity screening. The hOCT2 and hMATE1 pcDNA5/FRT constructs were developed as described above. The full-length cDNA encoding hOCT2 was then subcloned into the pcDNA3.1+ mammalian expression vector (Life Technologies). The cDNA encoding hMATE1 was then subcloned into pcDNA3.1/Hygro(+) expression vector. The new constructs were co-transfected at 1:1 molar ratio into MDCK cells. Transfected cells were selected by G418 (500 μg/ml) and hygromycin B (200 μg/ml) for 3-4 weeks. Colonies with normal cellular morphology and growth rate were isolated and expanded. The cell colonies were screened in functional transport assays by determining B-to-A and A-to-B permeability of [^{14}C]metformin as described below. Tight junction formation in transfected MDCK monolayers was assessed by measuring permeability of [^{3}H]mannitol. A colony with the highest metformin B-to-A/A-to-B ratio but low and similar B-to-A and A-to-B mannitol permeability was selected and used in transport studies. A control cell line co-transfected with empty pcDNA3.1+ and

pcDNA3.1/Hygro(+) vectors at 1:1 molar ratio was obtained using similar transfection and selection procedures.

3.2.5 Uptake and Inhibition Assays in HEK293 Cells.

The assays were performed as previously described (Duan and Wang, 2010) with some modifications. Control cells and transporter-expressing cells were seeded in poly-D-lycine-coated 24-well plates and allowed to grow for 2 to 3 days to reach 80-90% confluence. Uptake assays were performed at 37 °C in KRH buffer (5.6 mM glucose, 125 mM NaCl, 4.8 mM KCl, 1.2 mM KH_2PO_4, 1.2 mM $CaCl_2$, 1.2 mM $MgSO_4$, and 25 mM HEPES) containing cold substrates and trace amounts of radiolabeled substrates. For uptake studies in hMATE1- and hMATE2-K-expressing cells, KRH buffer was adjusted to pH 8.0 to generate an outwardly directed proton gradient since these transporters function as proton/organic cation exchangers (Otsuka et al., 2005). For all other transporters, uptake was performed at pH 7.4. After incubating the cells with a substrate for a specified time, uptake was terminated by washing cells three times with ice-cold KRH buffer. Cells were then solubilized with 0.5 ml 1 M NaOH at 37 °C for 2 hrs and neutralized with 0.5 ml 1 M HCl. Radioactivity of cell lysates was measured by a liquid scintillation counter (PerkinElmer, Tri-Carb B3110TR, Waltham, MA). For atenolol inhibition studies, uptake was performed in the presence of atenolol (500 μM). Protein content in the lysates was measured by the BCA Protein Assay Kit (Pierce Chemical, Rockford, IL) and the uptake in cells was normalized to their protein concentrations. Transporter-specific uptake was calculated by subtracting the background uptake in control cells.

3.2.6 Atenolol Inhibition Study Using A Fluorescent Substrate.

ASP+ is a fluorescent analog of the MPP+ that has been used as a probe substrate to determine ligand-transporter interaction using fluorescence based assays (Mason et al., 2005).

Uptake was performed with an ASP+ cocktail (2 μM ASP+ and 10 μM trypan blue in KRH buffer) using a previously described procedure (Ahlin et al., 2008; Duan et al., 2015). pcDNA5 control cells and transporter-expressing cells were seeded in poly-D-lycine-coated 96-well plates and grown for 48 hrs until approximately 90% confluence. The experiment was initiated by incubating cells with the ASP+ cocktail at 37 °C and relative fluorescence unit (RFU) was measured immediately (time 0) and at various time points (5, 10 and 15 min) using a PerkinElmer Wallac 1420 Multilabel Counter (Waltham, MA) with excitation/emission wavelengths of 475 nm/609 nm. Specific uptake was calculated by subtracting the RFU at time 0 from the RFU at the end point ($RFU_{end} - RFU_0$). ASP+ uptake were measured at various times to determine the initial uptake range; and a time point within the linear range was chosen as the time point for inhibition studies. For inhibition studies with atenolol stereoisomers, the cells were pre-incubated with each isomer and uptake was performed in the presence of the stereoisomers at varying concentrations.

3.2.7 Transport Studies in hOCT2/hMATE1 Double-transfected MDCK Cells.

Atenolol flux across MDCK monolayer expressing hOCT2/hMATE1 was determined using a previously described protocol with some modifications (Muller et al., 2013). MDCK cells were seeded on Falcon™ cell culture inserts at a density of 2 x $10^5/cm^2$. Five days after seeding, transport experiments were performed. After removing culture medium from both sides of the inserts, cells were pre-incubated for 10 min at 37 °C in KRH buffer with pH adjusted to pH 6.0 and 7.4 respectively at the apical and basal chamber. For apical-to-basal (A-to-B) transport, 2 ml of KRH buffer (pH 7.4) was added to the basal chamber, and transport was initiated by adding 0.8 ml of KRH buffer (pH 6.0) containing [^{3}H]atenolol (1 μM) to the apical chamber. For basal-to-apical (B-to-A) transport, 0.8 ml of KRH buffer (pH 6.0) was added to

the apical chamber and 2 ml of KRH buffer (pH 7.4) containing [^{3}H]atenolol (1 μM) was added to the basal chamber. The use of an apical pH of 6.0 was based on the average urine pH of 6.3 as well as previously published methods by other groups (Tsuda et al., 2009; Roland and Tozer, 2010; Muller et al., 2011). To measure transcellular transport, an aliquot of the incubation medium (100 μl from the basal chamber, 50 μl from the apical chamber) in the receiving chamber was periodically collected and replaced with equal volume of fresh buffer. At the end of the transport study, intracellular drug accumulation was measured by rinsing inserts three times with ice-cold KRH buffer (pH 7.4) followed by cell lysis with 1 M NaOH and then neutralization with 1 M HCl. The radioactivity of the collected medium and cell lysate was determined by a liquid scintillation counter (PerkinElmer, Tri-Carb B3110TR, Waltham, MA). Protein concentrations in cell lysate were measured by a BCA Protein Assay Kit (Pierce Chemical, Rockford, IL). The tightness of the MDCK monolayer was verified by measuring [^{3}H]mannitol permeability and transepithelial electrical resistance (TEER) using a Millicell-ERS system (Millipore Corporation, Bedford, MA) before and after each experiment to ensure monolayer integrity. Data generated in MDCK cells with TEER value < 180 Ω·cm^2 were not accepted.

3.2.8 Membrane Protein Preparation and LC-MS/MS Quantification of Transporter Protein.

Total membrane proteins were prepared from transporter-transfected HEK 293 cells and MDCK cells using the ProteoExtract Native Membrane Protein Extraction Kit (Calbiochem/EMD Millipore, San Diego, CA). The total membrane protein concentration was determined by the BCA Protein Assay Kit (Pierce Chemical, Rockford, IL). To quantify the membrane transporter protein in each cell line, an LC-MS/MS proteomic approach (Lee et al.,

2013; Prasad and Unadkat, 2014) was used. Agilent 6460A Triple Quadrupole Mass Spectrometer coupled to Agilent 1290 Infinity LC system (Agilent Technologies, Santa Clara, CA) operated in ESI positive ionization mode was used for LC-MS/MS analysis of the peptides (Table 3.1). Approximately 1.5 µg or less of the trypsin digest (5 µl) was injected onto the column (Kinetex™ 2.6 µm, C18, 100 x 3 mm, Phenomenex, Torrance, CA) and eluted at 0.3 ml/min. The mobile phase gradient conditions were 97% A (0.1% v/v formic acid) and 3% B (acetonitrile containing 0.1% v/v formic acid) held for 2.5 min, followed by three steps of linear gradient of mobile phase B concentrations of 3% to 8%, 8% to 21%, and 21% to 30%. 30% mobile phase B was maintained for 2 min. This was followed by the washing step using 80% mobile phase B for 1.6 min and re-equilibration for 3.3 min. The doubly/triply charged parent to singly charged product transitions for the analyte peptides and their respective SIL peptides were monitored using optimized LC-MS/MS parameters (Table 3.1). The data were processed by integrating the peak areas generated from the reconstructed ion chromatograms for the analyte peptides and the respective SIL internal standards using the MassHunter software V (Agilent Technologies, Santa Clara, CA).

3.2.9 Data Analysis.

All uptake experiments were performed in triplicates and repeated at least two times. Data were presented as mean ± SD ($n \geq 3$). The transport kinetics data were fitted through nonlinear regression using GraphPad Prism 6.0 (GraphPad Software, Inc, La Jolla, CA). The K_m and V_{max} values were obtained by fitting the Michaelis-Menten equation $V = V_{max}*S / (K_m + S)$ to the data, where V is the velocity of uptake, V_{max} is the maximum velocity of uptake, S is the substrate concentration, and K_m is the Michaelis-Menten constant. In addition, kinetic data fitting was also performed using a Michaelis-Menten equation plus a diffusional component.

The transporter turnover number (k_{cat}) was obtained by normalizing V_{max} to the amount of transporter protein quantified. The IC_{50} values were obtained by fitting data with log (inhibitor concentration) versus normalized response using the equation: V = Bottom + (Top - Bottom) / [1 + $(I/IC_{50})^{nH}$], where "V" is the rate of uptake in the presence of inhibitor, "Bottom" is the residual noninhibitable baseline value, "Top" is the rate of uptake in the absence of inhibitor, "I" is the inhibitor concentration, and "nH" is the Hill coefficient. For transport experiments, under the assumption that the substrate concentration at the donor side is constant, the apparent permeability (P_{app}) of compounds across cell monolayers was calculated as P_{app} = (dQ/dt) / ($A*C_0$), where Q is the amount of compound transported over time t, A is the insert membrane surface area, and C_0 is the initial compound concentration in the donor chamber. Statistic analysis was performed using unpaired Student's *t* test and a P value less than 0.05 was considered statistically significant.

3.3 Results

3.3.1 Functional Validation of Transporter-expressing Cell Lines.

The HEK293 cell line, which has negligible expression of endogenous organic cation and anion transporters (Ahlin et al., 2009), was used to generate various stable cell lines expressing major organic solute transporters using the Flp-in system. To assess the activity of the expressed transporters, uptake of a probe substrate was measured in both pcDNA5 (control) and transporter-expressing cell lines. Metformin was used for hOCT1-3 and hMATE1/2-K; PAH was used for hOAT1; and ES was used for hOAT3. Compared with the control cells (Figure 3.1), significantly enhanced uptake activity was observed for all transporter-expressing cells, demonstrating that all transporters are functionally expressed in the HEK293 cell lines used in this study.

3.3.2 Inhibitory Effect of Atenolol on Selected Drug Transporters.

To determine if atenolol interacts with hOCT1, hOCT2, hOCT3, hMATE1, hMATE2-K, hOAT1, and hOAT3, the uptake of a probe substrate in the presence and absence of atenolol (500 μM) was measured in both control and transporter-expressing cells. The uptake in the presence of atenolol was expressed as a percentage of the specific uptake in the absence of atenolol. As shown in Figure 3.2, atenolol at 500 μM inhibited hOCT1, hMATE1, and hMATE2-K by about 70%. Less but significant inhibition was also observed for hOCT2, hOAT1 and hOAT3. hOCT3 showed no interaction with atenolol.

3.3.3 Uptake of Atenolol by Selected Drug Transporters.

To determine if atenolol is a substrate of the seven selected transporters, uptake of ^{3}H-labeled atenolol (1 μM) was measured in both control cells and transporter-expressing cells. Compared to vector-transfected cells, atenolol uptake was significantly increased in cells expressing hOCT1, hOCT2, hMATE1 and hMATE2-K (Figure 3.3). Cells expressing hOCT2 and hMATE1 showed the highest uptake activity towards atenolol. In contrast, no significant uptake of atenolol was observed in cells expressing hOCT3, hOAT1 or hOAT3.

3.3.4 Atenolol Uptake Kinetics by hOCT1 and hOCT2.

To determine the kinetics of atenolol uptake by hOCT1 and hOCT2, time-dependent uptake of atenolol (1 μM) was performed in KRH buffer (pH7.4) at 37 °C. Uptake in hOCT1- and hOCT2-expressing cells was linear up to 15 and 5 min respectively (Figure 3.4A and 3.4B). Concentration-dependent uptake was then performed at 2 min incubation time and specific uptake was obtained by subtracting uptake in control cells. hOCT1- and hOCT2-specific atenolol uptake was saturable, and the K_m values derived from nonlinear regression fitting to the Michaelis-Menten equation were 128 ± 16 and 280 ± 41 μM, respectively (Figure 3.4C and

3.4D, Table 3.2). The Eadie-Hofstee plots were consistent with single-enzyme kinetics (Figure 3.4C and 3.4D insets). In addition, we also fitted the kinetic data by adding a first order diffusional component to the Michaelis-Menten equation. The resulting K_m and V_{max} values were essentially the same since diffusion was negligible due to subtraction of uptake in vector-transfected cells (Table 3.3).

3.3.5 Atenolol Uptake Kinetics by hMATE1 and hMATE2-K.

Atenolol transport kinetics towards the renal efflux transporters hMATE1 and hMATE2-K was determined using uptake assays in KRH buffer at pH 8.0 to provide an outwardly directed proton gradient. This method has been used previously to measure the transport kinetics for the MATE transporters (Otsuka et al., 2005; Muller et al., 2013). Uptake increased progressively till 15 min but declined at 30 min in both hMATE1 and hMATE2-K transfected cells (Figure 3.5A and 3.5B), probably due to the dissipation of the proton gradient with time. Because uptake was linear within 2 min, concentration-dependent uptake was performed at 2-min. hMATE1- and hMATE2-K-mediated atenolol uptake was saturable (Figure 3.5C and 3.5D) with the K_m and V_{max} values shown in Table 3.2 and Table 3.3. Compared to hOCT2, hMATE1 and 2-K showed 4-9 fold higher affinity towards atenolol.

3.3.6 Transporter Quantification and Turnover Number (k_{cat}) Determination.

To determine atenolol transport efficiency at the single transporter level, we quantified transporter protein expression levels in membrane fractions prepared from transfected HEK293 cell lines using targeted LC-MS/MS proteomics. The hOCT1, hOCT2, hMATE1 and hMATE2-K expression in HEK293 cell lines varied within 4 fold and the protein levels for each transporter are shown in Table 3.4. The transporter turnover number (k_{cat}), which is the maximum number of substrate that can be transported during a transport cycle, was calculated by normalizing V_{max}

to the number of transporters determined (Table 3.4). When single transporter efficiency (k_{cat}/K_m) was compared, hOCT2 and hMATE1 showed similar transport efficiency for atenolol. hOCT1 and hMATE2-K had similar transport efficiencies, which were about three time higher than those of hOCT2 and hMATE1.

3.3.7 Inhibition of hOCT1, hOCT2, hMATE1, and hMATE2-K by R- and S- Atenolol.

Like many other beta blockers, atenolol has two stereoisomers. To evaluate if R- and S-atenolol have different affinities toward hOCT1, hOCT2, hMATE1, and hMATE2-K, the inhibitory effects of R- and S- atenolol on these transporters were determined using a rapid fluorescent substrate uptake assay. As shown in Figure 3.6 and Table 3.5, the IC_{50} values of R- and S- atenolol for all four transporters were very similar with less than 25% difference, suggesting that hOCT1, hOCT2, hMATE1, and hMATE2-K have little steroselectivity for R- and S- atenolol.

3.3.8 Establishment of A hOCT2/hMATE1 Double-transfected MDCK Cell Line.

Double transfected MDCK cells stably expressing hOCT2/hMATE1 were previously shown as a useful model to elucidate vectorial transport pathway for organic cations (Sato et al., 2008; Konig et al., 2011). To demonstrate unidirectional transcellular transport of atenolol, we generated a MDCK cell line stably expressing hOCT2 and hMATE1. The membrane expression of hOCT2 and hMATE1 in these cells was quantified using LC-MS/MS. The hOCT2 and hMATE1 protein levels determined were 28.6 and 6.9 fmol/μg membrane protein, respectively. We then evaluated the barrier properties of the double transfected cells by measuring TEER and transcellular transport of mannitol, a model compound for paracellular diffusion. The flux of mannitol was very low and similar in both B-to-A and A-to-B directions in double-transfected and control cells (Figure 3.7A and 3.7B). There was no statistical difference in mannitol

transport between B-to-A and A-to-B directions at all time-points except the last sampling point (120 min). However, the difference at 120 min was very small and showed an opposite direction in vector and hOCT2/hMATE1-transfected cells. The calculated mannitol permeability was about 1.6 x 10^{-6} cm/s, which is in the reported range of 0.4 – 3.5 x 10^{-6} cm/s in polarized MDCK monolayer culture (Avdeef, 2010). The measured TEER values were between 180-200 $\Omega \cdot cm^2$, which is also within the reported range (Dukes et al., 2011). These data suggest proper formation of tight junctions and good integrity of barrier function in our transfected cell lines. The B-to-A transport of metformin, a widely used probe substrate for organic cation transporters, was much greater (up to 65-fold at 120 min) than A-to-B transport in the hOCT2/hMATE1 double transfected cells (Figure 3.7C). The B-to-A/A-to-B ratio at 30 min was estimated to be 56, which is similar to what was reported by Sato et al (Sato et al., 2008). In contrast, control cells showed much lower metformin transport in both directions and there was little difference between A-to-B and B-to-A flux (Figure 3.7D).

3.3.9 Transcellular Transport of Atenolol in hOCT2/hMATE1-transfected MDCK Cells.

To determine the role of hOCT2 and hMATE1 in unidirectional transport of atenolol, time-dependent flux of [^{3}H]atenolol was examined using hOCT2/hMATE1-transfected MDCK cells. Transport studies were performed under pH gradient conditions (apical pH 6.0 and basal pH 7.4) based on physiological conditions. As shown in Figure 3.8A, transport of atenolol in the B-to-A direction was much greater than in the A-to-B direction in double transfected cells. In contrast, transport of atenolol in the vector-transfected control cell was much slower in both directions and was only slightly higher in B-to-A direction (Figure 3.8B). Although MDCK cells have generally negligible expression of many endogenous drug transporters, low expression of canine P-gp and Oct2 were reported (Shu et al., 2001; Kuteykin-Teplyakov et al., 2010). The

slightly higher transport of atenolol in the B-to-A direction in the control cells is probably due to the expression of endogenous transporters, which may also accept atenolol as a substrate. In both control and hOCT2/hMATE1 cells, the atenolol flux rate was constant over 120 min. Based on the time course, atenolol permeability was subsequently calculated and shown in Figure 3.8C. In hOCT2/hMATE1-transfected cells, the atenolol B-to-A/A-to-B permeability ratio was 27 whereas that in control cells was only 2. The overall permeability of atenolol in the B-to-A direction was 44-fold higher in hOCT2/hMATE1-transfected cells than in control cells. Intracellular accumulation of atenolol was measured at the end of the transport study. The hOCT2/hMATE1-transfected cells showed higher intracellular accumulation than control cells in both directions; and the B-to-A accumulation was higher than A-to-B in both cells lines (Figure 3.8D).

3.4 Discussion

Despite a critical role of the kidney in atenolol disposition, the molecular mechanisms involved in renal handling of atenolol have not been well understood. In this study, we characterized the interaction of atenolol with major renal drug transporters and showed that atenolol is an excellent substrate for hOCT2, hMATE1 and hMATE2-K in single transfected HEK cells. In addition, atenolol is an inhibitor but not a substrate for hOAT1 and hOAT3. Using double-transfected MDCK monolayer culture, we further demonstrated unidirectional transepithelial flux of atenolol mediated by hOCT2/hMATE1. Together, our data suggest that the tubular secretion of atenolol in the kidney is mediated by the hOCT2/hMATEs secretion pathway, as depicted in Figure 3.9.

While atenolol interacted with both organic cation and anion transporters, it was only transported by hOCT1, hOCT2, hMATE1 and hMATE2-K (Figures 3.2 and 3.3), consistent with

the drug carrying a positive charge at physiological pH. Detailed kinetic analysis coupled with absolute quantification of transporter protein levels provided further insights into transport efficiencies for individual transporters towards atenolol. While atenolol is an excellent substrate for hOCT1, hOCT2, hMATE1, and hMATE2-K (Figure 3.3, 3.4, 3.5 and Table 3.2, 3.4), hMATE1 appears to transport atenolol with a high affinity but low capacity. In contrast, hOCT2 appeared to be a high capacity and low affinity transporter for atenolol (Tables 3.2). However, the calculated single transporter transport efficiency (k_{cat}/K_m) was similar for hOCT2 and hMATE1 (Table 3.4), whereas hOCT1 and hMATE2-K appeared to be 2-3 fold more effective. In the human kidney, tubular secretion of organic cation is mediated by the sequential action of the basolateral hOCT2 and the apical hMATE1 and 2K. Under non-saturable conditions such as those commonly seen in clinical settings, the total transporter-mediated clearance at each membrane domain will be determined by the product of transport efficiency and transporter protein level (i.e. k_{cat}/K_m x E_{total}). The step with lower transport clearance will be rate-limiting and will determine if there is intracellular accumulation of the substrate. In our hOCT2/hMAT1 double-transfected MDCK cell model, the hOCT2 and hMATE1 protein levels determined by LS-MS/MS were 28.6 and 6.9 fmol/μg membrane protein, respectively. The predicted hOCT2-mediated basolateral and hMATE1-mediated apical clearance is 17.0 and 5.3 μl/min/μg membrane protein respectively, suggesting that hMATE1-mediated apical efflux is the rate-limiting step in atenolol secretion in our *in vitro* model. Indeed, the much higher intracellular accumulation of atenolol in hOCT2/hMATE1 cells (Figure 3.8D) is consistent with our prediction. Currently, the protein expression levels for hOCT2, hMATE1 and hMATE2-K in the human kidney proximal tubule are unknown. If these data become available, it might be possible to predict transporter clearance and the rate-limiting step in atenolol renal secretion *in vivo* based

on individual transporter expression levels and single transporter kinetics of atenolol determined in our study (Table 3.4). In addition, given the structural similarity of atenolol to other β-blockers, it is reasonable to suspect that the hOCT2/hMATEs secretion pathway may also be involved in renal handling of other hydrophilic β-blockers.

hOCT2 is one of the seven drug transporters currently recommended by the US Food and Drug Administration (FDA) and the International Transporter Consortium (ITC) for evaluation of potential drug interaction risk during drug development (FDA, 2012). hMATE1 and hMATE2-K were recently identified by the ITC as emerging transporters of clinical importance in pharmacokinetics and drug–drug interactions in humans (Hillgren et al., 2013). Metformin, a well-established substrate for hOCTs and hMATES, is currently recommended by the FDA as the probe substrate for *in vivo* renal DDI studies for hOCT2 (FDA, 2012). Interestingly, metformin and atenolol share a number of similarities in their physiochemical and pharmacokinetic characteristics (Table 3.6). Both atenolol and metformin are small hydrophilic cations at physiological pH. Atenolol and metformin have similar bioavailabilities (40-60%) and large distributional volumes (Kirch and Gorg, 1982; Scheen, 1996). Both drugs are not protein bound and exclusively eliminated by the kidney unchanged. Our data demonstrated that similar to metformin, atenolol is actively secreted by hOCT2/hMATEs pathway (Figures 3.7 and 3.8). Our data revealed that atenolol is an excellent substrate for hOCT2 and hMATE1/2-K (Figure 3.3 and 3.4) and achieved a B-to-A/A-to-B ratio comparable to metformin in our hOCT2/hMATE1 transfected MDCK cells (Figure 3.7 and 3.8). However, the renal clearance of atenolol (~168 to mL/min) is only 1.4 fold of GFR (120 mL/min), which is about 3-fold lower than the renal clearance of metformin (Mason et al., 1979; Pentikainen et al., 1979). It is possible that atenolol is efficiently secreted by hOCT2/hMATEs but undergoes substantial

reabsorption in the nephron tubules. Metformin, on the other hand, is much less reabsorbed in the nephron. Atenolol is less hydrophilic than metformin (Log $D_{7.4}$ -2.0 versus -5.5) and has a smaller faction of protonization (pKa 9.6 for atenolol and 12.4 for metformin). Thus, atenolol may undergo passive back diffusion (reabsorption) to a larger extent than metformin in the nephrons. Compared to metformin, few studies reported positive atenolol interactions with prototype renal organic cation transport inhibitors (e.g. cimetidine). This is also likely due to a smaller contribution of secretion clearance to total renal clearance of the drug. Nevertheless, the efficient transport of atenolol by hOCT2 and hMATEs *in vitro* and its lower *in vivo* DDI risk suggest that atenolol may be a useful and clinically relevant substrate for hOCT2 and hMATE1/2-K substrate.

Like many β-blockers, atenolol is dosed as two enantiomers. Because radio-labeled R- or S- isomers are not available, we performed inhibition studies with each stereoisomer. Our data suggest that hOCT1, hOCT2, hMATE1, and hMATE2-K do not exhibit pronounced stereoselectivity toward atenolol enantiomers (Figure 3.6, Table 3.5). Our *in vitro* data are in agreement with clinical observations showing little to very small difference in the renal clearance of R- and S- atenolol (Boyd et al., 1989; Mehvar et al., 1990). To date, very few studies reported stereoselective interaction of organic cations with hOCTs or hMATEs (Zhou et al., 2014). Gross and Somogyi previously evaluated the interaction of the stereoisomers of chiral basic drugs with the uptake of [^{14}C]tetraethylammonium in rat renal membrane vesicles. No differences were observed for many enantiomers (Gross and Somogyi, 1994). Small difference was observed only when the center of chirality is adjacent to the basic functional group (Gross and Somogyi, 1994). This is not the case for atenolol as its chiral center is separated from the amine group by one carbon length.

In contrast to a previous study that indicated no transport of atenolol by hOCT1 (Ciarimboli et al., 2013), our data clearly demonstrated that atenolol is an excellent substrate of hOCT1 (Figure 3.3, 3.4 and Table 3.2, 3.4). The role of hOCT1 in atenolol disposition is currently unclear. hOCT1 is mainly expressed in the sinusoidal membrane of hepatocytes (Giacomini et al., 2010), and also found in small intestine (Koepsell et al., 2007). Therefore, this transporter may play a role in oral absorption and tissue distribution of atenolol. Interestingly, several case reports have been described liver injury associated with atenolol use (Schwartz et al., 1989; Yusuf and Mishra, 1995; Dumortier et al., 2009). It would be reasonable to suspect an involvement of hepatic organic cation transporters (e.g. hOCT1, hMATE1) in atenolol disposition and toxicity in the liver. In addition, atenolol has been reported to be a substrate of OATP1A2 and P-gp (Augustijns and Mols, 2004; Wang et al., 2005; Kato et al., 2009). Therefore, these transporters could also influence atenolol disposition and pharmacokinetics *in vivo*.

In summary, we showed that atenolol is an excellent substrate for the renal organic cation transporters hOCT2, hMATE1 and hMATE2-K and that atenolol tubular secretion is mediated by the hOCT2/hMATEs secretion pathway. Our studies elucidated the molecular mechanisms involved in renal handling of atenolol and established the importance of organic cation transporters in transport and disposition of an important antihypertensive drug. Finally, our data suggest that atenolol could be used as a clinically relevant probe substrate for assessing hOCT1/2 and hMATE1/2-K function *in vitro* and *in vivo*.

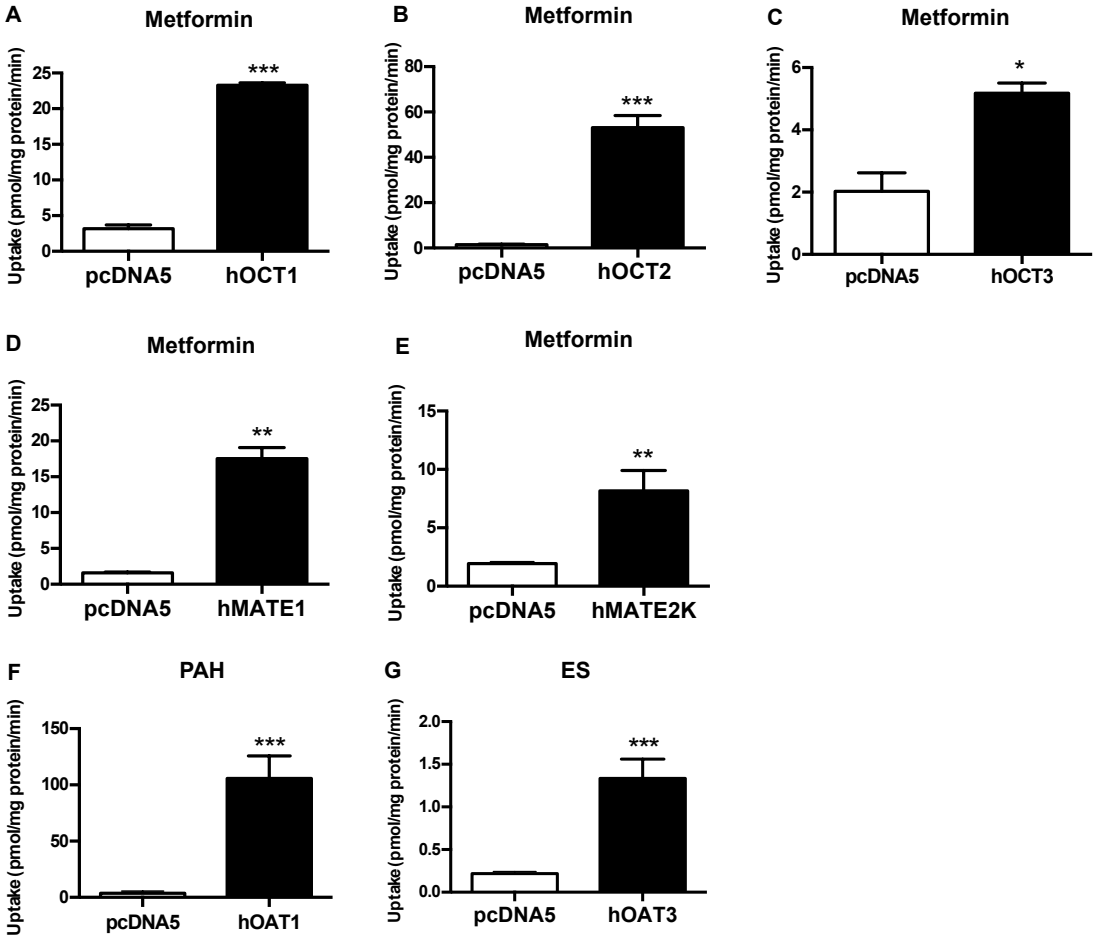

Figure 3.1 Functional characterization of HEK293 cells stably expressing selected drug transporters. The uptake of probe substrate for each drug transporter was measured in both transporter-transfected and pcDNA5-transfected control HEK293 cells. **(A) - (C)**: uptake of 6.1 μM metformin for 2 min by hOCT1, hOCT2, and hOCT3. **(D)** and **(E)**: uptake of 6.1 μM metformin for 5 min by hMATE1 and hMATE2-K. **(F)**: uptake of 2 μM PAH for 2 min by hOAT1. **(G)**: uptake of 0.06 μM ES for 2 min by hOAT3. Data are presented as mean ± SD. Uptake in transporter-expressing cells were compared with that in control cells, *** $P < 0.001$, ** $P < 0.01$, * $P < 0.05$.

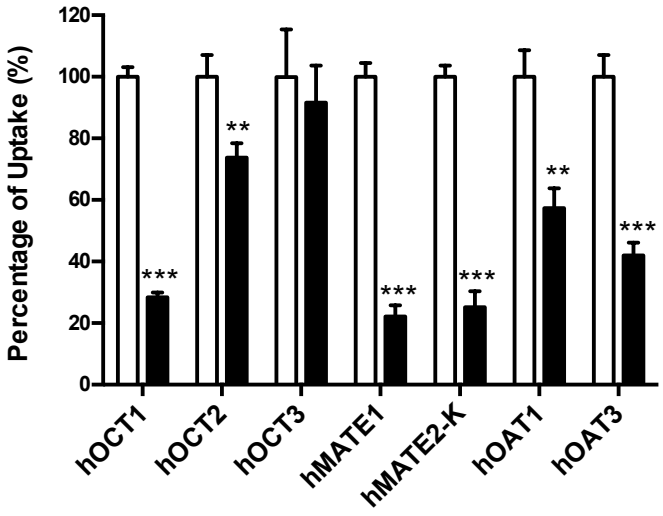

Figure 3.2 Inhibitory effect of atenolol on the uptake of probe substrates by selected drug transporters. Uptake of 6.1μM metformin by hOCT1, hOCT2, hOCT3, hMATE1, and hMATE2-K, 2 μM PAH by hOAT1, and 0.06 μM ES by hOAT3 in the absence and presence of 500 μM atenolol was measured in both transporter-expressing and control HEK293 cells. Transporter-specific uptake was obtained by subtracting the uptake in control cells from the uptake in transporter-expressing cells. The uptake in the absence of atenolol (□) was set as 100 percent. The uptake in the presence of atenolol (n) was expressed as a percentage of the uptake in the absence of atenolol. The uptake was measured after a 2 min incubation at 37 °C. Data are presented as mean ± SD. Uptake in the presence of atenolol was compared with that in the absence of atenolol (*** $P < 0.001$, ** $P < 0.01$).

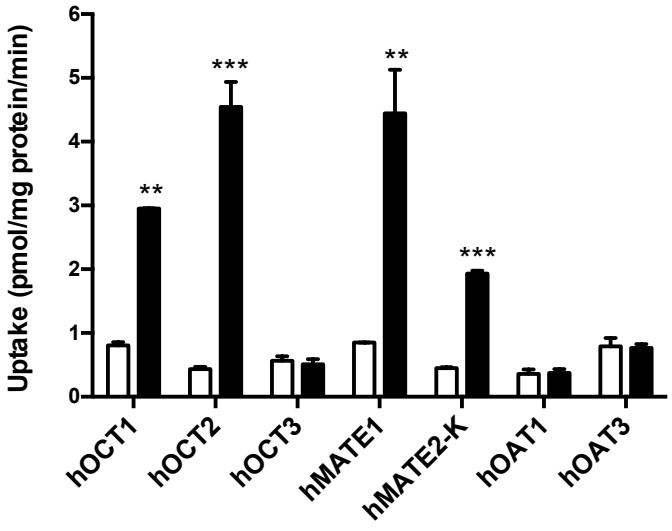

Figure 3.3 Uptake of atenolol by selected drug transporters. The uptake of 1 μM atenolol in transporter-expressing (black) and control (empty) HEK293 cells was measured. The uptake was measured after a 2 min incubation at 37 °C. Data are presented as mean ± SD. Uptake in transporter-expressing cells was compared with that in control cells (*** $P < 0.001$, ** $P < 0.01$).

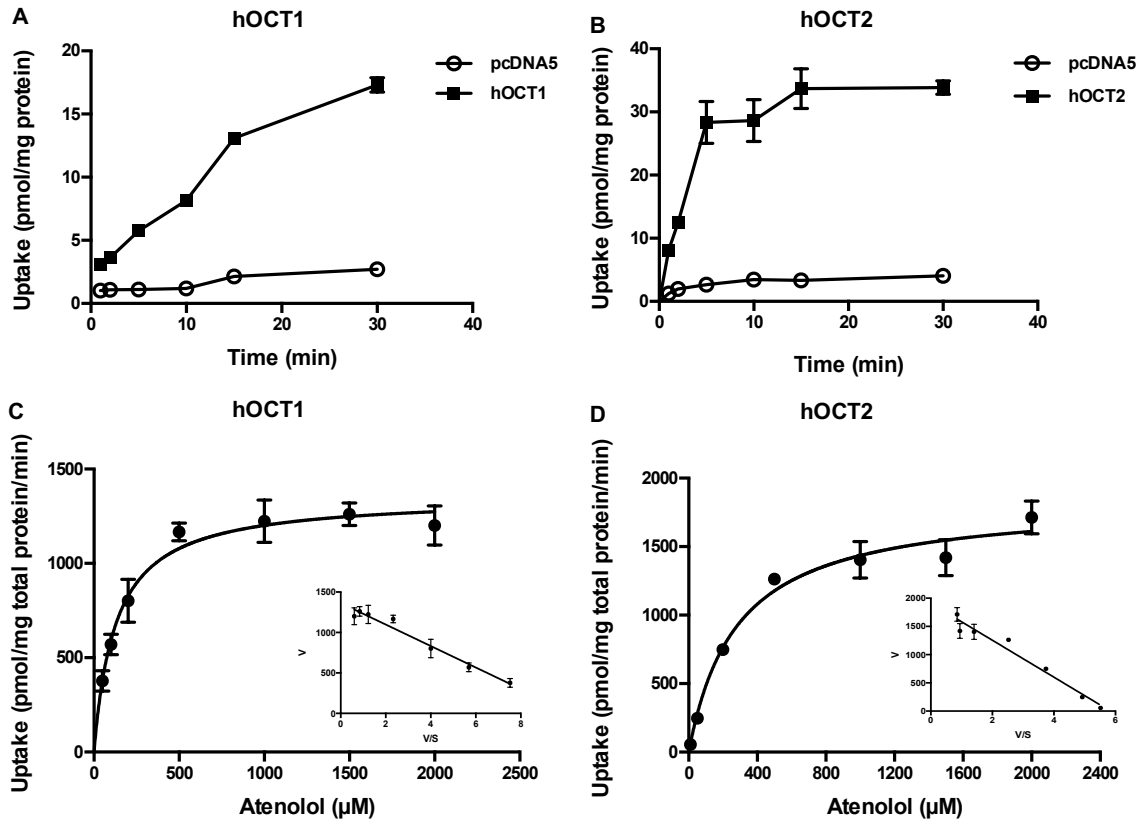

Figure 3.4 Atenolol uptake kinetics by hOCT1 and hOCT2. The uptake of 1 μM atenolol was measured in control and transporter-expressing HEK293 cells at specified time points (3A and 3B). Concentration-dependent uptake of atenolol was measured in both transporter-expressing and control HEK293 cells after a 2 min incubation at 37 °C (3C and 3D). Transporter-specific uptake was obtained by subtracting the uptake in control cells from the uptake in transporter-expressing cells. The Michaelis-Menten equation was fit to the data using nonlinear regression. . The insets are Eadie-Hofstee transformation of the kinetics data. Each data point represents mean ± SD.

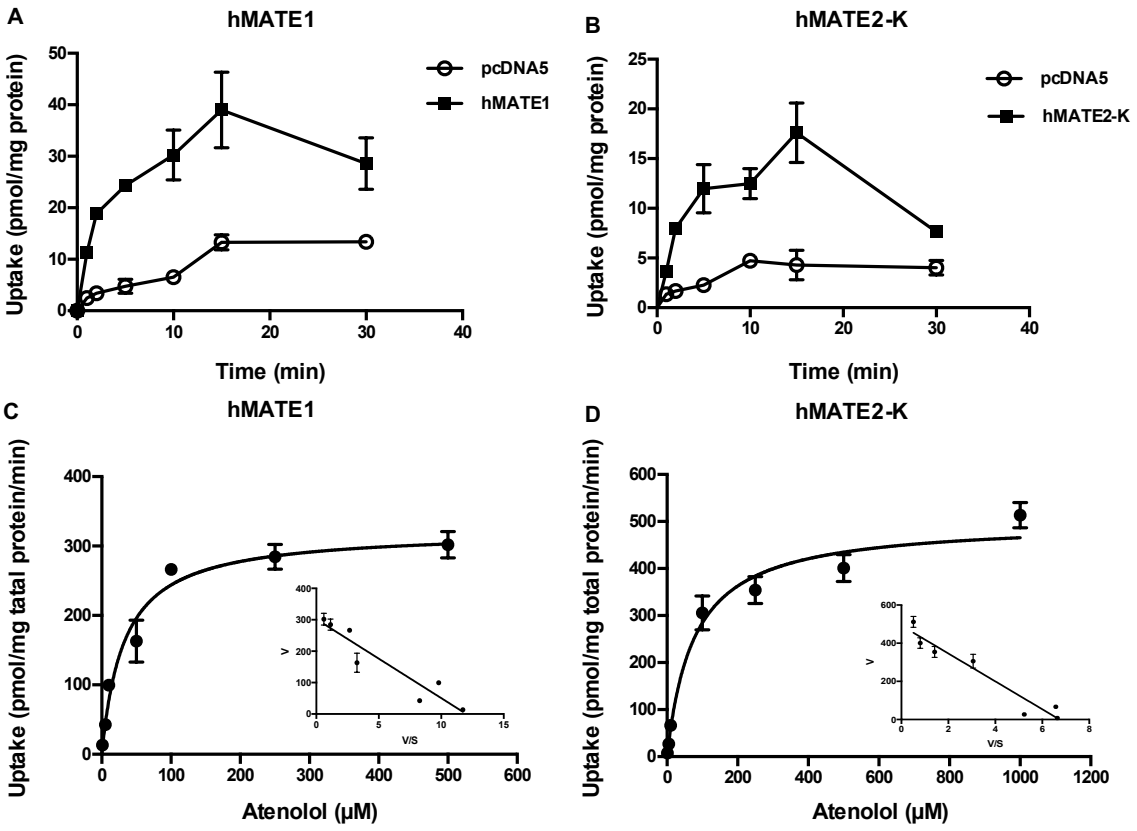

Figure 3.5 Atenolol uptake kinetics by hMATE1 and hMATE2-K. The uptake of 1 μM atenolol was measured in control and transporter-expressing HEK293 cells at specified time points (4A and 4B). Concentration-dependent uptake of atenolol was measured in both transporter-expressing and control HEK293 cells after a 2 min incubation at 37 °C (4C and 4D). Transporter-specific uptake was obtained by subtracting the uptake in control cells from the uptake in transporter-expressing cells. The Michaelis-Menten equation was fit to the data using nonlinear regression. The insets are Eadie-Hofstee transformation of the kinetics data. Each data point represents mean ± SD.

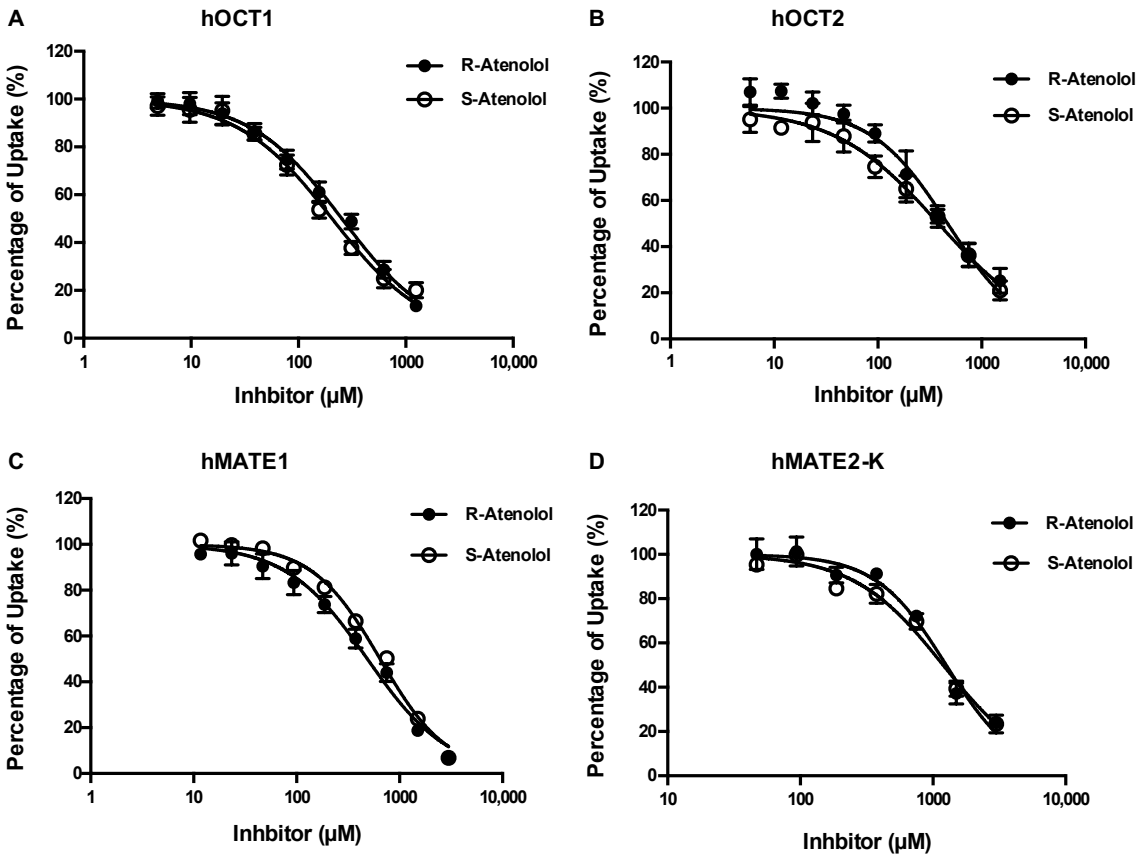

Figure 3.6 Inhibition of hOCT1, hOCT2, hMATE1, and hMATE2-K by R- and S- atenolol. Uptake of 1 μM ASP+ in the absence and presence of R- and S- atenolol was measured in both transporter-expressing and control HEK cells. The uptake of ASP+ in the presence of R- and S-atenolol was expressed as a percentage of the uptake in the absence of R- and S- atenolol. 5 min was chosen as the end point for specific uptake. Each data point represents mean ± SD.

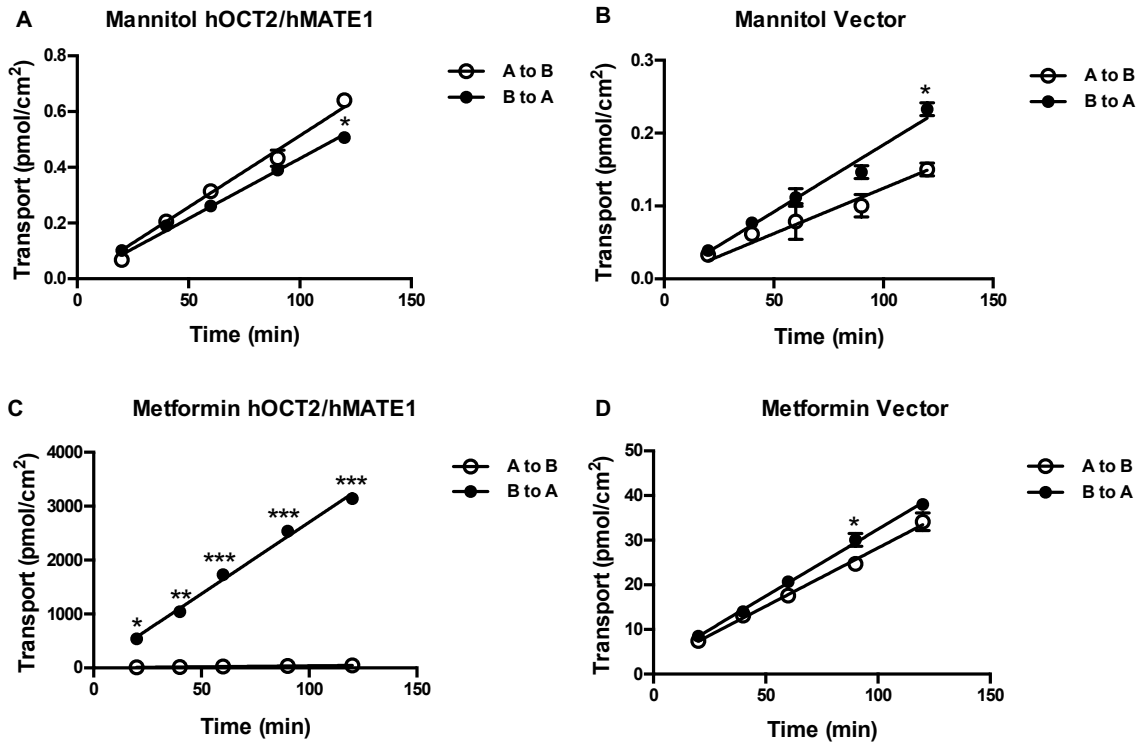

Figure 3.7 Transcelluar flux of mannitol and metformin in hOCT2/hMATE1 double-transfected and control MDCK cells. Cells were incubated in KRH buffer containing 0.05 μM mannitol (A and B) and 5.5 μM metformin (C and D) in either the apical (open circle) or basal (closed circle) chamber. An aliquot of buffer was taken periodically from the receiving chamber (100 μl from the basal chamber, 50 μl from the apical chamber) and radioactivity was subsequently measured. The pH of the apical and basal chambers were 6.0 and 7.4, respectively. Data were fitted with linear regression. Each data point represents mean ± SD. Transport in the basal-to-apical direction was compared with that in the apical-to-basal direction (*** $P < 0.001$, ** $P < 0.01$, * $P < 0.05$). (A to B: apical to basal; B to A: basal to apical)

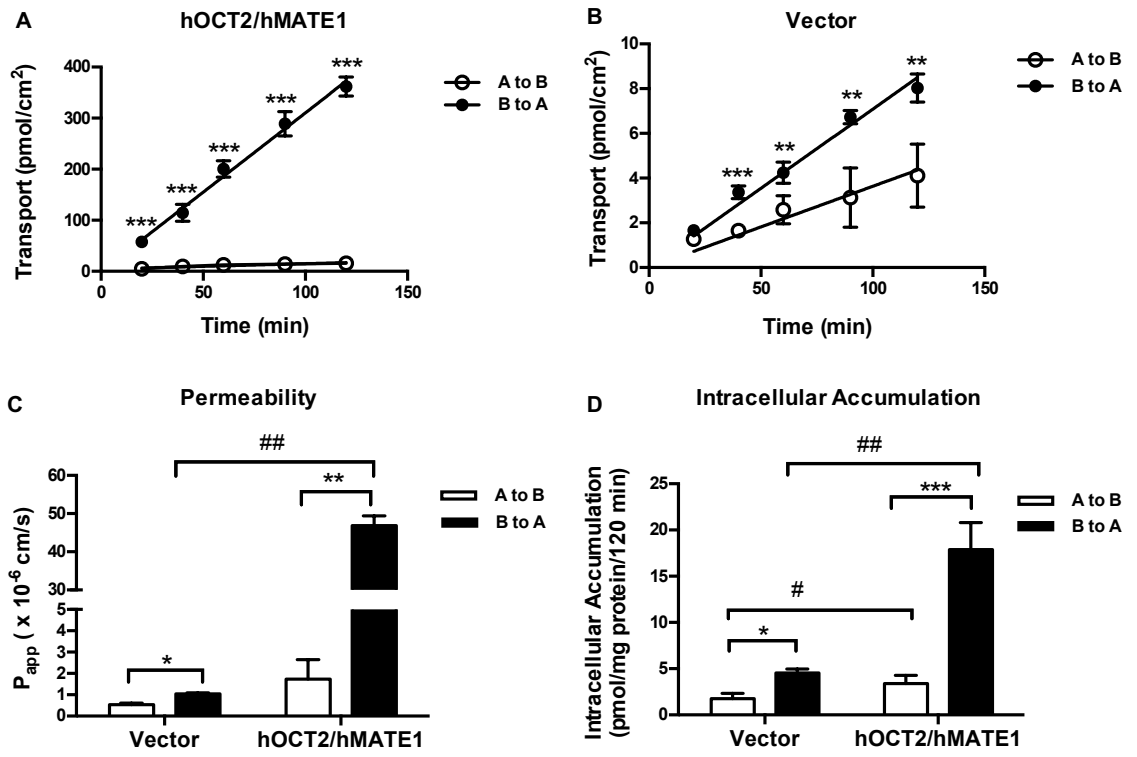

Figure 3.8 Transcelluar flux and permeability and intracelluar accumulation of atenolol in hOCT2/hMATE1 double-transfected and control MDCK cells. Cells were incubated in KRH buffer containing 1 μM atenolol in either the apical (open circle) or basal (closed circle) chamber (A and B). An aliquot of buffer was taken periodically from the receiving chamber (100 μl from the basal chamber, 50 μl from the apical chamber) and radioactivity was subsequently measured. The pH of the apical and basal chambers were 6.0 and 7.4, respectively. Permeability of atenolol was calculated using the equation described in Materials and Methods section (C). Intracellular accumulation of atenolol was measured at the end of the 120 min incubation (D). Data were fitted with linear regression. Transport, permeability and accumulation in the basal-to-apical direction were compared with that in the apical-to-basal direction (*** $P < 0.001$, ** $P < 0.01$, * $P < 0.05$). Permeability and accumulation in hOCT2/hMATE1 MDCK cells were compared with that in control cells (## $P < 0.01$, # $P < 0.05$). Each data point represents mean ± SD. (A to B: apical to basal; B to A: basal to apical).

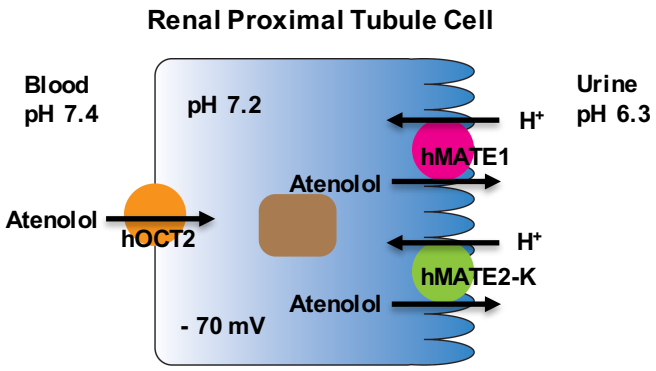

Figure 3.9 Proposed scheme of atenolol transport in human renal proximal tubule cells.

Table 3.1 Surrogate peptides of hOCT1, hOCT2, hMATE1 and hMATE2-K and their MS/MS parameters for protein quantification.

Protein	Compound Name	Parent Ion	Product Ions	Fragmentor	Collision Energy	LLOQ (fmol on column)
hOCT1	LSPSFADLFR	576.7	476.6, 855	25	16	0.20
	LSPSFADLF<u>R</u>	581.8	778.4, 865.4	25	23	
hOCT2	LNPSFLDLVR	587.34	228.13, 946.54	140	15	0.62
	LNPSFLDLV<u>R</u>	592.34	228.13, 956.54	140	15	
hMATE1	GGPEATLEVR	514.9	617.3, 817.6	130	14	0.64
	GGPEATLEV<u>R</u>	519.9	827.6, 627.3	130	15	
hMATE2-K	TPEEAHALSAPTSR	489.7	618.3, 460.2	130	15	2.50
	TPEEAHALSAPTS<u>R</u>	494.7	628.3, 470.2	130	15	

Table 3.2 Kinetic parameters of atenolol uptake by hOCT1, hOCT2, hMATE1 and hMATE2-K.

Kinetic Parameters	hOCT1	hOCT2	hMATE1	hMATE2-K
K_m (μM)	128 ± 16	280 ± 41	32 ± 5	76 ± 14
V_{max} (pmol/min/mg protein)	1355 ± 40	1836 ± 71	323 ± 12	500 ± 22

Table 3.3 Comparison of K_m and V_{max} values derived from Michaelis-Menten (MM) equation and MM with a diffusional component.

Transporter	MM fitting [a]			MM with diffusional component fitting [b]		
	K_m (μM)	V_{max} (pmol/min/mg protein)	R^2	K_m (μM)	V_{max} (pmol/min/mg protein)	R^2
hOCT1	128 ± 16	1355 ± 40	0.9404	128 ± 50	1356 ± 156	0.9404
hOCT2	280 ± 41	1836 ± 71	0.9715	278 ± 120	1838 ± 284	0.9714
hMATE1	32 ± 5	323 ± 12	0.9641	37 ± 9	318 ± 17	0.9630
hMATE2-K	76 ± 14	500 ± 22	0.9730	78 ± 21	500 ± 26	0.9730

[a.] $V = V_{max}*S / (K_m + S)$ was fit to the data, where V is the velocity of uptake, V_{max} is the maximum velocity of uptake, S is the substrate concentration, and K_m is the Michaelis-Menten constant. [b.] $V = V_{max}*S / (K_m + S) + P_{dif}*S$ was fit to the data, where a first order diffusional process is included. The P_{dif} is the nonsaturable passive diffusion rate constant.

Table 3.4 Turnover number and transport efficiency of atenolol uptake by hOCT1, hOCT2, hMATE1 and hMATE2-K.

	hOCT1	hOCT2	hMATE1	hMATE2-K
Amount of transporter (fmol/μg membrane)	19.0 ± 0.02	41.1 ± 3.6	36.9 ± 4.8	9.7 ± 1.3
k_{cat} (s^{-1})	4.57	2.76	0.41	2.20
k_{cat}/K_m ($s^{-1}*\mu M^{-1}$)	36 x 10^{-3}	9.9 x 10^{-3}	12.8 x 10^{-3}	28.9 x 10^{-3}

Table 3.5 IC_{50} of R- and S- atenolol inhibition of ASP+ uptake by hOCT1, hOCT2, hMATE1 and hMATE2-K.

Transporter	R-Atenolol IC_{50} (μM)	S-Atenolol IC_{50} (μM)	Ratio [a]	P Value
hOCT1	254.1 ± 11.9	206.1 ± 11.4	1.2	< 0.05
hOCT2	470.0 ± 15.2	384.0 ± 20.6	1.2	< 0.05
hMATE1	486.9 ± 22.1	645.2 ± 41.4	0.8	< 0.05
hMATE2-K	1258 ± 101.9	1194 ± 117.6	1.1	= 0.52

[a.] Ratio = R-Atenolol IC_{50}/S-Atenolol IC_{50}

Table 3.6 A comparison of physiochemical properties and human pharmacokinetic parameters for atenolol and metformin.

Parameters	Atenolol [a]	Metformin [a]
MW	266	129
$LogD_{7.4}$	-2.0	-5.5
pKa	9.6	12.4
F (%)	52 ~ 63	40 ~ 60
f_u (%)	> 95	100
V_d (L)	95	63 ~ 276
CL (ml/min)	178	459
CL_R (ml/min)	168	454
f_e (%)	> 95	99.9
$t_{1/2}$ (hr)	6	8 ~ 20

[a.] Human pharmacokinetic parameters were compiled from Mason et al., 1979, Goodman et al, 2011, Brown et al., 1976, Wadworth et al., 1991, Pentikainen et al., 1979, and Scheen et al., 1996. MW, molecular weight; $LogD_{7.4}$, distribution coefficient at pH 7.4; pKa, acid dissociation constant; F, oral bioavailability; f_u, plasma unbound fraction; V_d, volume of distribution; CL, total plasma clearance; CL_R, renal clearance; f_e, fraction excreted unchanged in urine after i.v. dosing; $t_{1/2}$, terminal elimination half-life

Chapter 4. Renal Secretion of Hydrochlorothiazide Involves both Organic Anion and Organic Cation Transporters

4.1 Introduction

Hydrochlorothiazide (HCTZ), a drug on the World Health Organization (WHO) list of essential medicines, is the most commonly prescribed thiazide diuretic for the treatment of hypertension (Feldman et al., 2015). In 2013, HCTZ was the 12th most commonly prescribed drug in the US with 50 million prescriptions (Roush and Sica, 2016). It belongs to the thiazide class of diuretics, which are the first-line treatment for patients with uncomplicated hypertension (Chobanian et al., 2003; Salvetti and Ghiadoni, 2006). Thiazide diuretics lowers blood pressure by blocking the electroneutral Na^+/Cl^- cotransporter located on the apical membrane of the early segment of renal distal convoluted tubule, resulting in reduced Na^+ reabsorption and increased water loss (Tamargo et al., 2014). Among the thiazide diuretics, HCTZ remains the cornerstone for treatment of hypertension, either alone or in combination with other classes of antihypertensive drugs, such as angiotensin-converting enzyme (ACE) inhibitors, angiotensin receptor blockers (ARBs), beta-blockers, and calcium channel blockers (CCBs) (Chobanian et al., 2003; Tamargo et al., 2014). While generally safe at low doses, HCTZ at high doses significantly increases the risk of hydroelectrolytic and metabolic adverse effects such as hypokalemia, hyperuricemia, and hyperglycemia (Tamargo et al., 2014).

HCTZ is a hydrophilic (Log $D_{7.4}$ of -0.57), small molecule drug (MW 297). Orally administrated HCTZ is rapidly absorbed in the gastrointestinal track with a reported bioavailability of ~60-80% (Beermann et al., 1976). The drug is primarily eliminated by the kidney with more than 95% of the absorbed dose being excreted unchanged in the urine (Beermann et al., 1976; Tamargo et al., 2014). The binding of HCTZ to plasma protein is more

than 50% (Baur et al., 1977), which significantly reduces its elimination by glomerular filtration. The reported renal clearance of HCTZ (~ 320 ml/min) is more than 5-fold higher than its filtration clearance, suggesting a dominating role of tubular secretion in HCTZ renal excretion (Beermann and Groschinsky-Grind, 1977). Secretion is also important for delivering HCTZ to its site of action in the distal convoluted tubule (Tamargo et al., 2014). Despite the importance of renal secretion in HCTZ pharmacology, the mechanisms underlying HCTZ tubular secretion have not been clearly defined at the molecular level.

Tubular secretion of drug molecules is mediated by the sequential action of transporters located at the basolateral and apical membranes of the proximal tubular cells (Morrissey et al., 2012). Two major secretion systems exist for organic anion and organic cation drugs. In the human kidney, negatively charged drugs are first transported from blood into the renal tubular cells by the basolateral organic anion transporters 1 and 3 (hOAT1 and 3) (You, 2004; Burckhardt, 2012). Once inside the cells, these organic anion drugs are further effluxed into the lumen by apical membrane transporters such as the multidrug resistance-associated proteins 2 and 4 (hMRP2 and 4) (Hillgren et al., 2013). In contrast, positively charged drugs are first transported into renal tubular cells by the electrogenic basolateral organic cation transporter 2 (hOCT2) and then effluxed into urine by the apical proton/organic cation exchangers including multidrug and toxin extrusion proteins 1 and 2-K (hMATE1 and 2-K) (Motohashi and Inui, 2013). Although these transporters are generally charge selective, hOAT3 is also able to transport certain positively charged drugs such as cimetidine (Giacomini et al., 2010). hMATEs have also been reported to transport certain anionic and zwitterion drugs (Tanihara et al., 2007; Matsushima et al., 2009; Yonezawa and Inui, 2011). These renal transporters are increasingly recognized as the target for clinically significant drug-drug interactions (DDIs); and among them,

hOCT2, hOAT1 and hOAT3 are recommended by the US Food and Drug Administration (FDA) for assessing DDI potentials during drug development (FDA, 2012).

Like most thiazide diuretics, HCTZ contains a central backbone of benzothiadiazine and two sulfonamide groups (Tamargo et al., 2014). At physiological pH, a significant portion of HCTZ is de-protonated, carrying a negative charge that is stabilized by resonance (Vujic et al., 2012). HCTZ was previously shown to be an in vitro substrate of hMRP4 (Hasegawa et al., 2007). In Mrp4 knockout mice, HCTZ renal clearance is significantly reduced (Hasegawa et al., 2007). These data suggest that apical efflux of HCTZ, the second step in its tubular secretion, is mediated by at least in part by hMRP4 (Hasegawa et al., 2007). The molecular mechanisms of HCTZ uptake at the basolateral membranes have not been well characterized, although uptake of thiazide diuretics in general is assumed to be mediated by the OATs since many of the these drugs exist as organic anions at physiologic pH (Tamargo et al., 2014). HCTZ was previously shown to inhibit rat Oat1 and human OAT1 and 3 with half inhibitory concentration (IC_{50}) values ranging ~ 70-1,000 μM (Uwai et al., 2000; Hasannejad et al., 2004). However, its substrate potential and transport kinetics towards human hOAT1 and 3 have not been characterized. In addition, using stop-flow peritubular capillary perfusion studies in rat kidney, Ullrich et al. provided evidence that HCTZ may also interact with the renal organic cation transport system (Ullrich et al., 1994). However, it is not known if HCTZ is a transportable substrate for the renal organic cation transporters hOCT2 and hMATEs. In this study, we investigated the molecular mechanisms involved in renal handling of HCTZ. We first characterized the interaction of HCTZ with major renal organic anion and cation transporters. Detailed transport kinetics of HCTZ was analyzed in conjunction with transporter protein

quantification with targeted LC-MS/MS proteomics. Lastly, we evaluated the drug interaction potential of HCTZ at the site of hOAT1/3 using in vitro inhibition assays.

4.2 Materials and Methods

4.2.1 Materials.

[^{14}C]metformin (98 mCi/mmol) was purchased from Moravek Biochemicals, Inc. (Brea, CA). [^{3}H]Estrone sulfate (ES) (50 Ci/mmol) and [^{3}H]para-aminohippurate (PAH) (3 Ci/mmol) were purchased from American Radiolabeled Chemicals, Inc. (St. Louis, MO). Nonradiolabeled compounds of analytical grade were purchased from Sigma-Aldrich (St. Louis, MO) and were. Synthetic signature peptides (Table 4.1) for protein quantification were obtained from New England Peptides (Boston, MA) and the corresponding stable isotope labeled (SIL) internal standards were obtained from Thermo Fisher Scientific (Rockford, IL). Cell culture media and reagents were purchased from Invitrogen (Carlsbad, CA).

4.2.2 Cell Lines and Cell Culture.

Flp-In HEK293 cell lines stably expressing hOAT1, hOAT3, hOCT2, hMATE1 and hMATE2-K and pcDNA5 vector-transfected control HEK293 cells were previously established (Duan et al., 2015; Yin et al., 2015a). All expressed transporters showed high transport activity compared with control (Yin et al., 2015a). Both transporter-expressing and control Flp-In HEK293 cells were cultured in Dulbecco's modified Eagle's medium (high glucose) supplemented with 10% FBS, 2 mM L-glutamine, 100 U/ml penicillin, 100 μg/ml streptomycin, and 150 μg/ml hygromycin B. For better attachment of Flp-In 293 cells, cell culture plastic surfaces were coated with 0.01% poly-D-lysine. Cells were maintained in a 37 °C humidified incubator with 5% CO_2.

4.2.3 Uptake and Inhibition Assays in HEK293 Cells.

The assays were performed as previously described (Yin et al., 2015a) with some modifications. Control and transporter-expressing cells were seeded in poly-D-lycine-coated 96-well plates and allowed to grow for 2 to 3 days to reach 80-90% confluence. Uptake experiments were performed at 37 °C in KRH buffer (5.6 mM glucose, 125 mM NaCl, 4.8 mM KCl, 1.2 mM KH_2PO_4, 1.2 mM $CaCl_2$, 1.2 mM $MgSO_4$, and 25 mM HEPES) containing substrates. For uptake experiments in hMATE1- and hMATE2-K-expressing cells, KRH buffer was adjusted to pH 8.0 to generate an outwardly directed proton gradient because hMATEs function as proton/organic cation exchangers (Otsuka et al., 2005). For all other transporters, uptake experiment was performed at pH 7.4. After incubating the cells with a substrate for a specified time, uptake was terminated by washing cells three times with ice-cold KRH buffer. For intracellular radioactivity measurement, cells were solubilized with 100 µl 1M NaOH and neutralized by equal volume 1 M HCl and the lysates were measured by a liquid scintillation counter (PerkinElmer, Tri-Carb B3110TR, Waltham, MA). For LC-MS-MS quantification of hydrochlorothiazide inside the cells, cells were lysed with 100 µl 80% acetonitrile and 20% H_2O containing internal standard then diluted with HPLC water. For inhibition studies, uptake was measured in both absence and presence of inhibitors. Protein content in cell lysates was measured by the BCA Protein Assay Kit (Pierce Chemical, Rockford, IL) and the uptake in cells was normalized to their protein concentrations. Transporter-specific uptake was calculated by subtracting the baseline uptake in control cells.

4.2.4 Quantification of HCTZ by LC-MS/MS.

A sensitive method was developed to quantify HCTZ by liquid chromatography-tandem mass spectrometry (LC-MS/MS) with diclofenac as the internal standard. An AB Sciex 4000 QTRAP Mass Spectrometer (AB Sciex, Framingham, MA) coupled to an Acquity UPLC system

(Waters Corporation, Milford, MA) was operated in electrospray ionization (ESI) negative mode. Ten microliter of sample was injected into column (Zorbax Eclipse Plus 1.8 µm, C18, 2.1 x 50 mm, Agilent Technologies, Santa Clara, CA) and eluted at 0.4 ml/min. The mobile phase conditions used for liquid chromatography were 90% A (0.1% v/v formic acid) and 10% B (acetonitrile containing 0.1% v/v formic acid) held for 0.1 min, followed by a linear gradient from 10% B to 90% B over 0.01 min. The 90% mobile phase B was maintained for 1.39 min and then returned to 10% B within 0.01 min. This was followed by re-equilibration for 1.49 min. The quantification limit of this method was 0.2 ng/ml in cell lysate. Instrument control and data processing were performed using Analyst software 1.6 from AB. Product ions m/z 268.9 for HCTZ and m/z 249.7 for internal standard were monitored using optimized LC-MS/MS parameters.

4.2.5 Membrane Protein Preparation and LC-MS/MS Quantification of Transporter Protein.

Membrane proteins were prepared from transporter-transfected HEK 293 cells using the ProteoExtract Native Membrane Protein Extraction Kit (Calbiochem/EMD Millipore, San Diego, CA) and concentration of the membrane proteins were determined by the BCA Protein Assay Kit (Pierce Chemical, Rockford, IL). To quantify the membrane transporter protein in each cell line, an LC-MS/MS proteomic approach (Lee et al., 2013; Prasad and Unadkat, 2014) was used. An Agilent 6460A Triple Quadrupole Mass Spectrometer coupled to Agilent 1290 Infinity LC system (Agilent Technologies, Santa Clara, CA) operated in ESI positive ionization mode was used for LC-MS/MS analysis of the peptides (Table 4.1). Approximately 1.5 µg or less of the trypsin digest (5 µl) was injected onto the column (Kinetex™ 2.6 µm, C18, 100 x 3 mm, Phenomenex, Torrance, CA) and eluted at 0.3 ml/min. The mobile phase gradient conditions

were 97% A (0.1% v/v formic acid) and 3% B (acetonitrile containing 0.1% v/v formic acid) held for 2.5 min, followed by three steps of linear gradient of mobile phase B concentrations of 3% to 8%, 8% to 21%, and 21% to 30%. 30% mobile phase B was maintained for 2 min. This was followed by a washing step using 80% mobile phase B for 1.6 min and re-equilibration for 3.3 min. The doubly/triply charged parent to singly charged product transitions for the analyte peptides and their respective SIL peptides were monitored using optimized LC-MS/MS parameters (Supplemental Table 1). The data were processed by integrating the peak areas generated from the reconstructed ion chromatograms for the analyte peptides and the respective SIL internal standards using the MassHunter software V (Agilent Technologies, Santa Clara, CA).

4.2.6 Data Analysis.

All uptake and inhibition experiments were performed in triplicates and repeated at least two times. Data were presented as mean ± SD ($n \geq 3$). The transport kinetics data were fitted by nonlinear regression using GraphPad Prism 6.0 (GraphPad Software, Inc, La Jolla, CA). The K_m and V_{max} values were obtained by fitting the Michaelis-Menten equation $V = V_{max}*S / (K_m + S)$ to the data, where V is the velocity of uptake, V_{max} is the maximum velocity of uptake, S is the substrate concentration, and K_m is the Michaelis-Menten constant. The IC_{50} values were obtained by fitting log (inhibitor concentration) versus normalized response to the data using the equation: $V = Bottom + (Top - Bottom) / [1 + (I/IC_{50})^{nH}]$, where "V" is the rate of uptake in the presence of inhibitor, "Bottom" is the residual noninhibitable baseline value, "Top" is the rate of uptake in the absence of inhibitor, "I" is the inhibitor concentration, and "nH" is the Hill coefficient. Statistic analysis was performed using unpaired Student's *t* test and a P value less than 0.05 was considered statistically significant.

4.3 Results

4.3.1 Inhibitory Effect of HCTZ on Renal Drug Transporters.

To determine if HCTZ interacts with renal organic anion transporters hOAT1, hOAT3 and organic cation transporters hOCT2, hMATE1 and hMATE2-K, the uptake of a probe substrate in the presence and absence of HCTZ (0.5 and 2 mM) was measured in both control and transporter-expressing cells. The uptake of probe substrate in the presence of HCTZ was expressed as a percentage of the specific uptake in the absence of HCTZ. As shown in Figure 4.1, at 0.5 mM concentration, HCTZ only inhibited hOAT1 and hOAT3. At 2 mM concentration, all tested transporters were inhibited, although hOCT2, hMATE1 and hMATE2-K were inhibited to a lesser degree than hOAT1 and hOAT3.

4.3.2 Uptake of HCTZ by Renal Drug Transporters.

To determine if HCTZ is a substrate of the five tested transporters, uptake of HCTZ (10 μM) was measured in both control and transporter-expressing cells. Compared with the uptake in control cells, HCTZ uptake was significantly increased in cells expressing hOAT1, hOAT3, hOCT2 and hMATE2-K (Figure 4.2). Cells expressing hOAT1 showed the highest uptake activity towards HCTZ. In contrast, no significant uptake of HCTZ was observed in cells expressing hMATE1.

4.3.3 HCTZ Uptake Kinetics by hOAT1 and hOAT3.

To determine the transport kinetics of HCTZ by renal organic anion transporters hOAT1 and hOAT3, time-dependent uptake of HCTZ (10 μM) was performed in KRH buffer (pH7.4) at 37 °C. Uptake in both hOAT1 and hOAT3 cells was linear up to 5-15 min (Figure 4.3A and B). Concentration-dependent uptake was thus performed at 5 min incubation time and the specific uptake was obtained by subtracting uptake in control cells. hOAT1- and hOAT3-specific HCTZ

uptake was saturable, and the K_m values derived from nonlinear regression fitting to the Michaelis-Menten equation were 112 ± 8 and 134 ± 13 μM, respectively (Figure 4.3C and D, Table 4.2). Eadie-Hofstee further revealed a pattern consistent with single-enzyme kinetics for both transporters (Figure 4.33, C and D insets).

4.3.4 HCTZ Uptake Kinetics by hOCT2 and hMATE2-K.

The kinetics of HCTZ uptake by the renal organic cation transporters hOCT2 and hMATE2-K was determined in a similar manner, except that the uptake assay for hMATE2-K was performed in KRH buffer at pH 8.0 in order to provide an outwardly directed proton gradient (Otsuka et al., 2005; Muller et al., 2013; Yin et al., 2015a). For hOCT2, the uptake of HCTZ increased sharply in the first 2 min then rapidly reached plateau (Figure 4.4A). Uptake in hMATE2-K cell increased progressively until 10 min and then reached plateau (Figure 4.4B). Concentration-dependent uptake was thus performed with 2-min incubation for both transporters. hOCT2- and hMATE2-K-mediated HCTZ uptake was saturable (Figure 4.4C and D) with the K_m and V_{max} values shown in Table 4.2. Compared to hOAT1 and hOAT3, hOCT2 and hMATE2-K showed a 5-6 fold lower affinity towards HCTZ. Time-dependent uptake of HCTZ was also performed in hMATE1-expressing cells. Consistent with Figure 4.2, no significant uptake was observed with hMATE1 (Figure 4.8).

4.3.5 Transporter Quantification and Turnover Number Determination.

To determine HCTZ transport efficiency at single transporter level, we quantified transporter protein expression levels in membrane fractions prepared from transfected HEK293 cell lines using targeted LC-MS/MS proteomics. As shown in Table 4.3, hOAT1 and hOAT3 have relatively lower expression levels whereas hOCT2 and hMATE2-K have higher expression in our Flp-In HEK293 cell lines. The transporter turnover number (k_{cat}), which represents the

maximum number of substrate that a carrier can transport during a transport cycle, was calculated by normalizing V_{max} to the number of transporters determined. As shown in Table 4.3, hOAT1 exhibited a k_{cat} value 3-7 times higher than hOAT3, hOCT2 and hMATE-2K. When single transporter efficiency (k_{cat}/K_m) was compared, it followed the rank order of hOAT1 > hOAT3 > hOCT2 and hMATE-2K. These data suggest that at a single transporter level, hOAT1 is the most efficient transporter for HCTZ whereas hOCT2 and hMATE-2K are least efficient. hOAT3 has an intermediate efficiency for HCTZ.

4.3.6 Inhibitory Potential of HCTZ towards hOAT1 and hOAT3.

The relatively higher affinity of HCTZ towards hOAT1 and hOAT3 (Table 4.2) raised a concern of potential inhibitory drug interaction with these transporters. To evaluate the potential for HCTZ to inhibit hOAT1 and hOAT3 in vivo, the IC_{50}'s for HCTZ inhibition of hOAT1- and hOAT3-mediated probe substrate transport were determined. The substrates used were PAH (1 μM) for hOAT1 and ES (0.06 μM) for hOAT3. As shown in Figure 4.5, HCTZ exhibited similar potency toward hOAT1 and hOAT3, with the IC_{50} values of 126 ± 13.7 and 213 ± 21.5 μM, respectively. These IC_{50} values are very similar to the K_m values of HCTZ determined in Table 1. The IC_{50} values of HCTZ for hOAT1 and hOAT3 are much higher than its plasma concentrations (0.7 ~ 0.9 μM) following a typical 25 mg clinical dose (Vaidyanathan et al., 2006; Jeon et al., 2012), suggesting that HCTZ is unlikely to significantly inhibit hOAT1 and hOAT3 activities in vivo.

4.3.7 Probenecid and Valsartan Inhibition of hOAT1- and hOAT3- Mediated HCTZ Transport.

Our data suggest that hOAT1 and hOAT3 play a major role in renal secretion of HCTZ. Inhibition of hOAT1 and hOAT3 by other drugs may alter the renal handling of HCTZ. We thus

determined the inhibitory potency of two known hOAT inhibitors, probenecid and valsartan, towards hOAT1- and hOAT3-mediated HCTZ uptake. As shown in Figure 4.6, probenecid and valsartan potently inhibited hOAT1- and hOAT3-mediated HCTZ transport, with IC_{50} values ranged between 2.3 and 9.0 μM.

4.4 Discussion

HCTZ is eliminated primarily by tubular secretion but the molecular mechanisms underlying its renal handling have not been well characterized. In this study, we systematically characterized the interaction of HCTZ with major renal organic anion and cation transporters and evaluated the drug interaction potential at the site of these transporters. Several novel findings were obtained from our studies. First, our data demonstrated that HCTZ is not only a substrate of renal organic anion transporters hOAT1 and 3, but also transported by organic cation transporters hOCT2 and hMATE2-K. Second, by quantifying transporter protein levels by LC-MS/MS, we determined the detailed transport kinetics of HCTZ at single transporter level. Our data revealed that hOAT1 is the most efficient HCTZ transporter followed by hOAT3. Compared to hOAT1/3, hOCT2 and hMATE2-K have lower affinity and lower transport efficiency for HCTZ. Lastly, we showed that HCTZ is not a clinically relevant inhibitor for renal hOATs or hOCTs. However, hOAT-mediated HCTZ secretion may be affected by potent clinical inhibitors of hOAT such as probenecid.

At high concentrations (e.g. 2 mM), HCTZ inhibited all tested renal transporters (Figure 4.1). When tested as a substrate, we found that HCTZ is a substrate for hOAT1, hOAT3, hOCT2 and hMATE2-K, but not hMATE1 (Figure 4.2). While OATs and OCTs generally show distinct charge preference for anionic and cationic compounds, several studies have suggested that there is some overlap in substrate specificity (Takeda et al., 2002b; Ahn et al., 2009). For example,

the antiviral drugs acyclovir and ganciclovir have been shown to be transported by both hOAT1 and hOCT1 (Takeda et al., 2002b). Cimetidine, a substrate and a classic inhibitor of OCTs, is a known substrate of hOAT3 (Tahara et al., 2005). OATs and OCTs are both encoded by the SLC22 gene family and share similar 12 transmembrane domain structures (Koepsell et al., 2007; Burckhardt, 2012). This substrate overlap among these transporters may reflect some similarity of their substrate recognition sites likely due to a common ancestry. The MATEs transporters, which are encoded by SLC47, generally accept organic cations as substrates but they are also capable of transporting certain zwitterion and anionic drugs (Yonezawa and Inui, 2011). For example, the zwitterion drug cephalexin is a reported substrate of hOAT1/3 and hMATE1 (Tanihara et al., 2007; Watanabe et al., 2010; Zhang et al., 2010). Here we show that HCTZ is a substrate for hOAT1, hOAT3, hOCT2 and hMATE2-K. Like other thiazide diuretics, HCTZ has a central backbone of benzothiadiazine and two sulfonamide groups (Tamargo et al., 2014). The amine center in the sulfonamide structure can lose one proton, resulting in a negatively charged conjugate that can be further stabilized by resonance (Vujic et al., 2012). With a pKa of 7.9, approximately ~ 30% of HCTZ exists in the negatively charged form whereas the remainder is in the neutral form. Based on their charge preference and transport modes, we suspect that hOAT1 and hOAT3 transport the anionic form of HCTZ whereas hOCT2 and hMATE2-K may prefer the uncharged form as substrate. More studies are needed to clearly define the specific HCTZ species for their interaction with renal organic anion and cation transporters.

Our substrate data suggest that the first step of HCTZ renal secretion is mediated by multiple uptake transporters (hOAT1, hOAT3, hOCT2) at the basolateral membrane. It would be crucial to know the relative importance of these transporters in HCTZ renal secretion. In

theory, this is determined by two factors--the intrinsic transport efficiency (k_{cat}/K_m) and the total expression level of the transporter (E_{total}) in the kidney. Although the protein expression of hOAT1, hOAT3 and hOCT2 have not been quantified in human kidneys, all three transporters are known to be highly expressed in the kidney (Koepsell et al., 2007; Burckhardt, 2012), suggesting that the intrinsic activity of these transporters towards HCTZ may be a determining factor of their in vivo significance in HCTZ renal uptake. We thus performed detailed kinetic analysis coupled with absolute quantification of transporter protein levels to provide further insights (Figures 4.3 and 4.4; Tables 4.2 and 4.3). Our data revealed that hOAT1 and hOAT3 have higher affinity toward HCTZ than hOCT2 and hMATE2-K. The calculated transport efficiency (k_{cat}/K_m) follows the rank order of hOAT1> hOAT3 > hOCT2 and hMATE-2K (Table 4.3), suggesting a major role of organic anion transporters in tubular secretion of HCTZ. As HCTZ acts on the Na^+/Cl^- cotransporter located on the luminal side of the renal distal tubule, our data also support that hOAT1, and to a less extent hOAT3, may also be important for delivering the diuretic to its site of action. Interestingly and consistent with our kinetic data, a recent pharmacogenetics study in hypertensive patients treated with HCTZ suggested that an intergenic polymorphism (rs10792367) between the *OAT1 and OAT3* genes was associate with antihypertensive response to HCTZ (Han et al., 2011).

In the kidney, basolateral hOAT1/3 and apical hMRP2/4 often work in tandem to secrete organic anions from blood into urine (You, 2004). Previously, hMRP4 was identified as an efflux transporter for HCTZ (Hasegawa et al., 2007). Renal clearance of HCTZ is significantly reduced in Mrp4 knockout mice, suggesting an important role of this transporter in HCTZ secretion (Hasegawa et al., 2007). Our data showing that HCTZ is also transported by the apical organic efflux transporter hMATE2-K suggests that in addition to MRP4, apical efflux of HCTZ

may also be assisted by hMATE2-K (Hasegawa et al., 2007). Based on these data, we proposed a molecular model for HCTZ secretion in renal proximal tubule cells consisting of at least two parallel pathways (Figure 4.7). In this model, hOAT1/3 and hMRP4 form a major route whereas hOCT2 and hMATE2-K serve as a secondary pathway for HCTZ tubular secretion.

HCTZ is frequently used in combination or co-formulated as fixed dose combination pills (known as "polypills") with other antihypertensive drugs to produce an additive effect in lowering blood pressure in order to treat patients with inadequately controlled hypertension by monotherapy (Sica et al., 2011). Some of the co-administered drugs may be an inhibitor or substrate of the renal organic anion or cation transporters, raising a concern of potential drug-drug interactions. For example, HCTZ is frequently used together with loop diuretics (e.g. furosemide) or beta-blockers (e.g. atenolol) (Sica et al., 2011; Tamargo et al., 2014). Furosemide and atenolol are also mainly eliminated by the kidney with involvement of renal organic anion or cation transporters (Ebner et al., 2015; Yin et al., 2015b). The combination of HCTZ with valsartan, an angiotensin II receptor antagonist, has also been developed as fixed-dose tablets under the trade name DIOVAN HCT (Chrysant, 2003). Valsartan has been shown in vitro as a potent inhibitor of hOAT1 and 3 (Duan et al., 2012; Ingraham et al., 2014). Our inhibition studies showed that HCTZ generally has low affinities towards hOAT1/3, hOCT2 and hMATEs (Figures 4.1 and 4.5, Table 4.2). With IC_{50} or K_m values (> 100-200 μM) much larger than its clinically encountered concentrations (< 1-10 μM), HCTZ is unlikely to significantly inhibit hOAT1/3, hOCT2, or hMATEs at clinically relevant doses. Therefore, concurrent use of HCTZ with a substrate drug of hOAT1/3 (e.g. furosemide) or hOCT2 (e.g. atenolol) may not affect the renal handling of these drugs.

Our data suggest that HCTZ is eliminated from the body primarily by hOAT1/3-mediated tubular secretion (Table 4.3, Figure 4.7). While HCTZ is not a clinically relevant inhibitor for hOAT1/3, the pharmacokinetics of HCTZ itself may be altered by potent inhibitors of these transporters, which may affect its pharmacodynamics and toxicity. We thus determined the inhibitory effect of two known hOAT1/3 inhibitors, valsartan and probenecid, using HCTZ as the substrate. Our data showed that both valsartan and probenecid potently inhibited hOAT1- and hOAT3-mediated HCTZ uptake in vitro with IC_{50} in low micromolar range (Figure 4.6, Table 4.4). However, valsartan is highly protein-bound and has lower plasma concentrations at clinically used doses (Table 4.4). Assuming that only the unbound drug interacts with the basolateral transporters, at maximal plasma concentration (I_{max}) following a typical dose of 320 mg(Jung et al., 2012), valsartan is predicted to only produce a moderate inhibition of hOAT1 and hOAT3 (Table 4.4). Several clinical studies have examined the interaction between HCTZ and valsartan in healthy subjects, and two studies reported no significant effect of valsartan on HCTZ pharmacokinetics (Bhad et al., 2011; Hedaya and Helmy, 2013). Compared to valsartan, probenecid is also highly protein-bound but has much higher plasma concentrations at clinically used dose. At a typical dose of 1 g (Selen et al., 1982), HCTZ uptake by hOAT1 and hOAT3 is predicted to be markedly inhibited by probenecid (Table 4.4). Probenecid is a recommended in vivo inhibitor of hOAT1/3 for evaluation of DDI risk of hOAT1/3 substrates (FDA, 2012). To date, there is no human study of probenecid and HCTZ interaction reported. However, in dogs, it has been shown that coadministration of probenecid reduced HCTZ renal clearance by more than 80% (Beyer and Baer, 1967). At higher doses, HCTZ significantly increases the risk of hydroelectrolytic and metabolic adverse effects (Tamargo et al., 2014). Considering the

importance of renal tubular secretion in HCTZ elimination, caution should be taken when HCTZ is co-administered with strong in vivo hOAT1/3 inhibitors such as probenecid.

In summary, we showed that HCTZ is an excellent substrate for the renal organic anion transporters hOAT1 and hOAT3. It is also transported by renal organic cation transporters hOCT2 and hMATE2-K. Renal tubular secretion of HCTZ likely occurs mainly through the hOAT1/3 and hMRP4 pathway with hOCT2/hMATE2-K being a secondary pathway. Our data also suggest that the pharmacokinetics of HCTZ may be significantly affected by potent hOAT1/3 inhibitors. Together, our studies elucidated the molecular mechanisms involved in renal handling of HCTZ and revealed that complex transport mechanisms are involved in the disposition of this important antihypertensive drug.

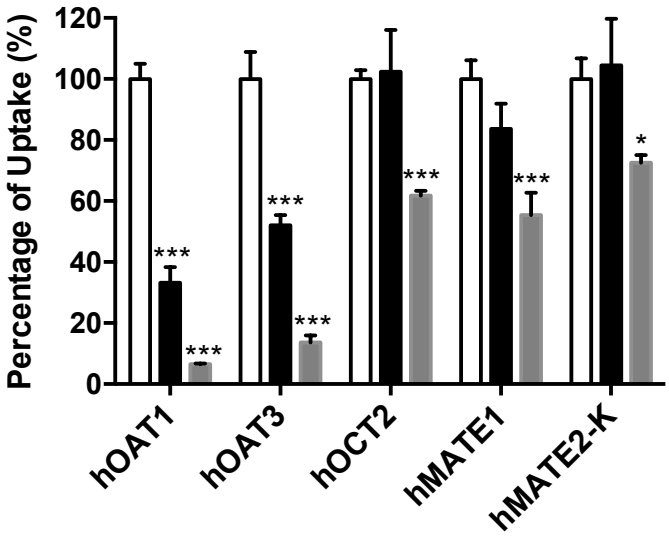

Figure 4.1 Inhibitory effect of hydrochlorothiazide on the uptake of probe substrates by renal transporters. Uptake of 5.5 μM metformin by hOCT2, hMATE1, and hMATE2-K, 1 μM PAH by hOAT1, and 0.06 μM ES by hOAT3 in the absence (unfilled bar) and presence of 500 μM hydrochlorothiazide (black bar) and 2 mM hydrochlorothiazide (grey bar) was measured in both transporter-expressing and control HEK293 cells. Transporter-specific uptake was obtained by subtracting the uptake in control cells from the uptake in transporter-expressing cells. The uptake was measured after a 2 min incubation at 37 °C. Data are presented as mean ± SD. *** $P < 0.001$ and * $P < 0.05$ indicate uptake in the presence of hydrochlorothiazide was significantly lower than that in the absence of hydrochlorothiazide.

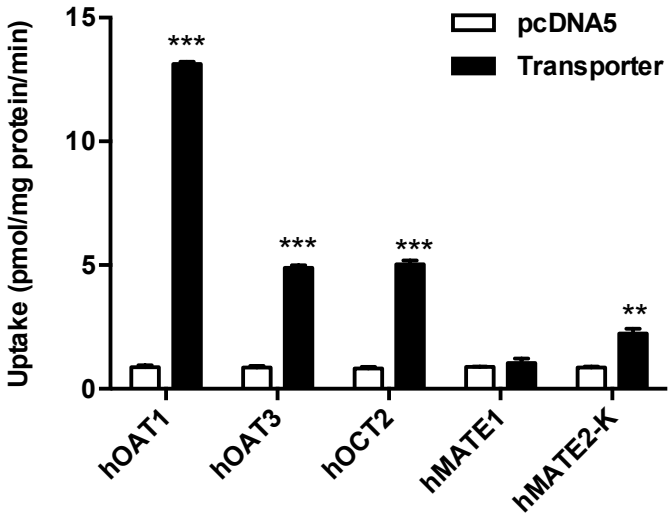

Figure 4.2 Uptake of hydrochlorothiazide by renal transporters. The uptake of 10 μM hydrochlorothiazide in transporter-expressing (filled) and control (unfilled) HEK293 cells was measured. The uptake was measured after a 5 min incubation at 37 °C. Data are presented as mean ± SD. *** $P < 0.001$ and ** $P < 0.01$ indicate uptake was significantly higher in transporter-expressing cells than that in control cells.

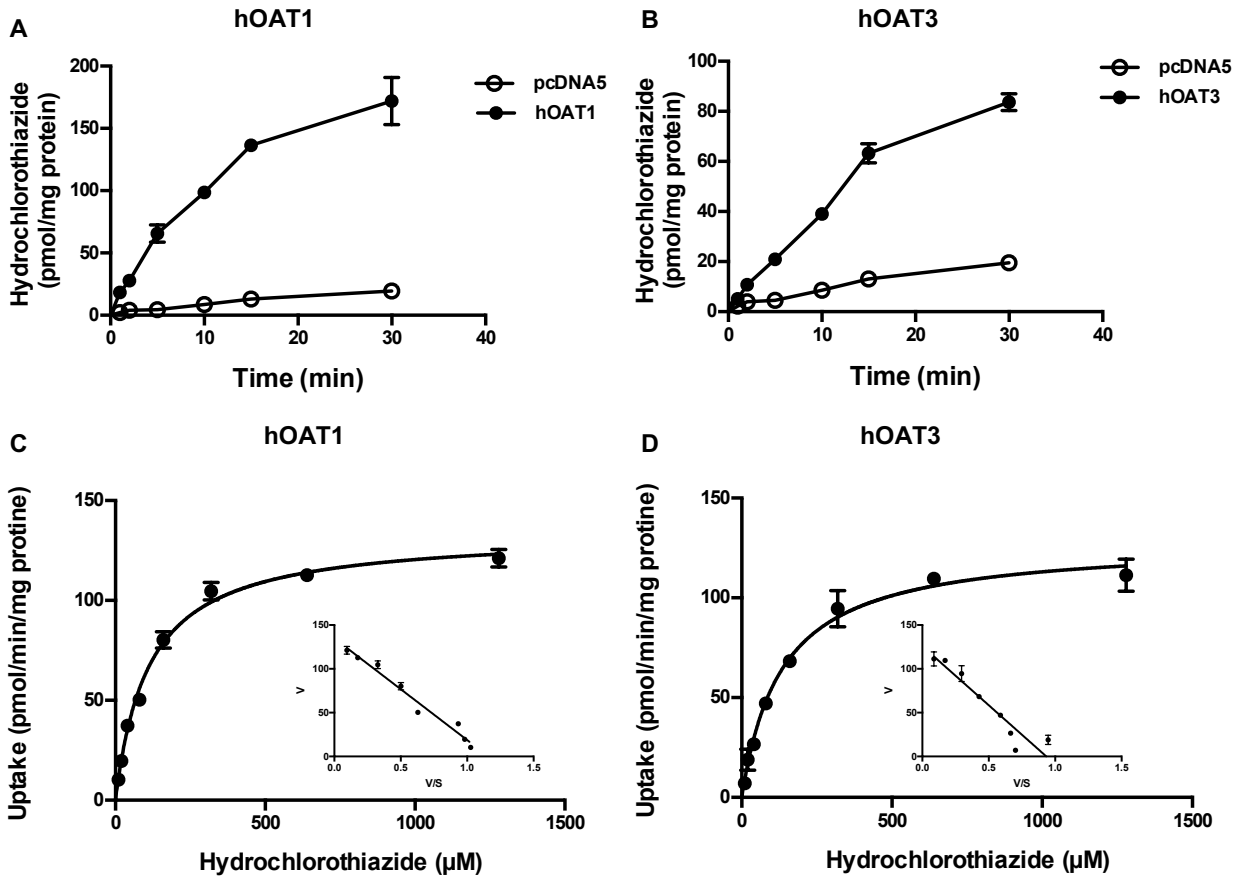

Figure 4.3 Hydrochlorothiazide uptake kinetics by hOAT1 and hOAT3. The uptake of 10 μM hydrochlorothiazide was measured in control and transporter-expressing HEK293 cells at specified time points (3A and 3B). Concentration-dependent uptake of HCT was measured in both transporter-expressing and control HEK293 cells after a 5 min incubation at 37 °C (3C and 3D). Transporter-specific uptake was obtained by subtracting the uptake in control cells from the uptake in transporter-expressing cells. Data were fitted with Michaelis-Menten equation using nonlinear regression. The insets are the Eadie-Hofstee transformation of the kinetics data. Each data point represents mean ± SD.

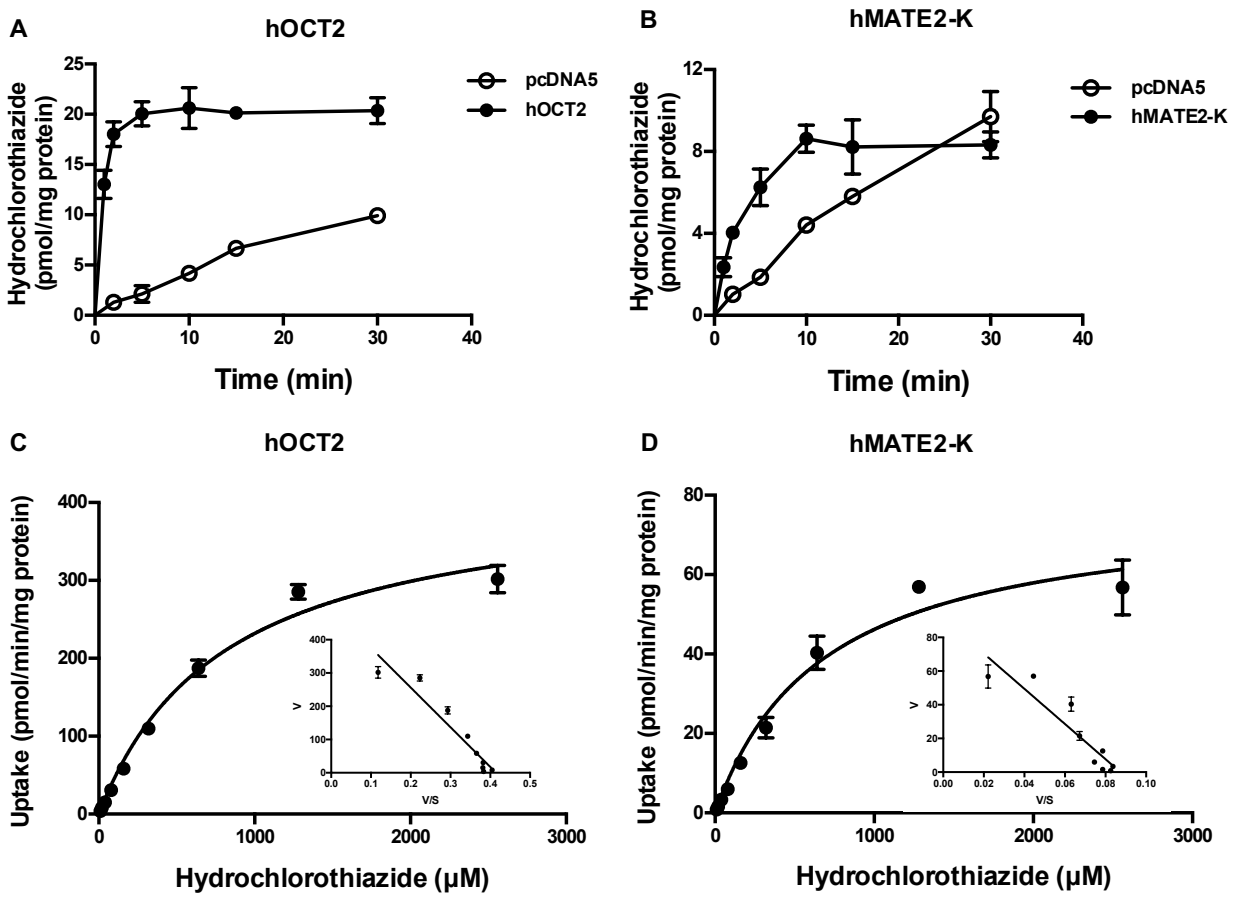

Figure 4.4 Hydrochlorothiazide uptake kinetics by hOCT2 and hMATE2-K. The uptake of 10 μM hydrochlorothiazide was measured in control and transporter-expressing HEK293 cells at specified time points (4A and 4B). Concentration-dependent uptake of atenolol was measured in both transporter-expressing and control HEK293 cells after a 2 min incubation at 37 °C (4C and 4D). Transporter-specific uptake was obtained by subtracting the uptake in control cells from the uptake in transporter-expressing cells. Data were fitted with Michaelis-Menten equation using nonlinear regression. The insets are the Eadie-Hofstee transformation of the kinetics data. Each data point represents mean ± SD.

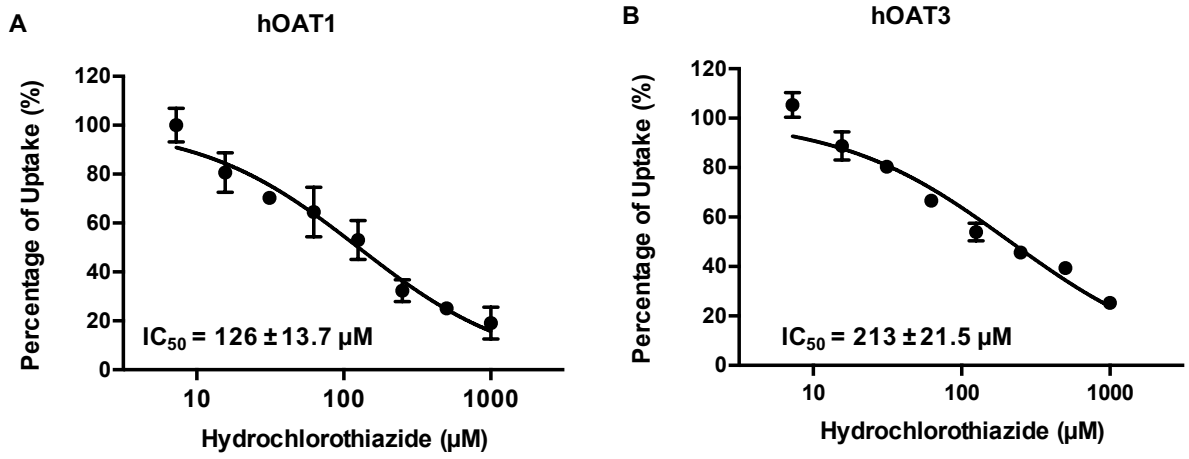

Figure 4.5 Inhibition of hOAT1 and hOAT3 by hydrochlorothiazide. Uptake of 1 µM PAH by hOAT1, and 0.06 µM ES by hOAT3 in the absence and presence of hydrochlorothiazide was measured in both transporter-expressing and control HEK293 cells. Transporter-specific uptake was obtained by subtracting the uptake in control cells from the uptake in transporter-expressing cells. The uptake was measured after a 2 min incubation at 37 °C. Data are presented as mean ± SD.

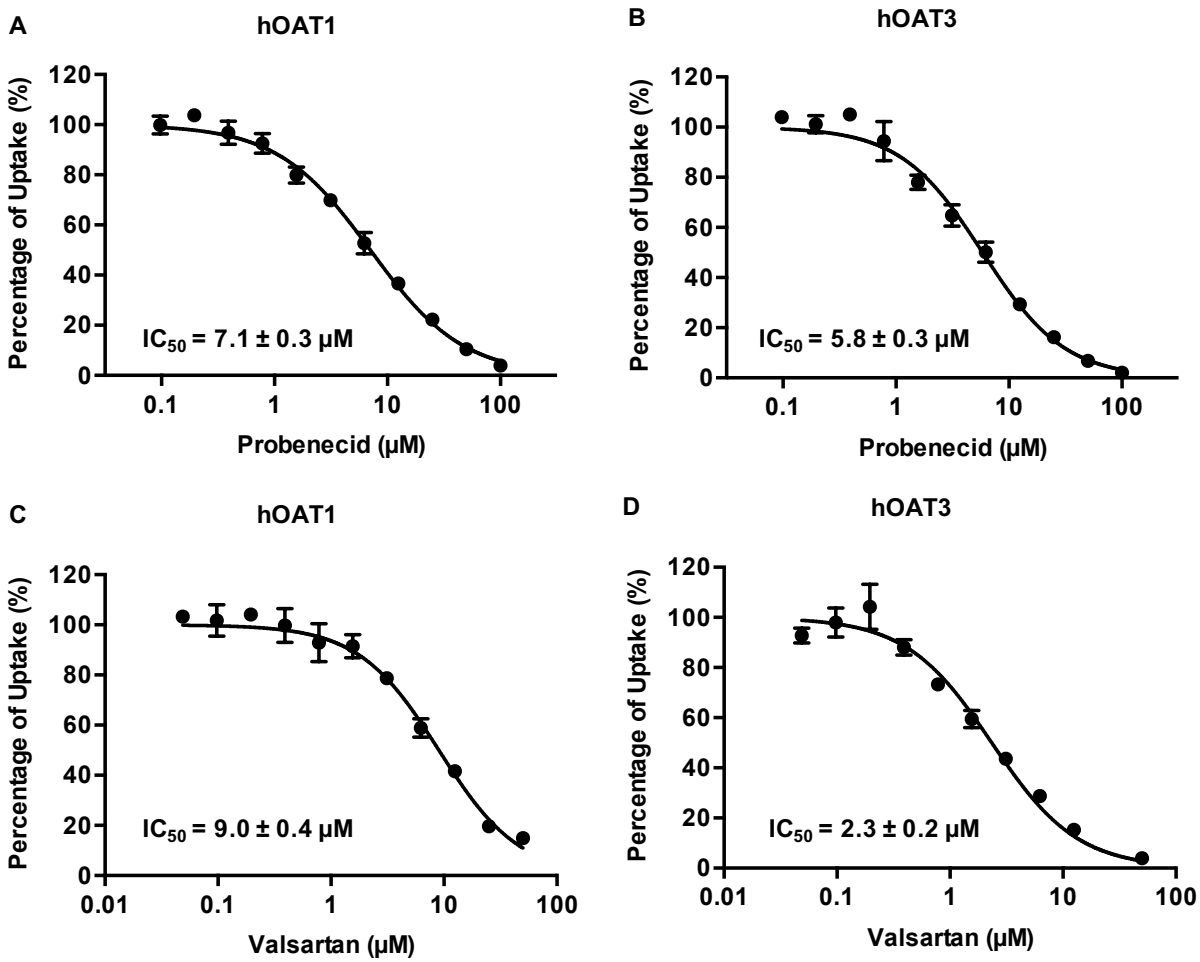

Figure 4.6 Inhibition of hOAT1- and hOAT3-mediated hydrochlorothiazide uptake by probenecid and valsartan. Uptake of 10 μM hydrochlorothiazide by hOAT1 and hOAT3 in the presence of increasing concentration of probenecid (A, B) and valsartan (C, D) was measured in both transporter-expressing and control HEK293 cells. Transporter-specific uptake was obtained by subtracting the uptake in control cells from the uptake in transporter-expressing cells. The uptake was measured after a 5 min incubation at 37 °C. Data are presented as mean ± SD.

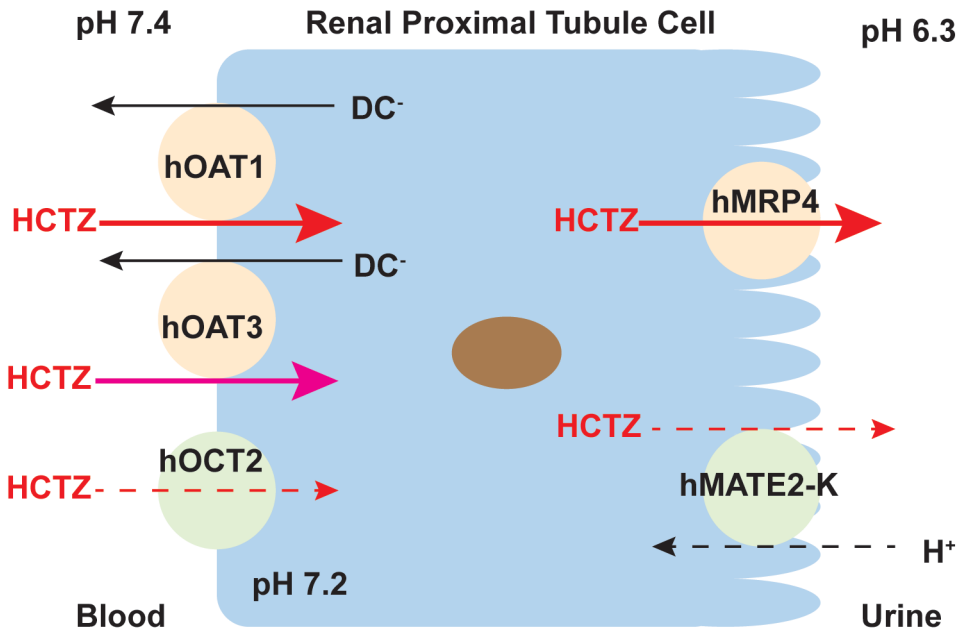

Figure 4.7 Proposed scheme of hydrochlorothiazide (HCT) transport in human renal proximal tubule cells. In this model, hOAT1/3 and hMRP4 form a major route (solid arrows) whereas hOCT2 and hMATE2-K represent as a secondary pathway (dashed arrows) for HCTZ tubular secretion.

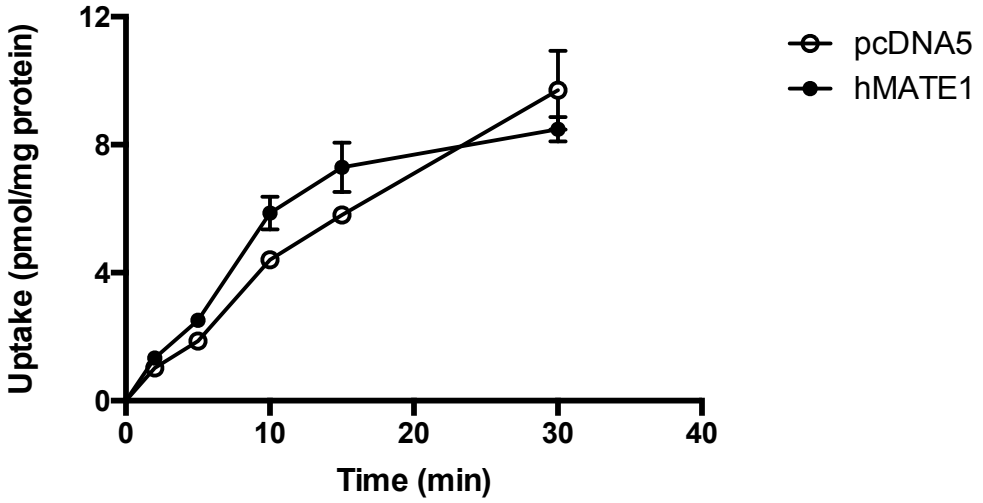

Figure 4.8 Hydrochlorothiazide uptake by hMATE1. The uptake of 10 μM hydrochlorothiazide was measured in control and transporter-expressing HEK293 cells at specified time points. Each data point represents mean ± SD.

Table 4.1: Surrogate peptides of hOAT1, hOAT3, hOCT2 and hMATE2-K and their MS/MS parameters for protein quantification.

Protein	Compound Name	Parent Ion	Product Ions	Fragmentor	Collision Energy	LLOQ (fmol on column)
hOAT1	TSLAVLGK	394.8	600.3, 487.2	35	13	0.19
	TSLAVLGK	398.8	608.3, 495.2	35	13	
hOAT3	TVLAVFGK	417.9	634.3, 521.2	35	15	0.37
	TVLAVFGK	421.9	642.3, 529.2	35	15	
hOCT2	LNPSFLDLVR	587.34	228.13, 946.54	140	15	0.62
	LNPSFLDLV<u>R</u>	592.34	228.13, 956.54	140	15	
hMATE2-K	TPEEAHALSAPTSR	489.7	618.3, 460.2	130	15	2.50
	TPEEAHALSAPTS<u>R</u>	494.7	628.3, 470.2	130	15	

Underlined residues are heavy peptide ([13C615N4]-arginine or [13C615N2]-lysine)

Table 4.2: Kinetic parameters of hydrochlorothiazide uptake by hOAT1, hOAT3, hOCT2 and hMATE2-K.

Kinetic Parameters	K_m	V_{max}
	μM	pmol/min/mg protein
hOAT1	112 ± 8	134 ± 3
hOAT3	134 ± 13	128 ± 4
hOCT2	812 ± 85	420 ± 18
hMATE2-K	681 ± 101	78 ± 5

Table 4.3: Turnover number and transport efficiency of hydrochlorothiazide uptake by hOAT1, hOAT3, hOCT2 and hMATE2-K.

	Amount of transporter	k_{cat}	k_{cat}/K_m
	fmol/μg membrane	s^{-1}	$s^{-1}*\mu M^{-1}$
hOAT1	1.3 ± 0.2	2.48	22.1×10^{-3}
hOAT3	3.2 ± 0.3	0.79	5.9×10^{-3}
hOCT2	41.1 ± 3.6	0.63	0.8×10^{-3}
hMATE2-K	9.7 ± 1.3	0.34	0.5×10^{-3}

Table 4.4: Prediction of % inhibition of hOAT1- and hOAT3-mediated hydrochlorothiazide transport in vivo by probenecid and valsartan.

Inhibitor	I_{max} (μM)	f_u (%)	$I_{max,u}$ (μM)	Transporter	IC_{50} (μM)	% Inhibition *
Probenecid §	240	11	26.4	hOAT1	7.1 ± 0.3	79
				hOAT3	5.8 ± 0.3	82
Valsartan ‡	24.6	5	1.2	hOAT1	9.0 ± 0.4	12
				hOAT3	2.3 ± 0.2	34

* % Inhibition is calculated by $(1 - 1/ (1 + I_{u,max}/IC_{50}))*100\%$. I_{max} is the maximum plasma concentration; f_u is the unbound plasma concentration; $I_{max,u}$ is the maximum unbound plasma concentration and is calculated by $I_{max}*f_u$.

§ I_{max} and f_u of probenecid were obtained from Selen et al., 1982. The I_{max} is following a 1 g dose.

‡ I_{max} and f_u of valsartan were collected from Jung et al., 2012 and Flesch et al., 1997. I_{max} is following a 320 mg dose.

Chapter 5. Substrate-Dependent Inhibition of Renal Organic Cation Uptake and Efflux Transporters and its Impact on Predicting Transporter-mediated Drug Interaction and Intracellular Accumulation

5.1 Introduction

Renal excretion is a major elimination pathway for many drugs and drug metabolites. Besides glomerular filtration, circulating drugs and metabolites are actively secreted by carrier-mediated pathways in the renal proximal tubules. In humans, secretion of organic cation (OC) drugs is primarily accomplished via basolateral uptake by the electrogenic organic cation transporter 2 (hOCT2) followed by apical efflux involving the proton/OC exchangers multidrug and toxin extrusion proteins 1 and 2-K (hMATE1 and 2-K) (Li et al., 2006b; Giacomini, 2010; Morrissey et al., 2012; Motohashi and Inui, 2013). Anionic drug molecules, on the other hand, are typically first transported into tubular cells by the basolateral organic anion transporters 1 and 3 (hOAT1 and 3) and then effluxed into the tubular lumen by apical transporters such as the multidrug resistance-associated proteins 2 and 4 (Li et al., 2006b; Giacomini, 2010; Morrissey et al., 2012). These kidney transporters are important pharmacokinetic and pharmacodynamic determinants for a wide array of therapeutic agents (Giacomini, 2010; Morrissey et al., 2012). Furthermore, an imbalance between transporter-mediated uptake and efflux may result in drug accumulation in proximal tubule cells, leading to drug-induced nephrotoxicity and kidney injury (Li et al., 2006b; Morrissey et al., 2012).

Numerous clinically significant DDIs in the kidney are attributed to the inhibition of renal organic cation and anion secretion systems (Masereeuw and Russel, 2001; Li et al., 2006b; Morrissey et al., 2012). Historically, cimetidine has been used as the prototypical inhibitor for the OC system whereas probenecid is the prototypical inhibitor of the anion system (Masereeuw

and Russel, 2001; Li et al., 2006b; Morrissey et al., 2012). Renal transporter-mediated DDIs are of significant clinical concern as they can adversely impact drug disposition, efficacy, and toxicity. Recognizing the important roles of transporters in drug disposition and interactions, the US Food and Drug Administration (FDA) and the International Transporter Consortium (ITC) have recently published a series of recommendations and decision trees to guide industry in assessment of DDI potentials of new molecular entities (NMEs) towards clinically important transporters, including hOCT2, hOAT1/3, and hMATE1/2-K (Giacomini, 2010; Zhang et al., 2011; FDA, 2012; Brouwer et al., 2013; Hillgren et al., 2013). In general, if an NME is an in vitro inhibitor for these transporters and its unbound maximal plasma concentration (C_{max}) is greater than one-tenth of its half maximal inhibitory concentration (IC_{50}), further in vivo DDI assessment is recommended (Giacomini, 2010; FDA, 2012). A key parameter essential in the prediction of DDI risk is the IC_{50} (or the inhibition constant K_i) of the NME, which is typically determined in transporter-expressing cell lines using a probe substrate (Brouwer et al., 2013). Several in vitro substrates, including metformin and 1-methyl-4-phenylpyridinium (MPP+), have been recommended as the probe substrates in preclinical DDI assessment with hOCT2 and hMATEs (FDA, 2012; Hillgren et al., 2013). This approach assumes that the K_i or IC_{50} values of an NME determined with a probe substrate are a constant and can be extrapolated to predict its in vivo DDI potential with clinically encountered drugs. However, several drug-metabolizing enzymes, including CYP3A4 and 2D6, are known to exhibit substrate-dependent inhibition, where the K_i or IC_{50} values of an inhibitor can vary considerably depending on the probe substrate used (Kenworthy et al., 1999; VandenBrink et al., 2012). To mitigate the risk of false-negative prediction, the use of two or more probe substrates or sensitive drug substrates for these enzymes was suggested (Yuan et al., 2002; FDA, 2012).

Emerging evidence suggests substrate-dependent inhibition can also occur with drug transporters (Belzer et al., 2013; Martinez-Guerrero and Wright, 2013; Izumi et al., 2015). Using metformin and several experimental compounds as probe substrates, Wright and coworkers showed that inhibition of hOCT2 and hMATE1 is substrate-dependent (Belzer et al., 2013; Martinez-Guerrero and Wright, 2013). However, except metformin, all other substrates used in these studies were experimental compounds not given to humans, making it difficult to infer the clinical impact of substrate-dependent inhibition on DDI prediction. Moreover, the influence of substrate-dependent inhibition on overall tubular secretion has never been studied. Its impact on intracellular drug accumulation, an important predictor for drug-induced nephrotoxicity, is also unknown. In this study, we investigated the influence of probe substrate choice on predicting transporter-mediated DDI using metformin and a newly identified drug substrate, atenolol, of hOCT2 and hMATEs (Yin et al., 2015a). The overall impact of substrate-dependent inhibition on tubular secretion and intracellular accumulation was also investigated using a double-transfected in vitro cell culture model for renal OC secretion.

5.2 Materials and Methods

5.2.1 Materials.

[^{3}H]atenolol (3.3 Ci/mmol) and [^{14}C]metformin (98 mCi/mmol) were purchased from Moravek Biochemicals, Inc. (Brea, CA) and [^{3}H]cimetidine (80 Ci/mmol) was from American Radiolabeled Chemicals, Inc. (St. Louis, MO). All other chemicals were purchased from Sigma-Aldrich (St. Louis, MO) and are of analytical grade.

5.2.2 Cell Lines and Cell Culture.

Control (pcDNA5-transfected) and Flp-In HEK293 cell lines stably expressing hOCT2, hMATE1 and hMATE2-K were previously established and maintained in Dulbecco's modified

Eagle's medium (Duan et al., 2015; Yin et al., 2015a). Transporter-expressing HEK293 cells showed high activity in transporting probe substrates compared with control HEK293 cells (Yin et al., 2015a). Both transporter-expressing and control HEK293 cells were maintained in Dulbecco's modified Eagle's medium (high glucose) supplemented with 10% FBS, 2 mM L-glutamine, 100 U/ml penicillin, 100 μg/ml streptomycin, and 150 μg/ml hygromycin B. MDCK cell transfected with empty vectors or double-transfected with hOCT2 and hMATE1 were also established in our laboratory (Yin et al., 2015a). The stably transfected MDCK cells formed proper tight junction and the MDCK-hOCT2/hMATE1 cells showed high activity in directional transport of the model substrate metformin (Yin et al., 2015a). MDCK cells were maintained in minimum essential medium supplemented with 10% FBS, 500 μg/ml G418, and 200 μg/ml hygromycin B. All cell lines were cultured in a 37 °C humidified incubator with 5% CO_2.

5.2.3 Uptake and Inhibition Assays in HEK293 Cells.

In vitro transport and inhibition studies were performed as previously described (Duan and Wang, 2010; Yin et al., 2015a). Briefly, Transporter-expressing and control cells were seeded in poly-D-lysine-coated plates and allowed to grow for 2 to 3 days to reach 80-90% confluence. Uptake of [^{14}C]metformin (5.5 μM) or [^{3}H]atenolol (1 μM) in control and transporter-expressing HEK293 cells were performed at 37 ºC in KRH buffer (5.6 mM glucose, 125 mM NaCl, 4.8 mM KCl, 1.2 mM KH_2PO_4, 1.2 mM $CaCl_2$, 1.2 mM $MgSO_4$, and 25 mM HEPES) for 2 min in the presence or absence of an inhibitor. Because hMATEs function as proton/organic cation exchangers (Otsuka et al., 2005), for studies in hMATE1- and hMATE2-K-expressing cells, KRH buffer was adjusted to pH 8.0 to generate an outwardly directed proton gradient to drive uptake. For hOCT2, uptake was performed at pH 7.4. Cells were incubated with a substrate for a specified time, and then the uptake was terminated by washing cells three

times with ice-cold KRH buffer. Cells were then solubilized with 1 M NaOH at 37 °C for and neutralized with equal volume 1 M HCl. The radioactivity of cell lysates was measured by a liquid scintillation counter (PerkinElmer, Tri-Carb B3110TR, Waltham, MA) and the protein content was measured by the BCA Protein Assay Kit (Pierce Chemical, Rockford, IL). Cellular uptake of substrates was normalized by total protein content and transporter-specific uptake was calculated by subtracting the background uptake in control cells.

5.2.4 Transwell Studies in MDCK-hOCT2/hMATE1 Cells.

Transepithelial flux across MDCK monolayer was determined as previously described (Yin et al., 2015a). Briefly, control and MDCK cells stably expressing hOCT2/hMATE1 were seeded on Falcon™ cell culture inserts at a density of 2 x $10^5/cm^2$ and transport experiments were performed 5 days after seeding. To ensure monolayer integrity, only cell cultures with transepithelial electrical resistance (TEER) greater than 150 $\Omega \bullet cm^2$ were used. After removing culture medium from both sides of the inserts, cells were pre-incubated at 37 °C for 10 min in KRH buffer with apical chamber pH 6.0 and basal chamber pH 7.4. For apical-to-basal (A-to-B) transport, 2 ml of KRH buffer (pH 7.4) was added to the basal chamber, and transport was initiated by adding 0.8 ml of KRH buffer (pH 6.0) containing radiolabeled substrates. Similarly, for basal-to-apical (B-to-A) transport, 0.8 ml of KRH buffer (pH 6.0) was added to the apical chamber and 2 ml of KRH buffer (pH 7.4) containing radiolabeled substrates was added to the basal chamber. To measure time-dependent trancellular transport, an aliquot of the incubation medium (100 µl from the basal chamber, 50 µl from the apical chamber) in the receiving chamber was periodically collected and replaced with equal volume of fresh buffer. For inhibition studies, cimetidine was applied to the basal, apical or both chambers at the start of the Transwell study. At the end of the experiment, inserts were rinsed three times with ice-cold

KRH buffer at the end of the transport study and cells were lysed with 1 M NaOH and then neutralized with 1 M HCl. The intracellular accumulation was measured by a liquid scintillation counter (PerkinElmer, Tri-Carb B3110TR, Waltham, MA) and normalized to total protein contents in cell lysate.

5.2.5 Data Analysis.

All experiments were repeated 2 -3 times and data were presented as mean ± SD ($n \geq 3$). The IC_{50} values were obtained by nonlinear regression fitting of Log (inhibitor concentration) vs. normalized response model in GraphPad Prism 6.0 to the uptake data using the equation: $V = Bottom + (Top - Bottom) / [1 + (I/IC_{50})^{nH}]$, where "V" is the rate of uptake in the presence of inhibitor, "Bottom" is the residual noninhibitable baseline value, "Top" is the rate of uptake in the absence of inhibitor, "I" is the inhibitor concentration, and "nH" is the Hill coefficient. For transport experiments, the apparent permeability (P_{app}) of compounds across cell monolayers was calculated as $P_{app} = (dQ/dt) / (A*C_0)$, where Q is the amount of compound transported over time t, A is the insert membrane surface area, and C_0 is the initial compound concentration in the donor chamber. Statistical significance was determined using unpaired Student's *t* test. A *P* value less than 0.05 was considered statistically significant.

5.3 Results

5.3.1 Inhibition of hOCT2 by Classic Inhibitors Is Highly Dependent on Substrate.

To determine if cimetidine, an H_2-receptor antagonist and a classic inhibitor of renal OC secretion, exhibits substrate-dependent inhibition of hOCT2 and hMATE1/2-K, inhibition studies were conducted using two drug substrates--metformin and atenolol. Metformin is a widely used antidiabetic drug and a well-established probe substrate for hOCT2 and hMATE1/2-K whereas atenolol is a major antihypertensive that was recently identified as an excellent

substrate for these transporters (Yin et al., 2015a). Two additional known drug inhibitors of these transporters, pyrimethamine (Kusuhara et al., 2011) and carvedilol (Zolk et al., 2009b; Wittwer et al., 2013), were also tested. Inhibition assays of the two substrates were conducted side-by-side in control and transporter-expressing HEK293 cells and the IC_{50} values were determined at a substrate concentration much lower than the K_m of the probe substrate. For hOCT2, substantial substrate-dependent inhibition was observed for all three tested inhibitors (Figure 5.1, Table 5.1). Cimetidine and pyrimethamine were approximately 10-fold more potent toward hOCT2 when atenolol was used as the substrate. Carvedilol also showed 6-fold higher potency for hOCT2 when atenolol was used. In contrast, substrate-dependent inhibition was much less pronounced for hMATE1 and 2-K (Figure 5.1, Table 5.1). Not all inhibitors showed substrate dependency; and for those that showed dependency, the difference in IC_{50} was significantly smaller (< 5 fold) as compared to hOCT2. Interestingly, atenolol is a more sensitive substrate to detect hOCT2 inhibition, whereas metformin appears to be a more sensitive substrate for hMATE1 and 2-K inhibition.

To examine the inhibition mechanisms of cimetidine towards hOCT2 and hMATE1/2-K, concentration-dependent uptake of atenolol or metformin was performed in the presence of different concentrations of cimetidine (0, IC_{50}, and 5xIC_{50}). Lineweaver-Burk plots indicate that cimetidine is a mixed-type inhibitor of hOCT2 for atenolol, but became a competitive inhibitor when metformin was used (Figure 5.2). Cimetidine acted as a mixed-type inhibitor for both hMATE1 and 2-K regardless of the substrate used. The K_i values of cimetidine obtained by Dixon plot analysis were similar to its IC_{50} values (Table 5.2).

5.3.2 Substrate-dependent Inhibition Results in Different Prediction of DDI Potential.

According to the latest FDA draft guidance for hOCT2-mediated DDI studies, an in vivo DDI study is recommended for a compound if its unbound C_{max}/IC_{50} is greater than 0.1 (FDA, 2012). Cimetidine is 20% protein bound in the plasma and the reported unbound C_{max} after a typical 400 mg oral dose is around 8 μM (Somogyi et al., 1980; Somogyi et al., 1989). Our study showed that the IC_{50} values of cimetidine towards hOCT2 differ by 10-fold when different drug substrates are used. To examine if substrate-dependent inhibition leads to different recommendations for in vivo DDI assessment, the unbound C_{max}/IC_{50} values of cimetidine were calculated for atenolol and metformin. In addition, the reported cimetidine IC_{50} towards MPP+ (Ito et al., 2012), a recommended in vitro probe for hOCT2, was also used for prediction. Very different recommendations for cimetidine in vivo DDI study were obtained for hOCT2 with a "Yes" for atenolol, a "No" for MPP^+, and a borderline for metformin (Table 5.3). These data demonstrated that substrate-dependent inhibition can significantly impact the outcome of in vivo DDI prediction for hOCT2. Compared to hOCT2, cimetidine is generally a more potent inhibitor for hMATE1/2-K and showed less pronounced substrate-dependent inhibition (Table 5.1). The unbound C_{max}/IC_{50} values of cimetidine are all greater than 0.1 for hMATE1/2-K, resulting in a consensus in recommendations for all three substrates.

5.3.3 Cimetidine Applied in the Basal Chamber Inhibited B-to-A Flux of Atenolol and Metformin in MDCK-hOCT2/hMATE1 Monolayer.

In the human kidney proximal tubules, organic cation secretion is sequentially mediated by basolateral hOCT2 and apical hMATE1/2-K. To determine the overall effect of cimetidine on hOCT2 and hMATEs-mediated OC secretion, we examined the inhibitory effect of cimetidine on basolateral-to-apical (B-to-A) flux of atenolol and metformin using a hOCT2/hMATE1 double transfected MDCK cell line we previously established (Yin et al., 2015a). Two clinically

relevant concentrations of cimetidine (2 and 10 μM) were chosen based on its IC_{50} values towards hOCT2 and hMATE1 (Table 5.1). To evaluate whether a difference in membrane access of the inhibitor can influence the inhibitory effect, cimetidine was applied to the basal, apical or both chambers in the Transwell studies. As expected, B-to-A flux of atenolol and metformin in the absence of cimetidine was much greater in hOCT2/hMATE1 transfected cells than in vector-transfected cells (Figure 5.3). When applied to the basal or both chambers, cimetidine dose-dependently inhibited B-to-A flux of atenolol and metformin (Figure 5.3A, C, D, F). Surprisingly, when applied to the apical chamber, cimetidine at the concentrations used had little effect on B-to-A flux of either atenolol or metformin (Figure 5.3B, E).

5.3.4 Cimetidine Differentially Impacted Intracellular Drug Accumulation in A Substrate-dependent Manner.

Transporter-mediated drug accumulation within renal tubular cells is a frequent cause underlying drug-induced nephrotoxicity and kidney injury (DeGorter et al., 2012; Morrissey et al., 2012). Inhibitors affecting renal drug secretion can have very different effects on intracellular drug accumulation depending on whether the interaction occurs at the apical or the basolateral membranes. Our inhibition data (Table 5.1 and Figure 5.1) showed that cimetidine is an equally potent inhibitor for hOCT2 and hMATE1 when atenolol is used as the substrate, but becomes an hMATE1-selective inhibitor if metformin is used. These data suggest that while cimetidine can reduce tubular secretion for all hOCT2/hMATE substrates, its effect on intracellular drug accumulation may be substrate-dependent. Indeed, when apparent permeability was calculated for the Transwell study, cimetidine applied to the basal or both chambers showed a marked inhibitory effect on the B-to-A permeability of atenolol and metformin (Figure 5.4A, B). When intracellular drug accumulation was measured in the absence

of cimetidine at the end of the study, intracellular drug accumulation is higher in hOCT2/hMATE1 cells than in vector-transfected cells (Figure 5.4C and D). Interestingly, cimetidine, either applied to basal or both chambers, had no effect on intracellular atenolol accumulation (Figure 5.4C), which is consistent with its equal inhibition potency for hOCT2- and hMATE1-mediated atenolol transport (Table 5.1). In contrast, cimetidine dose-dependently increased intracellular accumulation of metformin when applied to either basal or both chambers (Figure 5.4D), reflecting a predominant inhibition of apical hMATE1 when metformin is used as the substrate (Table 5.1). These data, obtained from a cell culture model of renal OC secretion, suggest that drugs affecting tubular secretion can impact intracellular drug accumulation in a substrate-dependent manner and the dominant substrate-inhibitor interacting site for a given inhibitor can shift between apical and basolateral transporters depending on the substrate.

5.3.5 Basally Applied Cimetidine Accumulated in MDCK-hOCT2/MATE1 Cells.

An intriguing observation in our studies is that the effect of cimetidine on hOCT2/hMATE1 mediated substrate flux and accumulation is only manifested when the inhibitor is applied to the basal chamber. To explore what could be the possible cause of the differential effect of cimetidine on substrate transport when placed on the opposing sides of the MDCK monolayer, we measured and compared monolayer permeability and intracellular accumulation of ^{3}H-labeled cimetidine under different experimental conditions. Cimetidine showed a minor directional transport in vector-transfected control cells. Consistent with being a reported substrate for hOCT2 and hMATE1 (Tahara et al., 2005; Tanihara et al., 2007), cimetidine exhibited a B-to-A/A-to-B ratio of 2.3 in hOCT2/hMATE1-transfected MDCK cells (Figure 5.5A), suggesting a role of hOCT2/hMATE1 in its renal secretion. Importantly, intracellular accumulation of cimetidine (10 μM) is much greater when it was applied to the

basal side than the apical side in MDCK-hOCT2/hMATE1 cells (Figure 5.5B). Similar results were also observed in the double-transfected cells when cold atenolol (1 μM) or metformin (5.5 μM) were added in the basal chamber (Figure 5.5C and D), which simulate the experimental conditions used in the inhibition studies in Figures 5.3 and 5.4. In vector-transfected control cells, cimetidine intracellular accumulation was also slightly higher when applied basally, which is probably due to its uptake by a low level of endogenously expressed canine Oct2 in MDCK cells (Shu et al., 2001).

5.4 Discussion

In this study, we investigated the impact of substrate-dependent inhibition on predicting transporter-mediated drug interaction and accumulation by focusing on the hOCT2/hMATE-mediated renal secretion pathway. Several novel findings were obtained. First, our data showed that the choice of a probe substrate has a larger impact on hOCT2 than hMATEs in their interactions with inhibitors. Atenolol is a more sensitive substrate than metformin for evaluating hOCT2-inhibitor interactions. Further, substrate-dependent inhibition can complicate in vitro-to-in vivo DDI prediction for hOCT2 and lead to different recommendations for in vivo DDI studies. Second, we showed that while cimetidine inevitably reduced hOCT2/hMATE1-mediated transepithelial flux of a drug substrate, its impact on intracellular drug accumulation, thus toxicity, can be unpredictable due to substrate-dependent shifting of the major inhibition site between apical and basolateral transporters. Lastly, our data provided the first evidence that cimetidine concentrations at the basolateral side (i.e. blood) may be more relevant than those in the apical side (i.e. filtrate) to estimate its inhibitory effects towards renal hOCT2 and hMATE1/2-K.

Using two drug substrates, we showed that cimetidine, as well as pyrimethamine and carvedilol, are much more potent inhibitors of hOCT2 when atenolol is used as the substrate (Figure 5.1, Table 5.1). In contrast, substrate-dependent inhibition was less pronounced for hMATE1 and 2-K (Figure 5.1, Table 5.1). These data suggest that the choice of a probe substrate can greatly influence the inhibition potency of a potential inhibitor (e.g. an NME), especially for hOCT2, leading to very different recommendations for in vivo DDI studies as exemplified in Table 5.3. Accordingly, it may be necessary to evaluate two or more probe substrates in in vitro studies for drug transporters that display substantial substrate-dependent inhibition. To mitigate the risk of false-negative predictions, a sensitive substrate, which consistently produces lower IC_{50} or K_i values for a range of known inhibitors, should be included. Lastly, if a co-mediation that is likely to be used with an NME clinically (e.g. two anti-hypertensive drugs used simultaneously), direct in vitro DDI analyses should be performed using the co-medicated drug as the substrate.

In the current ITC and FDA recommendations, MPP+ and metformin are suggested as the probe substrates for assessing the inhibition potential of a NME towards hOCT2 (Giacomini, 2010; FDA, 2012; Hillgren et al., 2013). Belzer et al. previously reported that structurally diverse hOCT2 inhibitors were generally more effective (up to 9-10 fold) for inhibition of metformin than for MPP+ (Belzer et al., 2013), suggesting that metformin is a more sensitive substrate than MPP+ for hOCT2. Our data revealed that atenolol is an even more sensitive (up to 10-fold) hOCT2 substrate than metformin. Like metformin, atenolol is minimally metabolized in vivo and exclusively eliminated unchanged by the kidney. With a $LogD_{7.4}$ of -2.0, atenolol is highly hydrophilic with minimal passive membrane diffusion. We recently showed that atenolol is an excellent hOCT2 substrate and also has a higher apparent affinity for hOCT2 than

metformin (K_m 280 μM vs. 2,750 μM) (Song et al., 2008a; Yin et al., 2015a). The radiolabeled form of atenolol is readily available. These characteristics suggest that atenolol is a clinically relevant, metabolically stable, and more sensitive probe substrate than metformin for assessing potential hOCT2 inhibitors in vitro. Nevertheless, data from available clinical studies do not suggest a positive interaction between cimetidine and atenolol in vivo (Houtzagers et al., 1982; Kirch et al., 1982; Mutschler et al., 1984) which is likely due to a small contribution of tubular secretion (< 30 %) to the total renal clearance of atenolol in vivo (Yin et al., 2015a). To assess hOCT2-mediated DDIs in vivo, metformin may be more revealing than atenolol to detect AUC changes as tubular secretion contributes more than 75% to its total renal clearance.

Drug-induced nephrotoxicity is a major concern during drug discovery and development (Morrissey et al., 2012). Renal transporter-mediated DDIs may not only affect the systemic exposure of a victim drug, but could also have profound toxicological effect on renal proximal tubule cells. Although inhibition of a basolateral or an apical transporter both decreases tubular secretion, the impact on intrarenal drug accumulation and kidney toxicity can be drastically different. Inhibition of a basolateral uptake transporter is generally nephron-protective as it reduces transporter-mediated drug accumulation within renal tubular cells. Indeed, co-administration of probenecid to inhibit hOAT1-mediated uptake of cidofovir is used clinically to prevent intrarenal accumulation and nephrotoxicity of this antiviral drug (Cundy et al., 1995; Cihlar et al., 1999). Inhibition of hOCT2-mediated cisplatin uptake is also being explored as a strategy to ameliorate cisplatin nephrotoxicity (Filipski et al., 2009; Sprowl et al., 2013; Pabla et al., 2015). In contrast, inhibition of apical efflux transporters diminishes drug exit from renal tubular cells, which may lead to increased drug accumulation and nephrotoxicity (Yonezawa and Inui, 2011). Because inhibitors of the renal organic cation or anion secretion systems often

interact with both apical and basolateral transporters, knowing the major site of interaction (i.e. apical vs. basolateral) is critical to accurate forecasting of a nephron-toxic or a nephron-protective effect of the inhibitor. In the case of cimetidine, inhibition of hOCT2-mediated uptake was historically thought to underlie its numerous clinical DDIs (Li et al., 2006b; Giacomini, 2010). However, based on the in vitro K_i or IC_{50} values of cimetidine determined with metformin or experimental substrates, Ito et al. suggested that the inhibition of the apical hMATEs, but not basolateral hOCT2, is the major mechanism underlying clinically observed renal DDIs with cimetidine (Ito et al., 2012). Here, our data revealed that cimetidine acts as an equally potent inhibitor of hOCT2 and hMATE1 for atenolol, but becomes an hMATE-selective inhibitor when metformin is used (Table 5.1). These data suggest that the specific site of cimetidine interaction with a victim drug is changeable between the apical and basolateral transporters depending on the substrate. Consequently, the effect of an inhibitor on intracellular accumulation is also substrate-dependent, leading to either a nephron-toxic or a nephron-protective effect. This concept, supported by our Transwell studies with atenolol and metformin (Figures 5.3 and 5.4), is illustrated in Figure 5.6. Our studies demonstrated that the effect of a transporter inhibitor on intracellular drug accumulation is dynamic and substrate-dependent; and information obtained with one inhibitor-substrate pair may not be extrapolated to other drug combinations containing the same inhibitor.

To predict transporter-mediated renal DDIs, the unbound plasma concentration of the inhibitor is often used (Giacomini, 2010; FDA, 2012). However, it is the inhibitor concentration at the site of interaction that determines the magnitude of inhibition. An intriguing observation of our study is that in hOCT2/hMATE1-trasfected MDCK cells, cimetidine at clinically relevant concentrations only exerted an inhibitory effect when applied to the basal compartment (Figures

5.3 and 5.4). Cimetidine had no inhibitory effect if applied to the apical compartment. This can be explained by the low passive permeability of cimetidine (LogP = 0.4) and its differential accessibility to transporter binding sites under different in vitro experimental conditions. The pH in the basal and apical chambers was respectively maintained at 7.4 and 6.0 to mimic the physiological environment in the nephron. Because cimetidine is a substrate of both hOCT2 and hMATE1, basally applied cimetidine not only directly interacts with hOCT2, but is also transported by hOCT2 into MDCK cells, where it can bind to hMATE1 and interfere with its efflux function. When cimetidine is applied apically, however, there is little active uptake by hMATE1 as the inwardly-directed proton gradient at the apical membrane drives efflux, not uptake. Cimetidine thus has little access to inhibit the basal hOCT2. The lack of an effect of apically applied cimetidine on hMATE1 function indicates that at an acidic apical pH, the substrate (or inhibitor) binding site in hMATE1 may only be accessible from the intracellular side, which is consistent with its physiological function as a drug efflux transporter in the kidney. Our data demonstrating that basally applied cimetidine accumulates to much higher levels in hOCT2/hMATE1-expressing MDCK cells (Figure 5.5) corroborates with this hypothesis. Together, our studies suggest that plasma and intracellular concentrations of cimetidine, as compare to its filtrate or urine concentrations, may be more relevant to predict hOCT2/hMATE1-mediated cimetidine-drug interactions in the kidney.

In summary, we demonstrated that the choice of a probe substrate can greatly impact the prediction of hOCT2-mediated renal drug interaction and accumulation. Our findings revealed the complex and dynamic nature of substrate-inhibitor interactions in multispecific drug transporters and highlighted the importance of considering substrate-dependent inhibition in assessing transporter-mediated renal drug interaction, accumulation and toxicity.

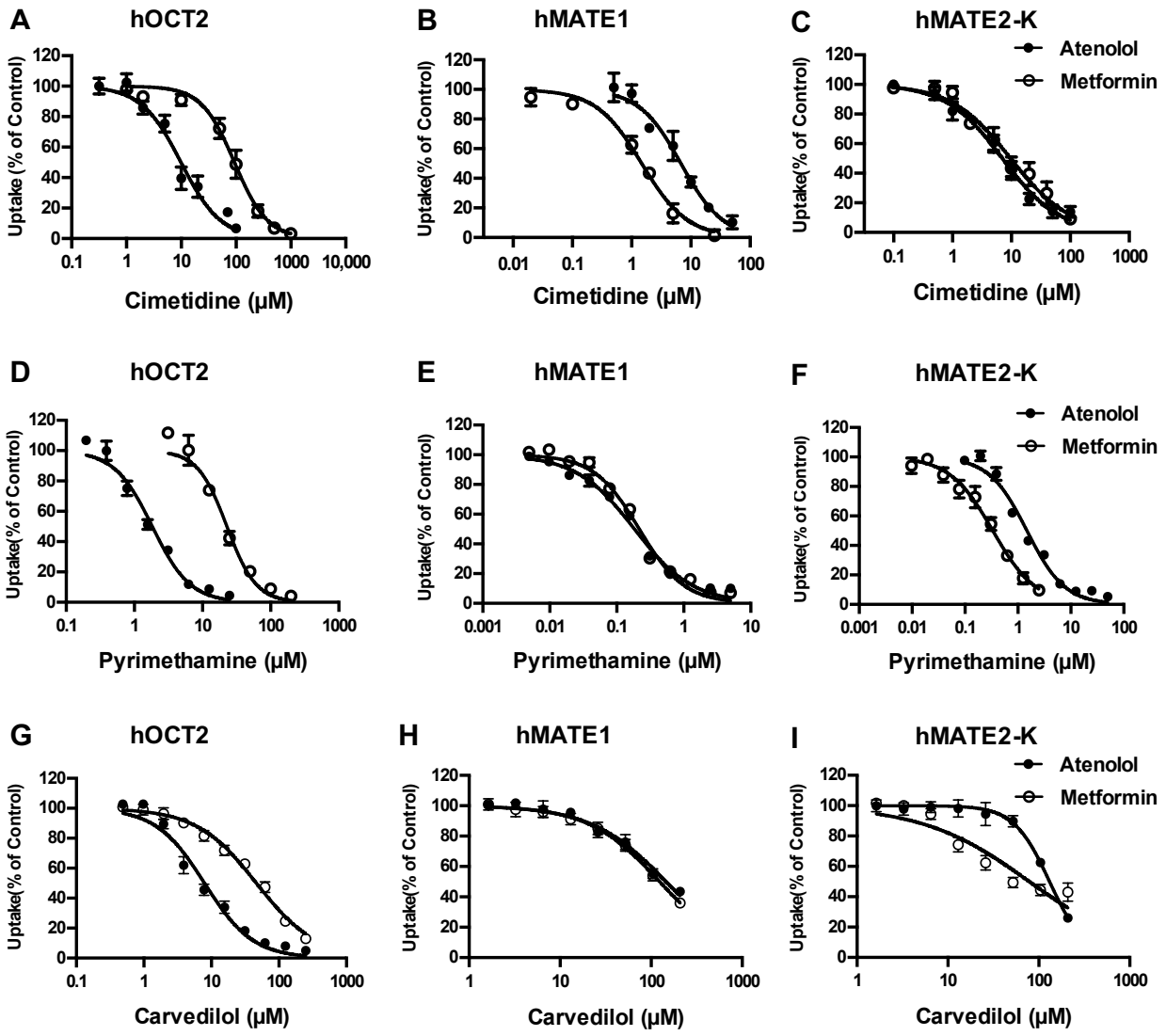

Figure 5.1 Inhibition of hOCT2, hMATE1 and hMATE2-K-by cimetidine, pyrimethamine and carvedilol using atenolol or metformin as the probe substrate. Cells were incubated in KRH buffer containing either 1 μM atenolol or 5.5 μM metformin for 2 min in the presence of an inhibitor at graded concentrations. Transporter-specific uptake was calculated by subtracting the uptake in vector-transfected HEK293 cells and presented as percentage of the uptake determined in the absence of an inhibitor. All experiments were repeated 2 -3 times and data were presented as mean ± SD.

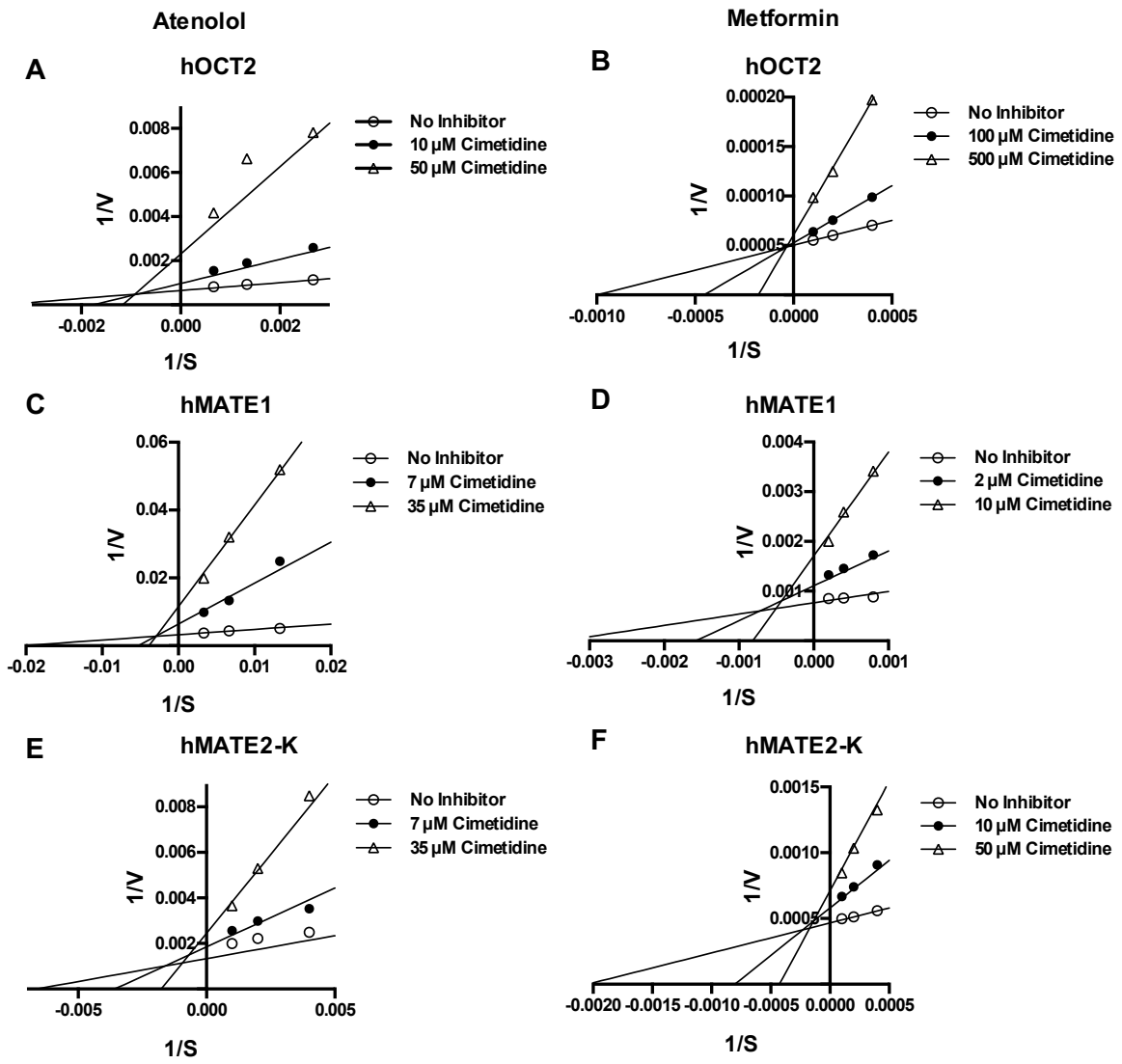

Figure 5.2 Effect of cimetidine inhibition on atenolol or metformin transport kinetics of hOCT2, hMATE1 and 2-K. Concentration-dependent uptake of atenolol and metformin was measured in both transporter-expressing and control HEK293 cells after a 2 min incubation in the presence of cimetidine at specified concentration (0, IC_{50}, and 5xIC_{50}). Transporter-specific uptake was obtained by subtracting the uptake in control cells from the uptake in transporter-expressing cells. While all kinetic data points were used for the generation of Lineweaver-Burk plots, only the close-up view at lower x and y range was presented in order to clearly show where the lines converge.

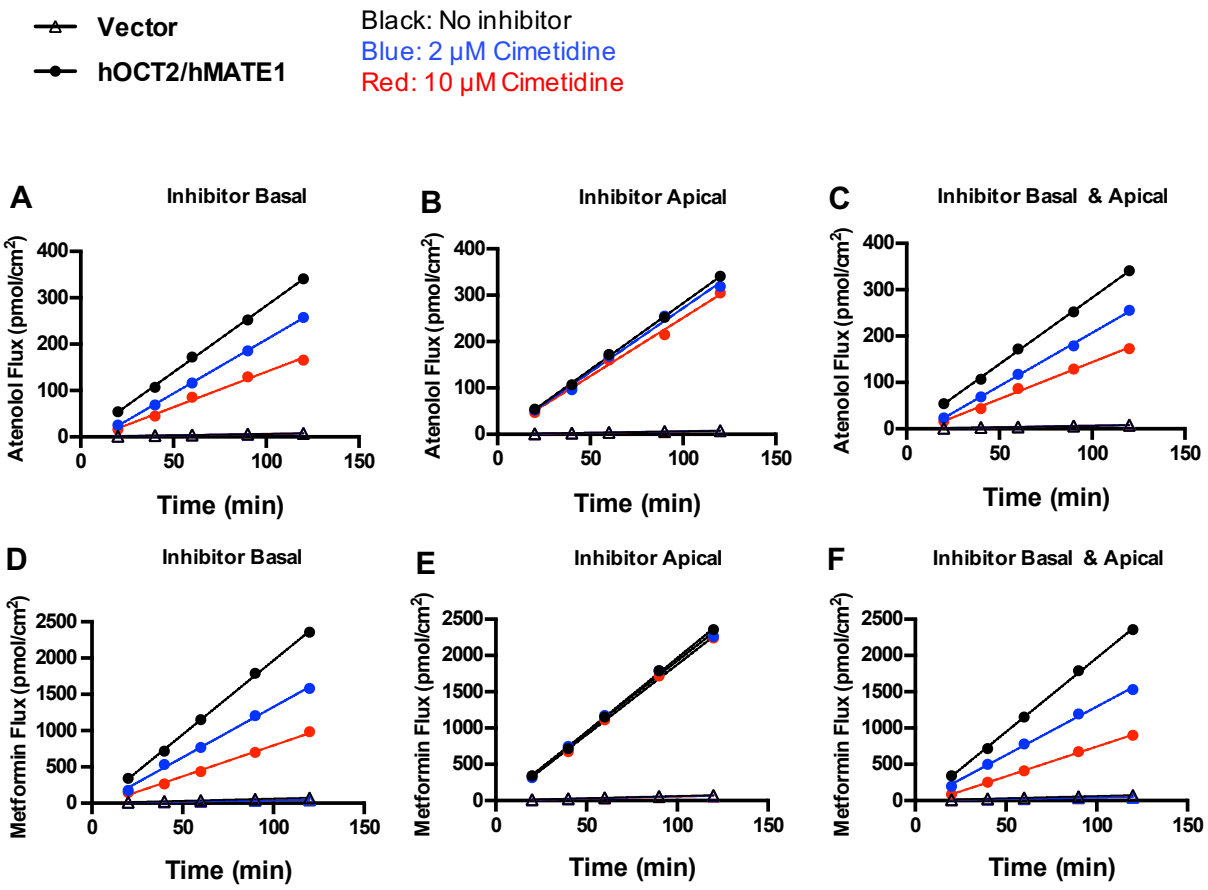

Figure 5.3 Effects of cimetidine on B-to-A flux of atenolol and metformin in MDCK-hOCT2/hMATE1 cells. Cells were incubated in KRH buffer containing 1 µM atenolol or 5.5 µM metformin in the basal chamber. The pH in the apical and basal chambers was maintained at 6.0 and 7.4, respectively. B-to-A flux of atenolol and metformin was measured in the absence or presence of 2 µM or 10 µM of cimetidine. Cimetidine was added to the basal (A, D), apical (B, E) or both chambers (C, F). At various time points, 50 µl of sample was taken from the apical chamber and replenished with an equal volume of fresh KRH buffer.

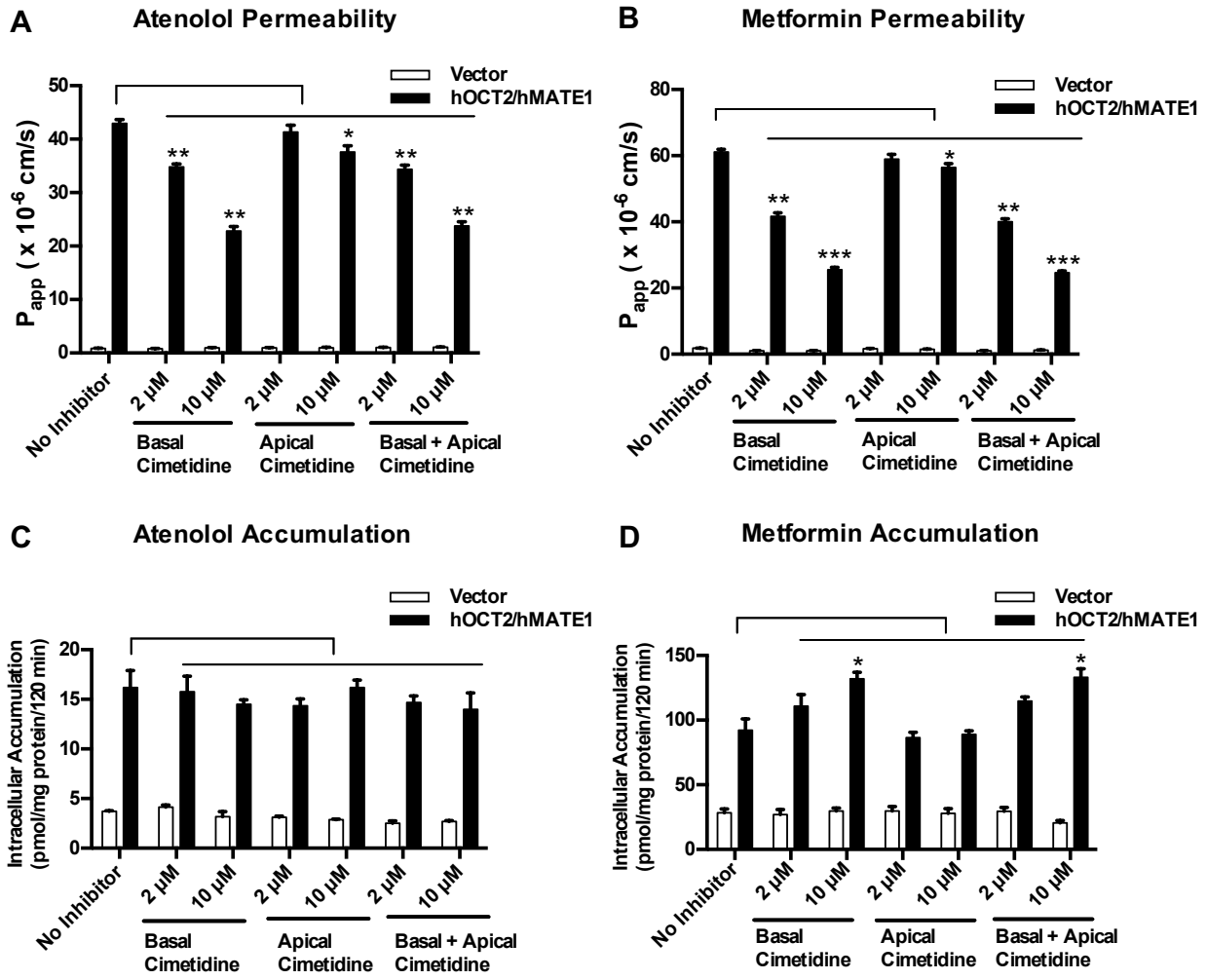

Figure 5.4 Effect of cimetidine inhibition on permeability and intracellular accumulation of atenolol and metformin in MDCK-hOCT2/hMATE1 cells. The B-to-A permeability of atenolol (A) and metformin (B) was calculated using the equation described in the Materials and Methods section. Intracellular accumulation of atenolol (C) and metformin (D) was measured at the end of the transwell study in the absence or presence of cimetidine (2 or 10 μM). Cimetidine was added to basal, apical, or both chambers at the start of the transwell experiment. *** $P < 0.001$, ** $P < 0.01$, * $P < 0.05$ indicates significantly different from no inhibitor control.

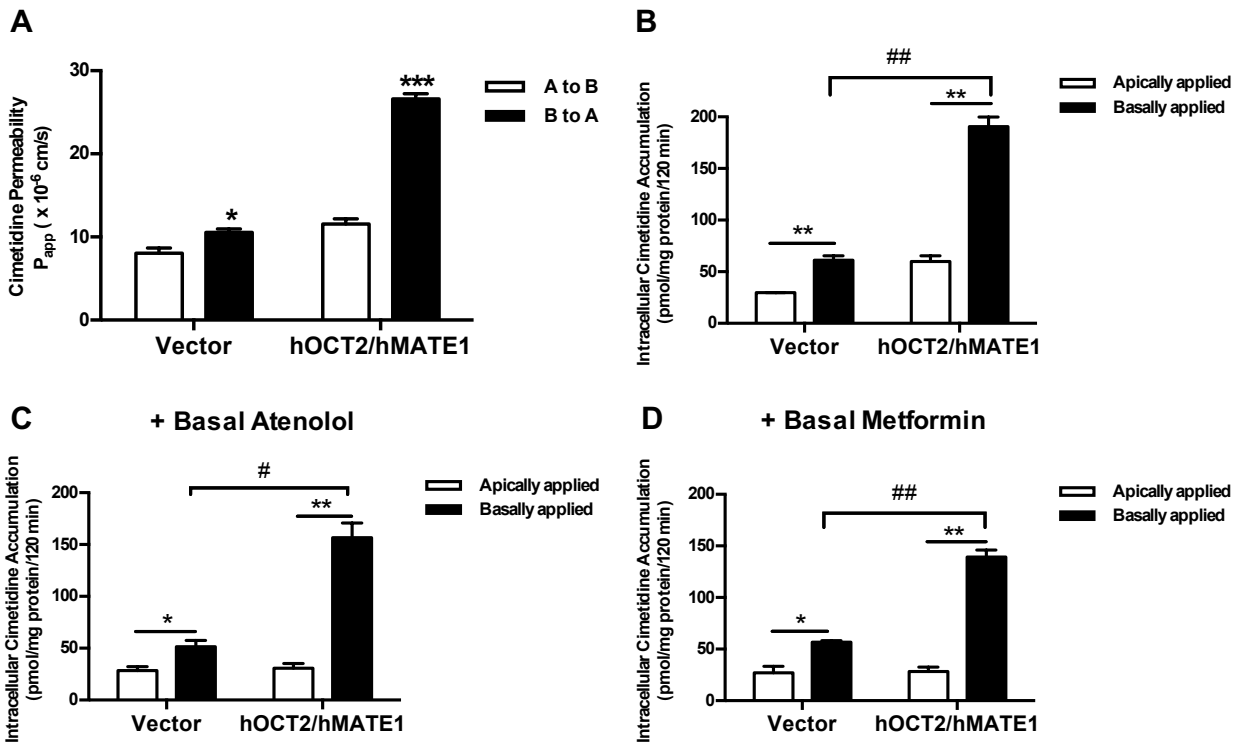

Figure 5.5 Cimetidine permeability and intracellular accumulation in MDCK-hOCT2/hMATE1 cells. Vector- and hOCT2/hMATE1-transfected MDCK cells growing on inserts were incubated in KRH buffer with [^{3}H]cimetidine (10 μM) added to either apical (pH 6.0) or basal chamber (pH 7.4). An aliquot of buffer in the receiving chamber was sampled periodically up to 120 min. (A) Cimetidine permeability in the B-to-A and A-to-B directions was measured and compared (*** $P < 0.001$, * $P < 0.05$). (B-D**)** Intracellular accumulation of [^{3}H]cimetidine (10 μM) after applying to basal or apical chamber alone or with cold atenolol (1 μM) or metformin (5.5 μM) added in the basal chamber. ** $P < 0.01$, * $P < 0.05$ indicates significantly higher accumulation when cimetidine is applied to the basal chamber than the apical chamber. ## $P < 0.01$, # $P < 0.05$ indicates significantly higher accumulation in hOCT2/hMATE1 cells than in vector control.

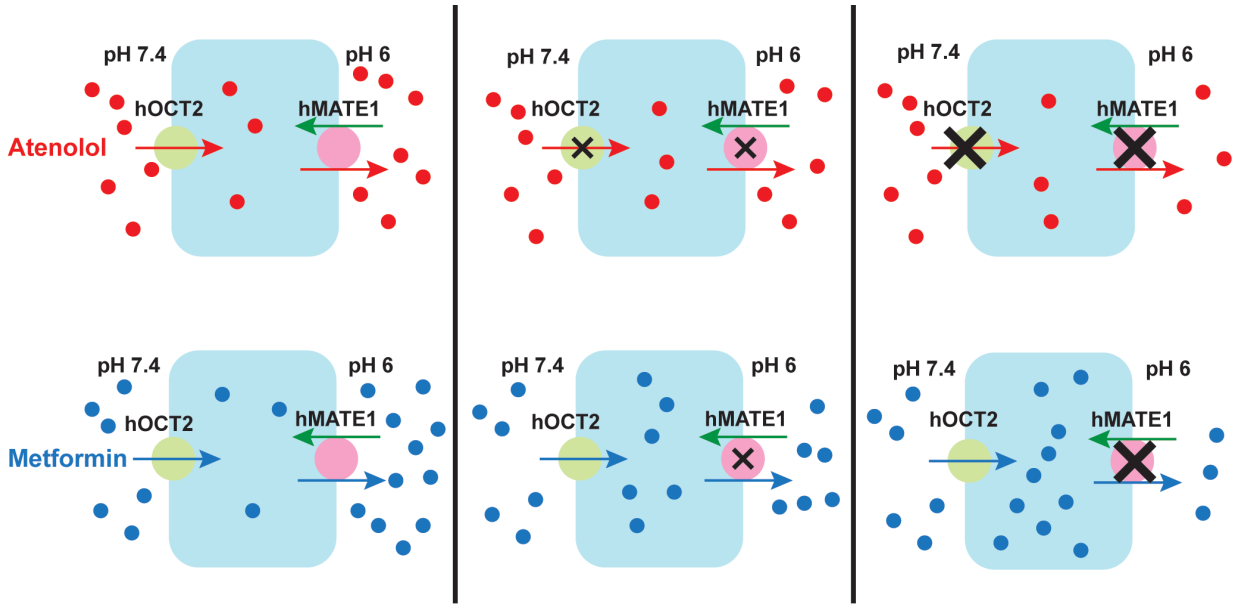

Figure 5.6. Hypothesized effects and sites of interaction for cimetidine on renal tubular secretion and intracellular accumulation of atenolol and metformin. For atenolol, cimetidine inhibits hOCT2 and hMATE1 with equal potency. At clinically relevant concentrations, cimetidine dose-dependently reduces atenolol tubular secretion but has no effect on intracellular accumulation. For metformin, cimetidine mainly inhibits hMATE1. Cimetidine not only reduces metformin tubular secretion but also increases its intracellular accumulation in a dose-dependent manner.

Table 5.1 Cimetidine IC_{50} values for atenolol and metformin.

Inhibitor	Transporter	IC_{50} (μM)		*P* Value	Fold Difference
		Atenolol	Metformin		
Cimetidine	hOCT2	9.9 ± 1.1	93.5 ± 1.1	$P < 0.001$	9.4 [a]
	hMATE1	6.7 ± 1.2	1.5 ± 1.0	$P < 0.01$	4.5 [b]
	hMATE2-K	7.1 ± 1.1	9.7 ± 1.3	$P = 0.057$	1.4 [a]
Pyrimethamine	hOCT2	1.8 ± 0.2	22.9 ± 1.9	$P < 0.001$	12.7 [a]
	hMATE1	0.18 ± 0.006	0.22 ± 0.01	$P < 0.01$	1.2 [a]
	hMATE2-K	1.5 ± 0.07	0.3 ± 0.06	$P < 0.001$	5.0 [b]
Carvedilol	hOCT2	7.9 ± 0.6	46.4 ± 0.4	$P < 0.001$	5.9 [a]
	hMATE1	146.4 ± 0.9	124.2 ± 4.3	$P < 0.001$	1.2 [b]
	hMATE2-K	131.2 ± 4.2	78.6 ± 12.5	$P < 0.001$	1.7 [b]

[a.] IC_{50} for metformin/IC_{50} for atenolol

[b.] IC_{50} for atenolol/IC_{50} for metformin

Table 5.2 Comparison of cimetidine IC_{50} and K_i values.

Transporter	Substrate	IC_{50} (μM)	K_i (μM)
hOCT2	Atenolol	9.9 ± 1.1	5.0
	Metformin	93.5 ± 1.1	94.5
hMATE1	Atenolol	6.7 ± 1.2	6.8
	Metformin	1.5 ± 1.0	1.4
hMATE2-K	Atenolol	7.1 ± 1.1	7.0
	Metformin	9.7 ± 1.3	9.2

Table 5.3 Prediction of hOCT2 DDIs following FDA decision tree.

	Atenolol	Metformin	MPP^+
hOCT2			
IC_{50}	9.9	93.5	146 [b]
Cimetidine unbound C_{max}/IC_{50} [a]	0.8	0.09	0.05
Recommendation for in vivo DDI study	Yes	Yes/No	No
hMATE1			
IC_{50}	6.7	1.5	2.7 [b]
Cimetidine unbound C_{max}/IC_{50} [a]	1.2	5.3	3.0
Recommendation for in vivo DDI study	Yes	Yes	Yes
hMATE2-K			
IC_{50}	7.1	9.7	4.0 [b]
Cimetidine unbound C_{max}/IC_{50} [a]	1.1	0.8	2.0
Recommendation for in vivo DDI study	Yes	Yes	Yes

[a.] Cimetidine unbound C_{max} = 8 μM was used for calculation. Value is from *Goodman & Gilman's The Pharmacological Basis of Therapeutics*. 11th edn. (McGraw-Hill Medical, New York, 2011).

[b.] Value is from Ito, S. et al. *J Pharmacol Exp Ther* **340**, 393-403 (2012).

Chapter 6. Conclusions and Future Directions

The kidney is a vital organ for elimination of therapeutic drugs and their metabolites. Cellular drug transport proteins localized in the renal proximal tubules play an important role in drug disposition, efficacy and toxicity. Like drug-metabolizing enzymes, they are also the target sites for drug-drug interactions. However, although substantial progress has been made in basic drug transporter research, the role of drug transporters in renal clearance of commonly prescribed drugs and the mechanisms of renal transporter-mediated DDIs are still poorly understood. This dissertation research focused on understanding the clinical significance of renal drug transporters and their role in drug interactions. The studies were designed to: 1) evaluate the clinical significance of renal transporter-mediated DDIs using top 200 prescribed drugs as sample dataset; 2) identify major drug transporters in renal elimination of two highly renally secreted antihypertensive drugs: atenolol and hydrochlorothiazide; 3) characterize the effect of substrate-dependent inhibition on hOCT2/hMATE-mediated drug secretion and evaluate its impact on renal DDI and toxicity assessment.

In Chapter 2, an analysis of the top 200 prescribed drugs in U.S. and their DDI studies suggests that renal transporter-mediated DDI risk is substantial. Potent drug transport inhibitors elicit significant interactions in vivo that approach maximums predicted from in vitro-derived inhibition kinetics. However, high-magnitude renal DDIs in the clinical setting appear to be rare, which may be due to 1) compensating transport pathways for the same drug, 2) a lack of potent in vivo inhibitors and 3) a lack of sensitive probes for renal drug transporters. By choosing the appropriate in vivo inhibitors and sensitive probe substrates, more clinically significant renal DDIs might be observed.

In Chapter 3, we showed that atenolol is an excellent substrate for the renal organic cation transporters hOCT2, hMATE1 and hMATE2-K, but not a substrate for renal organic anion transporters hOAT1 and hOAT3. Using hOCT2/hMATE1 double-transfected MDCK monolayer culture, we further demonstrated unidirectional transepithelial flux of atenolol mediated by hOCT2/hMATE1. Together, our data suggest that tubular secretion of atenolol in the kidney is mediated primarily by the hOCT2/hMATEs pathway. Because the radiolabeled form of atenolol is commercially available, it should be an ideal, clinically relevant in vitro and in vivo probe for assessing hOCT2 and hMATE1/2-K function.

In Chapter 4, we showed that hydrochlorothiazide is transported by both organic anion transporters, hOAT1 and hOAT3, and the organic cation transporters hOCT2 and hMATE2-K, although hOCT2 and hMATE2-K showed much lower affinity and efficiency in transporting hydrochlorothiazide. Combined with findings from other investigators, our data suggest that renal tubular secretion of hydrochlorothiazide is mediated by two parallel pathways, with hOATs/hMRP4 being the major one and hOCT2/hMATE2-K being a minor pathway. This concept may be further tested by comparing hydrochlorothiazide transepithelial permeability in double-transfected MDCK cell lines expressing hOAT1/hMRP4, hOAT3/hMRP4 or hOCT2/hMATE2-K. Our studies also suggest that caution should be taken when hydrochlorothiazide is co-prescribed with potent hOAT1/3 inhibitors, as renal secretion is not only important for its elimination but also its efficacy.

In Chapter 5, we investigated the impact of substrate-dependent inhibition on predicting transporter-mediated drug interaction and accumulation by focusing on the hOCT2/hMATE-mediated renal secretion pathway. Screening a series of drug substrates, our data clearly showed that inhibition of basolateral hOCT2 is highly dependent on the identity of the substrate, leading

to strikingly different predictions of hOCT2-mediated DDI risk. Using a cell culture model simulating tubular OC secretion, we further demonstrated that substrate-dependent inhibition can shift the major substrate-inhibitor interacting site between apical and basolateral transporters, leading to different effects on intracellular drug accumulation. These findings revealed the complex and dynamic nature of substrate-inhibitor interactions in multispecific drug transporters and highlighted the necessity of considering substrate-dependent inhibition in predicting transporter-mediated DDIs.

In summary, my dissertation research has contributed greatly to our understanding of the role of renal transporters in drug disposition, the clinical significance of renal DDIs and the impact of substrate-dependent inhibition on predicting transporter-mediated drug interaction and accumulation. However, there are still significant gaps in our knowledge and challenges to predict and understand DDIs medicated by renal drug transporters. For example, it is still difficult to precisely locate the actual sites (apical versus basal membranes) and magnitudes of renal DDIs in vivo. While the plasma concentrations of the inhibitor drug are used for DDI prediction, the actual concentrations of inhibitor that the transporter encounters at the site of inhibition may be significantly different and difficult to measure. Lastly, substrate-dependent as well as time-dependent inhibition, further complicates the assessment and in vitro-to-in vivo prediction of DDIs. Nevertheless, the field of drug transporter pharmacology is rapidly evolving. With the conceptual and technological advancements in drug transport research, we are now in position to gain a better understanding of renal drug transporters, predict and ameliorate the consequences of renal DDIs, and to design beneficial DDIs that might improve drug efficacy and minimize drug toxicity.

Bibliography

Agon P, Goethals P, Van Haver D, and Kaufman JM (1991) Permeability of the blood-brain barrier for atenolol studied by positron emission tomography. *J Pharm Pharmacol* **43:**597-600.

Agrawal H, Aggarwal K, Littrell R, Velagapudi P, Turagam MK, Mittal M, and Alpert MA (2015) Pharmacological and non pharmacological strategies in the management of coronary artery disease and chronic kidney disease. *Curr Cardiol Rev* **11:**261-269.

Aherne GW, Piall E, Marks V, Mould G, and White WF (1978) Prolongation and enhancement of serum methotrexate concentrations by probenecid. *Br Med J* **1:**1097-1099.

Ahlin G, Hilgendorf C, Karlsson J, Szigyarto CA, Uhlen M, and Artursson P (2009) Endogenous gene and protein expression of drug-transporting proteins in cell lines routinely used in drug discovery programs. *Drug Metab Dispos* **37:**2275-2283.

Ahlin G, Karlsson J, Pedersen JM, Gustavsson L, Larsson R, Matsson P, Norinder U, Bergstrom CA, and Artursson P (2008) Structural requirements for drug inhibition of the liver specific human organic cation transport protein 1. *J Med Chem* **51:**5932-5942.

Ahn SY, Eraly SA, Tsigelny I, and Nigam SK (2009) Interaction of organic cations with organic anion transporters. *J Biol Chem* **284:**31422-31430.

Akanuma S, Uchida Y, Ohtsuki S, Kamiie J, Tachikawa M, Terasaki T, and Hosoya K (2011) Molecular-weight-dependent, anionic-substrate-preferential transport of beta-lactam antibiotics via multidrug resistance-associated protein 4. *Drug Metab Pharmacokinet* **26:**602-611.

Andreasen F, Hansen U, Husted SE, and Jansen JA (1983) The pharmacokinetics of frusemide are influenced by age. *Br J Clin Pharmacol* **16:**391-397.

Annaert P, Ye ZW, Stieger B, and Augustijns P (2010) Interaction of HIV protease inhibitors with OATP1B1, 1B3, and 2B1. *Xenobiotica* **40:**163-176.

Augustijns P and Mols R (2004) HPLC with programmed wavelength fluorescence detection for the simultaneous determination of marker compounds of integrity and P-gp functionality in the Caco-2 intestinal absorption model. *J Pharm Biomed Anal* **34:**971-978.

Avdeef A (2010) Leakiness and size exclusion of paracellular channels in cultured epithelial cell monolayers-interlaboratory comparison. *Pharm Res* **27:**480-489.

Bachmakov I, Glaeser H, Endress B, Morl F, Konig J, and Fromm MF (2009) Interaction of beta-blockers with the renal uptake transporter OCT2. *Diabetes Obes Metab* **11:**1080-1083.

Bahn A, Ebbinghaus C, Ebbinghaus D, Ponimaskin EG, Fuzesi L, Burckhardt G, and Hagos Y (2004) Expression studies and functional characterization of renal human organic anion transporter 1 isoforms. *Drug Metab Dispos* **32:**424-430.

Bahn A, Hagos Y, Reuter S, Balen D, Brzica H, Krick W, Burckhardt BC, Sabolic I, and Burckhardt G (2008) Identification of a new urate and high affinity nicotinate transporter, hOAT10 (SLC22A13). *J Biol Chem* **283:**16332-16341.

Barriere SL, Catlin DH, Orlando PL, Noe A, and Frost RW (1990) Alteration in the pharmacokinetic disposition of ciprofloxacin by simultaneous administration of azlocillin. *Antimicrob Agents Chemother* **34:**823-826.

Baur G, Kurz H, and Trunk H (1977) Alteration of protein-binding during storage of human plasma preparations. *Anaesthesist* **26:**148-150.

Bednarczyk D (2010) Fluorescence-based assays for the assessment of drug interaction with the human transporters OATP1B1 and OATP1B3. *Anal Biochem* **405:**50-58.

Beermann B and Groschinsky-Grind M (1977) Pharmacokinetics of hydrochlorothiazide in man. *Eur J Clin Pharmacol* **12:**297-303.

Beermann B, Groschinsky-Grind M, and Rosen A (1976) Absorption, metabolism, and excretion of hydrochlorothiazide. *Clin Pharmacol Ther* **19:**531-537.

Belinsky MG, Bain LJ, Balsara BB, Testa JR, and Kruh GD (1998) Characterization of MOAT-C and MOAT-D, new members of the MRP/cMOAT subfamily of transporter proteins. *J Natl Cancer Inst* **90:**1735-1741.

Belzer M, Morales M, Jagadish B, Mash EA, and Wright SH (2013) Substrate-dependent ligand inhibition of the human organic cation transporter OCT2. *J Pharmacol Exp Ther* **346:**300-310.

Bentz J, O'Connor MP, Bednarczyk D, Coleman J, Lee C, Palm J, Pak YA, Perloff ES, Reyner E, Balimane P, Brannstrom M, Chu X, Funk C, Guo A, Hanna I, Heredi-Szabo K, Hillgren K, Li L, Hollnack-Pusch E, Jamei M, Lin X, Mason AK, Neuhoff S, Patel A, Podila L, Plise E, Rajaraman G, Salphati L, Sands E, Taub ME, Taur JS, Weitz D, Wortelboer HM, Xia CQ, Xiao G, Yabut J, Yamagata T, Zhang L, and Ellens H (2013) Variability in P-glycoprotein inhibitory potency (IC(5)(0)) using various in vitro experimental systems: implications for universal digoxin drug-drug interaction risk assessment decision criteria. *Drug Metab Dispos* **41:**1347-1366.

Berginc K, Zakelj S, and Kristl A (2010) In vitro interactions between aged garlic extract and drugs used for the treatment of cardiovascular and diabetic patients. *Eur J Nutr* **49:**373-384.

Bergman A, Ebel D, Liu F, Stone J, Wang A, Zeng W, Chen L, Dilzer S, Lasseter K, Herman G, Wagner J, and Krishna R (2007a) Absolute bioavailability of sitagliptin, an oral

dipeptidyl peptidase-4 inhibitor, in healthy volunteers. *Biopharm Drug Dispos* **28:**315-322.

Bergman AJ, Cote J, Yi B, Marbury T, Swan SK, Smith W, Gottesdiener K, Wagner J, and Herman GA (2007b) Effect of renal insufficiency on the pharmacokinetics of sitagliptin, a dipeptidyl peptidase-4 inhibitor. *Diabetes Care* **30:**1862-1864.

Beyer KH, Jr. and Baer JE (1967) Enzymes, drugs and transport phenomena. *Protoplasma* **63:**113-120.

Bhad P, Ayalasomayajula S, Karan R, Leon S, Riviere GJ, Sunkara G, and Jarugula V (2011) Evaluation of pharmacokinetic interactions between amlodipine, valsartan, and hydrochlorothiazide in patients with hypertension. *J Clin Pharmacol* **51:**933-942.

Bourdet DL, Pritchard JB, and Thakker DR (2005) Differential substrate and inhibitory activities of ranitidine and famotidine toward human organic cation transporter 1 (hOCT1; SLC22A1), hOCT2 (SLC22A2), and hOCT3 (SLC22A3). *J Pharmacol Exp Ther* **315:**1288-1297.

Boyd RA, Chin SK, Don-Pedro O, Williams RL, and Giacomini KM (1989) The pharmacokinetics of the enantiomers of atenolol. *Clin Pharmacol Ther* **45:**403-410.

Brouwer KL, Keppler D, Hoffmaster KA, Bow DA, Cheng Y, Lai Y, Palm JE, Stieger B, and Evers R (2013) In vitro methods to support transporter evaluation in drug discovery and development. *Clin Pharmacol Ther* **94:**95-112.

Brown HC, Carruthers SG, Johnston GD, Kelly JG, McAinsh J, McDevitt DG, and Shanks RG (1976) Clinical pharmacologic observations on atenolol, a beta-adrenoceptor blocker. *Clin Pharmacol Ther* **20:**524-534.

Brusch JL, Bergeron MG, Barza M, and Weinstein L (1974) An in vitro and pharmacological comparison of amoxicillin and ampicillin. *Am J Med Sci* **267:**41-48.

Burckhardt G (2012) Drug transport by Organic Anion Transporters (OATs). *Pharmacol Ther* **136:**106-130.

Chandra P and Brouwer KL (2004) The complexities of hepatic drug transport: current knowledge and emerging concepts. *Pharm Res* **21:**719-735.

Chatton JY, Munafo A, Chave JP, Steinhauslin F, Roch-Ramel F, Glauser MP, and Biollaz J (1992) Trimethoprim, alone or in combination with sulphamethoxazole, decreases the renal excretion of zidovudine and its glucuronide. *Br J Clin Pharmacol* **34:**551-554.

Chen C, Liu X, and Smith BJ (2003) Utility of Mdr1-gene deficient mice in assessing the impact of P-glycoprotein on pharmacokinetics and pharmacodynamics in drug discovery and development. *Curr Drug Metab* **4:**272-291.

Chen L, Pawlikowski B, Schlessinger A, More SS, Stryke D, Johns SJ, Portman MA, Chen E, Ferrin TE, Sali A, and Giacomini KM (2010) Role of organic cation transporter 3 (SLC22A3) and its missense variants in the pharmacologic action of metformin. *Pharmacogenet Genomics* **20:**687-699.

Chien SC, Rogge MC, Gisclon LG, Curtin C, Wong F, Natarajan J, Williams RR, Fowler CL, Cheung WK, and Chow AT (1997) Pharmacokinetic profile of levofloxacin following once-daily 500-milligram oral or intravenous doses. *Antimicrob Agents Chemother* **41:**2256-2260.

Chobanian AV, Bakris GL, Black HR, Cushman WC, Green LA, Izzo JL, Jr., Jones DW, Materson BJ, Oparil S, Wright JT, Jr., and Roccella EJ (2003) Seventh report of the Joint National Committee on Prevention, Detection, Evaluation, and Treatment of High Blood Pressure. *Hypertension* **42:**1206-1252.

Choi MK, Jin QR, Jin HE, Shim CK, Cho DY, Shin JG, and Song IS (2007) Effects of tetraalkylammonium compounds with different affinities for organic cation transporters on the pharmacokinetics of metformin. *Biopharm Drug Dispos* **28:**501-510.

Choi MK and Song IS (2012) Genetic variants of organic cation transporter 1 (OCT1) and OCT2 significantly reduce lamivudine uptake. *Biopharm Drug Dispos* **33:**170-178.

Chrysant SG (2003) Fixed combination therapy of hypertension: focus on valsartan/hydrochlorothiazide combination (Diovan/HCT). *Expert Rev Cardiovasc Ther* **1:**335-343.

Chu X, Cai X, Cui D, Tang C, Ghosal A, Chan G, Green MD, Kuo Y, Liang Y, Maciolek CM, Palamanda J, Evers R, and Prueksaritanont T (2013a) In vitro assessment of drug-drug interaction potential of boceprevir associated with drug metabolizing enzymes and transporters. *Drug Metab Dispos* **41:**668-681.

Chu X, Korzekwa K, Elsby R, Fenner K, Galetin A, Lai Y, Matsson P, Moss A, Nagar S, Rosania GR, Bai JP, Polli JW, Sugiyama Y, and Brouwer KL (2013b) Intracellular drug concentrations and transporters: measurement, modeling, and implications for the liver. *Clin Pharmacol Ther* **94:**126-141.

Chu XY, Bleasby K, Yabut J, Cai X, Chan GH, Hafey MJ, Xu S, Bergman AJ, Braun MP, Dean DC, and Evers R (2007) Transport of the dipeptidyl peptidase-4 inhibitor sitagliptin by human organic anion transporter 3, organic anion transporting polypeptide 4C1, and multidrug resistance P-glycoprotein. *J Pharmacol Exp Ther* **321:**673-683.

Ciarimboli G, Schroter R, Neugebauer U, Vollenbroker B, Gabriels G, Brzica H, Sabolic I, Pietig G, Pavenstadt H, Schlatter E, and Edemir B (2013) Kidney transplantation down-regulates expression of organic cation transporters, which translocate beta-blockers and fluoroquinolones. *Mol Pharm* **10:**2370-2380.

Cihlar T, Lin DC, Pritchard JB, Fuller MD, Mendel DB, and Sweet DH (1999) The antiviral nucleotide analogs cidofovir and adefovir are novel substrates for human and rat renal organic anion transporter 1. *Mol Pharmacol* **56:**570-580.

Cocquyt V, Kline WF, Gertz BJ, Van Belle SJ, Holland SD, DeSmet M, Quan H, Vyas KP, Zhang KE, De Greve J, and Porras AG (1999) Pharmacokinetics of intravenous alendronate. *J Clin Pharmacol* **39:**385-393.

Cummins CL, Jacobsen W, and Benet LZ (2002) Unmasking the dynamic interplay between intestinal P-glycoprotein and CYP3A4. *J Pharmacol Exp Ther* **300:**1036-1045.

Cundy KC, Petty BG, Flaherty J, Fisher PE, Polis MA, Wachsman M, Lietman PS, Lalezari JP, Hitchcock MJ, and Jaffe HS (1995) Clinical pharmacokinetics of cidofovir in human immunodeficiency virus-infected patients. *Antimicrob Agents Chemother* **39:**1247-1252.

Dahan A and Amidon GL (2009) Segmental dependent transport of low permeability compounds along the small intestine due to P-glycoprotein: the role of efflux transport in the oral absorption of BCS class III drugs. *Mol Pharm* **6:**19-28.

Dayton PG, Yu TF, Chen W, Berger L, West LA, and Gutman AB (1963) The physiological disposition of probenecid, including renal clearance, in man, studied by an improved method for its estimation in biological material. *J Pharmacol Exp Ther* **140:**278-286.

De Maine JB and Kirby WM (1970) Clinical pharmacology of cephalexin administered intravenously. *Antimicrob Agents Chemother (Bethesda)* **10:**190-194.

Debruyne D and Ryckelynck JP (1993) Clinical pharmacokinetics of fluconazole. *Clin Pharmacokinet* **24:**10-27.

Deeley RG, Westlake C, and Cole SP (2006) Transmembrane transport of endo- and xenobiotics by mammalian ATP-binding cassette multidrug resistance proteins. *Physiol Rev* **86:**849-899.

DeGorter MK, Xia CQ, Yang JJ, and Kim RB (2012) Drug transporters in drug efficacy and toxicity. *Annu Rev Pharmacol Toxicol* **52:**249-273.

Ding R, Tayrouz Y, Riedel KD, Burhenne J, Weiss J, Mikus G, and Haefeli WE (2004) Substantial pharmacokinetic interaction between digoxin and ritonavir in healthy volunteers. *Clin Pharmacol Ther* **76:**73-84.

Ding Y, Liu W, Jia Y, Lu C, Jin X, Yang J, Zhu Y, Yang L, Song Y, Ding L, and Wen A (2013) Effects of amlodipine on the oral bioavailability of cephalexin and cefuroxime axetil in healthy volunteers. *J Clin Pharmacol* **53:**82-86.

Dollery CT (2013) Intracellular drug concentrations. *Clin Pharmacol Ther* **93:**263-266.

Drusano GL, Standiford HC, Plaisance K, Forrest A, Leslie J, and Caldwell J (1986) Absolute oral bioavailability of ciprofloxacin. *Antimicrob Agents Chemother* **30:**444-446.

Duan H, Hu T, Foti R, Pan Y, Swaan P, and Wang J (2015) Potent and Selective Inhibition of Plasma Membrane Monoamine Transporter (PMAT) by HIV Protease Inhibitors. *Drug Metab Dispos*.

Duan H and Wang J (2010) Selective transport of monoamine neurotransmitters by human plasma membrane monoamine transporter and organic cation transporter 3. *J Pharmacol Exp Ther* **335:**743-753.

Duan P, Li S, Ai N, Hu L, Welsh WJ, and You G (2012) Potent inhibitors of human organic anion transporters 1 and 3 from clinical drug libraries: discovery and molecular characterization. *Mol Pharm* **9:**3340-3346.

Dukes JD, Whitley P, and Chalmers AD (2011) The MDCK variety pack: choosing the right strain. *BMC Cell Biol* **12:**43.

Dumortier J, Guillaud O, Gouraud A, Pittau G, Vial T, Boillot O, and Scoazec JY (2009) Atenolol hepatotoxicity: report of a complicated case. *Ann Pharmacother* **43:**1719-1723.

Ebner T, Ishiguro N, and Taub ME (2015) The Use of Transporter Probe Drug Cocktails for the Assessment of Transporter-Based Drug-Drug Interactions in a Clinical Setting-Proposal of a Four Component Transporter Cocktail. *J Pharm Sci* **104:**3220-3228.

Ekaratanawong S, Anzai N, Jutabha P, Miyazaki H, Noshiro R, Takeda M, Kanai Y, Sophasan S, and Endou H (2004) Human organic anion transporter 4 is a renal apical organic anion/dicarboxylate exchanger in the proximal tubules. *J Pharmacol Sci* **94:**297-304.

El-Sheikh AA, van den Heuvel JJ, Koenderink JB, and Russel FG (2007) Interaction of nonsteroidal anti-inflammatory drugs with multidrug resistance protein (MRP) 2/ABCC2- and MRP4/ABCC4-mediated methotrexate transport. *J Pharmacol Exp Ther* **320:**229-235.

Elsby R, Smith V, Fox L, Stresser D, Butters C, Sharma P, and Surry DD (2011) Validation of membrane vesicle-based breast cancer resistance protein and multidrug resistance protein 2 assays to assess drug transport and the potential for drug-drug interaction to support regulatory submissions. *Xenobiotica* **41:**764-783.

Enomoto A, Kimura H, Chairoungdua A, Shigeta Y, Jutabha P, Cha SH, Hosoyamada M, Takeda M, Sekine T, Igarashi T, Matsuo H, Kikuchi Y, Oda T, Ichida K, Hosoya T, Shimokata K, Niwa T, Kanai Y, and Endou H (2002) Molecular identification of a renal urate anion exchanger that regulates blood urate levels. *Nature* **417:**447-452.

FDA (2012) Guidance for Industry Drug Interaction Studies. http://wwwfdagov/downloads/Drugs/GuidanceComplianceRegulatoryInformation/Guidances/ucm292362pdf.

Feldman RD, Hussain Y, Kuyper LM, McAlister FA, Padwal RS, and Tobe SW (2015) Intraclass differences among antihypertensive drugs. *Annu Rev Pharmacol Toxicol* **55:**333-352.

Feng B, Hurst S, Lu Y, Varma MV, Rotter CJ, El-Kattan A, Lockwood P, and Corrigan B (2013) Quantitative prediction of renal transporter-mediated clinical drug-drug interactions. *Mol Pharm* **10:**4207-4215.

Fenner KS, Troutman MD, Kempshall S, Cook JA, Ware JA, Smith DA, and Lee CA (2009) Drug-drug interactions mediated through P-glycoprotein: clinical relevance and in vitro-in vivo correlation using digoxin as a probe drug. *Clin Pharmacol Ther* **85:**173-181.

Fenster PE, Hager WD, and Goodman MM (1984) Digoxin-quinidine-spironolactone interaction. *Clin Pharmacol Ther* **36:**70-73.

Filipski KK, Mathijssen RH, Mikkelsen TS, Schinkel AH, and Sparreboom A (2009) Contribution of organic cation transporter 2 (OCT2) to cisplatin-induced nephrotoxicity. *Clin Pharmacol Ther* **86:**396-402.

Flens MJ, Zaman GJ, van der Valk P, Izquierdo MA, Schroeijers AB, Scheffer GL, van der Groep P, de Haas M, Meijer CJ, and Scheper RJ (1996) Tissue distribution of the multidrug resistance protein. *Am J Pathol* **148:**1237-1247.

Flesch G, Muller P, and Lloyd P (1997) Absolute bioavailability and pharmacokinetics of valsartan, an angiotensin II receptor antagonist, in man. *Eur J Clin Pharmacol* **52:**115-120.

Fujita T, Urban TJ, Leabman MK, Fujita K, and Giacomini KM (2006) Transport of drugs in the kidney by the human organic cation transporter, OCT2 and its genetic variants. *J Pharm Sci* **95:**25-36.

Garg DC, Weidler DJ, and Eshelman FN (1983) Ranitidine bioavailability and kinetics in normal male subjects. *Clin Pharmacol Ther* **33:**445-452.

Giacomini KM (2010) Membrane transporters in drug development. *Nat Rev Drug Discov* **9:**215-236.

Giacomini KM, Huang SM, Tweedie DJ, Benet LZ, Brouwer KL, Chu X, Dahlin A, Evers R, Fischer V, Hillgren KM, Hoffmaster KA, Ishikawa T, Keppler D, Kim RB, Lee CA, Niemi M, Polli JW, Sugiyama Y, Swaan PW, Ware JA, Wright SH, Yee SW, Zamek-Gliszczynski MJ, and Zhang L (2010) Membrane transporters in drug development. *Nat Rev Drug Discov* **9:**215-236.

Goodman LS, Brunton LL, Blumenthal DK, Murri N, and Hilal-Dandan R (2011) *Goodman & Gilman's The Pharmacological Basis of Therapeutics*. McGraw-Hill Medical,, New York.

Gorboulev V, Ulzheimer JC, Akhoundova A, Ulzheimer-Teuber I, Karbach U, Quester S, Baumann C, Lang F, Busch AE, and Koepsell H (1997) Cloning and characterization of two human polyspecific organic cation transporters. *DNA Cell Biol* **16:**871-881.

Gramatte T, Oertel R, Terhaag B, and Kirch W (1996) Direct demonstration of small intestinal secretion and site-dependent absorption of the beta-blocker talinolol in humans. *Clin Pharmacol Ther* **59:**541-549.

Greene DS, Flanagan DR, Quintiliani R, and Nightingale CH (1976) Pharmacokinetics of cephalexin: an evaluation of one- and two-compartment model pharmacokinetics. *J Clin Pharmacol* **16:**257-264.

Greiner B, Eichelbaum M, Fritz P, Kreichgauer HP, von Richter O, Zundler J, and Kroemer HK (1999) The role of intestinal P-glycoprotein in the interaction of digoxin and rifampin. *J Clin Invest* **104:**147-153.

Gross AS and Somogyi AA (1994) Interaction of the stereoisomers of basic drugs with the uptake of tetraethylammonium by rat renal brush-border membrane vesicles. *J Pharmacol Exp Ther* **268:**1073-1080.

Grun B, Kiessling MK, Burhenne J, Riedel KD, Weiss J, Rauch G, Haefeli WE, and Czock D (2013) Trimethoprim-metformin interaction and its genetic modulation by OCT2 and MATE1 transporters. *Br J Clin Pharmacol* **76:**787-796.

Grundemann D, Gorboulev V, Gambaryan S, Veyhl M, and Koepsell H (1994) Drug excretion mediated by a new prototype of polyspecific transporter. *Nature* **372:**549-552.

Grundemann D, Harlfinger S, Golz S, Geerts A, Lazar A, Berkels R, Jung N, Rubbert A, and Schomig E (2005) Discovery of the ergothioneine transporter. *Proc Natl Acad Sci U S A* **102:**5256-5261.

Grundemann D, Schechinger B, Rappold GA, and Schomig E (1998) Molecular identification of the corticosterone-sensitive extraneuronal catecholamine transporter. *Nat Neurosci* **1:**349-351.

Guay DR (2000) Cefdinir: an expanded-spectrum oral cephalosporin. *Ann Pharmacother* **34:**1469-1477.

Gui C, Wahlgren B, Lushington GH, and Hagenbuch B (2009) Identification, Ki determination and CoMFA analysis of nuclear receptor ligands as competitive inhibitors of OATP1B1-mediated estradiol-17beta-glucuronide transport. *Pharmacol Res* **60:**50-56.

Hagenbuch B and Meier PJ (2003) The superfamily of organic anion transporting polypeptides. *Biochim Biophys Acta* **1609:**1-18.

Hagenbuch B and Meier PJ (2004) Organic anion transporting polypeptides of the OATP/ SLC21 family: phylogenetic classification as OATP/ SLCO superfamily, new nomenclature and molecular/functional properties. *Pflugers Arch* **447:**653-665.

Hagenbuch B and Stieger B (2013) The SLCO (former SLC21) superfamily of transporters. *Mol Aspects Med* **34:**396-412.

Hager WD, Fenster P, Mayersohn M, Perrier D, Graves P, Marcus FI, and Goldman S (1979) Digoxin-quinidine interaction Pharmacokinetic evaluation. *N Engl J Med* **300:**1238-1241.

Hagos Y, Stein D, Ugele B, Burckhardt G, and Bahn A (2007) Human renal organic anion transporter 4 operates as an asymmetric urate transporter. *J Am Soc Nephrol* **18:**430-439.

Han YF, Fan XH, Wang XJ, Sun K, Xue H, Li WJ, Wang YB, Chen JZ, Zhen YS, Zhang WL, Zhou X, and Hui R (2011) Association of intergenic polymorphism of organic anion transporter 1 and 3 genes with hypertension and blood pressure response to hydrochlorothiazide. *Am J Hypertens* **24:**340-346.

Hasannejad H, Takeda M, Taki K, Shin HJ, Babu E, Jutabha P, Khamdang S, Aleboyeh M, Onozato ML, Tojo A, Enomoto A, Anzai N, Narikawa S, Huang XL, Niwa T, and Endou H (2004) Interactions of human organic anion transporters with diuretics. *J Pharmacol Exp Ther* **308:**1021-1029.

Hasegawa M, Kusuhara H, Adachi M, Schuetz JD, Takeuchi K, and Sugiyama Y (2007) Multidrug resistance-associated protein 4 is involved in the urinary excretion of hydrochlorothiazide and furosemide. *J Am Soc Nephrol* **18:**37-45.

Haslam IS, Wright JA, O'Reilly DA, Sherlock DJ, Coleman T, and Simmons NL (2011) Intestinal ciprofloxacin efflux: the role of breast cancer resistance protein (ABCG2). *Drug Metab Dispos* **39:**2321-2328.

Hedaya MA and Helmy SA (2013) Pharmacokinetic interactions of valsartan and hydrochlorothiazide: an open-label, randomized, 4-period crossover study in healthy Egyptian male volunteers. *Clin Ther* **35:**846-861.

Heikkila AM and Erkkola RU (1993) The need for adjustment of dosage regimen of penicillin V during pregnancy. *Obstet Gynecol* **81:**919-921.

Hellinger E, Veszelka S, Toth AE, Walter F, Kittel A, Bakk ML, Tihanyi K, Hada V, Nakagawa S, Duy TD, Niwa M, Deli MA, and Vastag M (2012) Comparison of brain capillary endothelial cell-based and epithelial (MDCK-MDR1, Caco-2, and VB-Caco-2) cell-based surrogate blood-brain barrier penetration models. *Eur J Pharm Biopharm* **82:**340-351.

Hemauer SJ, Patrikeeva SL, Nanovskaya TN, Hankins GD, and Ahmed MS (2010) Role of human placental apical membrane transporters in the efflux of glyburide, rosiglitazone, and metformin. *Am J Obstet Gynecol* **202:**383 e381-387.

Hernandez-Canero A, Gonzalez A, Cardonne A, Perez-Medina T, and Garcia-Barreto D (1972) Effect of atenolol in angina pectoris of effort. *Cor Vasa* **20:**99-103.

Hill G, Cihlar T, Oo C, Ho ES, Prior K, Wiltshire H, Barrett J, Liu B, and Ward P (2002) The anti-influenza drug oseltamivir exhibits low potential to induce pharmacokinetic drug interactions via renal secretion-correlation of in vivo and in vitro studies. *Drug Metab Dispos* **30:**13-19.

Hillgren KM, Keppler D, Zur AA, Giacomini KM, Stieger B, Cass CE, Zhang L, and International Transporter C (2013) Emerging transporters of clinical importance: an update from the International Transporter Consortium. *Clin Pharmacol Ther* **94:**52-63.

Hoffken G, Lode H, Prinzing C, Borner K, and Koeppe P (1985) Pharmacokinetics of ciprofloxacin after oral and parenteral administration. *Antimicrob Agents Chemother* **27:**375-379.

Horikawa M, Kato Y, Tyson CA, and Sugiyama Y (2002) The potential for an interaction between MRP2 (ABCC2) and various therapeutic agents: probenecid as a candidate inhibitor of the biliary excretion of irinotecan metabolites. *Drug Metab Pharmacokinet* **17:**23-33.

Houtzagers JJ, Streurman O, and Regardh CG (1982) The effect of pretreatment with cimetidine on the bioavailability and disposition of atenolol and metoprolol. *Br J Clin Pharmacol* **14:**67-72.

Huls M, van den Heuvel JJ, Dijkman HB, Russel FG, and Masereeuw R (2006) ABC transporter expression profiling after ischemic reperfusion injury in mouse kidney. *Kidney Int* **69:**2186-2193.

Hulter HN, Licht JH, Ilnicki LP, and Singh S (1979) Clinical efficacy and pharmacokinetics of clonidine in hemodialysis and renal insufficiency. *J Lab Clin Med* **94:**223-231.

Humphrey MJ, Jevons S, and Tarbit MH (1985) Pharmacokinetic evaluation of UK-49,858, a metabolically stable triazole antifungal drug, in animals and humans. *Antimicrob Agents Chemother* **28:**648-653.

Ingraham L, Li M, Renfro JL, Parker S, Vapurcuyan A, Hanna I, and Pelis RM (2014) A plasma concentration of alpha-ketoglutarate influences the kinetic interaction of ligands with organic anion transporter 1. *Mol Pharmacol* **86:**86-95.

Inotsume N, Nishimura M, Nakano M, Fujiyama S, and Sato T (1990) The inhibitory effect of probenecid on renal excretion of famotidine in young, healthy volunteers. *J Clin Pharmacol* **30:**50-56.

Iqbal Z, Khan A, Naz A, Khan JA, and Khan GS (2009) Pharmacokinetic interaction of ciprofloxacin with diclofenac: a single-dose, two-period crossover study in healthy adult volunteers. *Clin Drug Investig* **29:**275-281.

Ito S, Kusuhara H, Kuroiwa Y, Wu C, Moriyama Y, Inoue K, Kondo T, Yuasa H, Nakayama H, Horita S, and Sugiyama Y (2010) Potent and specific inhibition of mMate1-mediated efflux of type I organic cations in the liver and kidney by pyrimethamine. *J Pharmacol Exp Ther* **333:**341-350.

Ito S, Kusuhara H, Yokochi M, Toyoshima J, Inoue K, Yuasa H, and Sugiyama Y (2012) Competitive inhibition of the luminal efflux by multidrug and toxin extrusions, but not basolateral uptake by organic cation transporter 2, is the likely mechanism underlying the

pharmacokinetic drug-drug interactions caused by cimetidine in the kidney. *J Pharmacol Exp Ther* **340:**393-403.

Izumi S, Nozaki Y, Komori T, Maeda K, Takenaka O, Kusano K, Yoshimura T, Kusuhara H, and Sugiyama Y (2013) Substrate-dependent inhibition of organic anion transporting polypeptide 1B1: comparative analysis with prototypical probe substrates estradiol-17beta-glucuronide, estrone-3-sulfate, and sulfobromophthalein. *Drug Metab Dispos* **41:**1859-1866.

Izumi S, Nozaki Y, Maeda K, Komori T, Takenaka O, Kusuhara H, and Sugiyama Y (2015) Investigation of the impact of substrate selection on in vitro organic anion transporting polypeptide 1B1 inhibition profiles for the prediction of drug-drug interactions. *Drug Metab Dispos* **43:**235-247.

Jacquemin E, Hagenbuch B, Stieger B, Wolkoff AW, and Meier PJ (1994) Expression cloning of a rat liver Na(+)-independent organic anion transporter. *Proc Natl Acad Sci U S A* **91:**133-137.

Jaehde U, Sorgel F, Reiter A, Sigl G, Naber KG, and Schunack W (1995) Effect of probenecid on the distribution and elimination of ciprofloxacin in humans. *Clin Pharmacol Ther* **58:**532-541.

Jeon H, Jang IJ, Lee S, Ohashi K, Kotegawa T, Ieiri I, Cho JY, Yoon SH, Shin SG, Yu KS, and Lim KS (2013) Apple juice greatly reduces systemic exposure to atenolol. *Br J Clin Pharmacol* **75:**172-179.

Jeon H, Lim KS, Shin KH, Kim J, Yoon SH, Cho JY, Shin SG, Jang IJ, and Yu KS (2012) Assessment of the drug-drug interactions between fimasartan and hydrochlorothiazide in healthy volunteers. *J Cardiovasc Pharmacol* **59:**84-91.

Jiang J, Tian L, Huang Y, Xie S, Xu L, Liu H, and Li Y (2011) Pharmacokinetic profiles of hydrochlorothiazide alone and in combination with benazepril or valsartan in healthy Chinese volunteers: evaluation of the potential interaction. *Int J Clin Pharmacol Ther* **49:**756-764.

Juliano RL and Ling V (1976) A surface glycoprotein modulating drug permeability in Chinese hamster ovary cell mutants. *Biochim Biophys Acta* **455:**152-162.

Jung JA, Noh YH, Jin S, Kim MJ, Kim YH, Jung JA, Lim HS, and Bae KS (2012) Pharmacokinetic interaction between pitavastatin and valsartan: a randomized, open-labeled crossover study in healthy male Korean volunteers. *Clin Ther* **34:**958-965.

K PA, Meda VS, Kucherlapati VS, Dubala A, M D, P RA, K E, and B S (2012) Pharmacokinetic drug interaction between gemfibrozil and sitagliptin in healthy Indian male volunteers. *Eur J Clin Pharmacol* **68:**709-714.

Karlgren M, Ahlin G, Bergstrom CA, Svensson R, Palm J, and Artursson P (2012) In vitro and in silico strategies to identify OATP1B1 inhibitors and predict clinical drug-drug interactions. *Pharm Res* **29:**411-426.

Kato Y, Miyazaki T, Kano T, Sugiura T, Kubo Y, and Tsuji A (2009) Involvement of influx and efflux transport systems in gastrointestinal absorption of celiprolol. *J Pharm Sci* **98:**2529-2539.

Kenworthy KE, Bloomer JC, Clarke SE, and Houston JB (1999) CYP3A4 drug interactions: correlation of 10 in vitro probe substrates. *Br J Clin Pharmacol* **48:**716-727.

Kimura N, Masuda S, Tanihara Y, Ueo H, Okuda M, Katsura T, and Inui K (2005a) Metformin is a superior substrate for renal organic cation transporter OCT2 rather than hepatic OCT1. *Drug Metab Pharmacokinet* **20:**379-386.

Kimura N, Okuda M, and Inui K (2005b) Metformin transport by renal basolateral organic cation transporter hOCT2. *Pharm Res* **22:**255-259.

Kirch W and Gorg KG (1982) Clinical pharmacokinetics of atenolol--a review. *Eur J Drug Metab Pharmacokinet* **7:**81-91.

Kirch W, Spahn H, Kohler H, Ohnhaus EE, and Mutschler E (1982) Interaction of metoprolol, propranolol and atenolol with concurrent administration of cimetidine. *Klin Wochenschr* **60:**1401-1407.

Kiser JJ, Carten ML, Aquilante CL, Anderson PL, Wolfe P, King TM, Delahunty T, Bushman LR, and Fletcher CV (2008) The effect of lopinavir/ritonavir on the renal clearance of tenofovir in HIV-infected patients. *Clin Pharmacol Ther* **83:**265-272.

Kiuchi Y, Suzuki H, Hirohashi T, Tyson CA, and Sugiyama Y (1998) cDNA cloning and inducible expression of human multidrug resistance associated protein 3 (MRP3). *FEBS Lett* **433:**149-152.

Koepsell H (2013) The SLC22 family with transporters of organic cations, anions and zwitterions. *Mol Aspects Med* **34:**413-435.

Koepsell H, Lips K, and Volk C (2007) Polyspecific organic cation transporters: structure, function, physiological roles, and biopharmaceutical implications. *Pharm Res* **24:**1227-1251.

Kolars JC, Lown KS, Schmiedlin-Ren P, Ghosh M, Fang C, Wrighton SA, Merion RM, and Watkins PB (1994) CYP3A gene expression in human gut epithelium. *Pharmacogenetics* **4:**247-259.

Kolars JC, Schmiedlin-Ren P, Schuetz JD, Fang C, and Watkins PB (1992) Identification of rifampin-inducible P450IIIA4 (CYP3A4) in human small bowel enterocytes. *J Clin Invest* **90:**1871-1878.

Komatsu T, Hiasa M, Miyaji T, Kanamoto T, Matsumoto T, Otsuka M, Moriyama Y, and Omote H (2011) Characterization of the human MATE2 proton-coupled polyspecific organic cation exporter. *Int J Biochem Cell Biol* **43:**913-918.

Konig J, Zolk O, Singer K, Hoffmann C, and Fromm MF (2011) Double-transfected MDCK cells expressing human OCT1/MATE1 or OCT2/MATE1: determinants of uptake and transcellular translocation of organic cations. *Br J Pharmacol* **163:**546-555.

Krishna R, Bergman A, Larson P, Cote J, Lasseter K, Dilzer S, Wang A, Zeng W, Chen L, Wagner J, and Herman G (2007) Effect of a single cyclosporine dose on the single-dose pharmacokinetics of sitagliptin (MK-0431), a dipeptidyl peptidase-4 inhibitor, in healthy male subjects. *J Clin Pharmacol* **47:**165-174.

Kroemer H and Klotz U (1987) Pharmacokinetics of famotidine in man. *Int J Clin Pharmacol Ther Toxicol* **25:**458-463.

Kullak-Ublick GA, Hagenbuch B, Stieger B, Schteingart CD, Hofmann AF, Wolkoff AW, and Meier PJ (1995) Molecular and functional characterization of an organic anion transporting polypeptide cloned from human liver. *Gastroenterology* **109:**1274-1282.

Kusuhara H, Ito S, Kumagai Y, Jiang M, Shiroshita T, Moriyama Y, Inoue K, Yuasa H, and Sugiyama Y (2011) Effects of a MATE protein inhibitor, pyrimethamine, on the renal elimination of metformin at oral microdose and at therapeutic dose in healthy subjects. *Clin Pharmacol Ther* **89:**837-844.

Kuteykin-Teplyakov K, Luna-Tortos C, Ambroziak K, and Loscher W (2010) Differences in the expression of endogenous efflux transporters in MDR1-transfected versus wildtype cell lines affect P-glycoprotein mediated drug transport. *Br J Pharmacol* **160:**1453-1463.

Kyrklund C, Backman JT, Neuvonen M, and Neuvonen PJ (2003) Gemfibrozil increases plasma pravastatin concentrations and reduces pravastatin renal clearance. *Clin Pharmacol Ther* **73:**538-544.

Landersdorfer CB, Kirkpatrick CM, Kinzig M, Bulitta JB, Holzgrabe U, Jaehde U, Reiter A, Naber KG, Rodamer M, and Sorgel F (2010) Competitive inhibition of renal tubular secretion of ciprofloxacin and metabolite by probenecid. *Br J Clin Pharmacol* **69:**167-178.

Laskin OL, de Miranda P, King DH, Page DA, Longstreth JA, Rocco L, and Lietman PS (1982) Effects of probenecid on the pharmacokinetics and elimination of acyclovir in humans. *Antimicrob Agents Chemother* **21:**804-807.

Lee N, Duan H, Hebert MF, Liang CJ, Rice KM, and Wang J (2014) Taste of a pill: organic cation transporter-3 (OCT3) mediates metformin accumulation and secretion in salivary glands. *J Biol Chem* **289:**27055-27064.

Lee N, Hebert MF, Prasad B, Easterling TR, Kelly EJ, Unadkat JD, and Wang J (2013) Effect of gestational age on mRNA and protein expression of polyspecific organic cation transporters during pregnancy. *Drug Metab Dispos* **41:**2225-2232.

Li M, Anderson GD, Phillips BR, Kong W, Shen DD, and Wang J (2006a) Interactions of amoxicillin and cefaclor with human renal organic anion and peptide transporters. *Drug Metab Dispos* **34:**547-555.

Li M, Anderson GD, and Wang J (2006b) Drug-drug interactions involving membrane transporters in the human kidney. *Expert Opin Drug Metab Toxicol* **2:**505-532.

Lilja JJ, Raaska K, and Neuvonen PJ (2005) Effects of orange juice on the pharmacokinetics of atenolol. *Eur J Clin Pharmacol* **61:**337-340.

Lin X, Skolnik S, Chen X, and Wang J (2011) Attenuation of intestinal absorption by major efflux transporters: quantitative tools and strategies using a Caco-2 model. *Drug Metab Dispos* **39:**265-274.

Liu S, Beringer PM, Hidayat L, Rao AP, Louie S, Burckart GJ, and Shapiro B (2008) Probenecid, but not cystic fibrosis, alters the total and renal clearance of fexofenadine. *J Clin Pharmacol* **48:**957-965.

Lockwood GF, Albert KS, Gillespie WR, Bole GG, Harkcom TM, Szpunar GJ, and Wagner JG (1983) Pharmacokinetics of ibuprofen in man. I. Free and total area/dose relationships. *Clin Pharmacol Ther* **34:**97-103.

Lowenthal DT, Matzek KM, and MacGregor TR (1988) Clinical pharmacokinetics of clonidine. *Clin Pharmacokinet* **14:**287-310.

MacGregor TR, Relihan GL, and Keirns JJ (1985) Pharmacokinetics of oral sustained release clonidine in humans. *Arzneimittelforschung* **35:**440-446.

Machavaram KK, Gundu J, and Yamsani MR (2006) Effect of ketoconazole and rifampicin on the pharmacokinetics of ranitidine in healthy human volunteers: a possible role of P-glycoprotein. *Drug Metabol Drug Interact* **22:**47-65.

Maeda K, Ieiri I, Yasuda K, Fujino A, Fujiwara H, Otsubo K, Hirano M, Watanabe T, Kitamura Y, Kusuhara H, and Sugiyama Y (2006) Effects of organic anion transporting polypeptide 1B1 haplotype on pharmacokinetics of pravastatin, valsartan, and temocapril. *Clin Pharmacol Ther* **79:**427-439.

Maeda K, Ikeda Y, Fujita T, Yoshida K, Azuma Y, Haruyama Y, Yamane N, Kumagai Y, and Sugiyama Y (2011) Identification of the rate-determining process in the hepatic clearance of atorvastatin in a clinical cassette microdosing study. *Clin Pharmacol Ther* **90:**575-581.

Mandery K, Balk B, Bujok K, Schmidt I, Fromm MF, and Glaeser H (2012) Inhibition of hepatic uptake transporters by flavonoids. *Eur J Pharm Sci* **46:**79-85.

Marcelin-Jimenez G, Angeles AP, Martinez-Rossier L, and Fernandez SA (2006) Ciprofloxacin bioavailability is enhanced by oral co-administration with phenazopyridine: a pharmacokinetic study in a Mexican population. *Clin Drug Investig* **26:**323-328.

Martin PD, Warwick MJ, Dane AL, Brindley C, and Short T (2003a) Absolute oral bioavailability of rosuvastatin in healthy white adult male volunteers. *Clin Ther* **25:**2553-2563.

Martin PD, Warwick MJ, Dane AL, Hill SJ, Giles PB, Phillips PJ, and Lenz E (2003b) Metabolism, excretion, and pharmacokinetics of rosuvastatin in healthy adult male volunteers. *Clin Ther* **25:**2822-2835.

Martinez V, Maguregui MI, Jimenez RM, and Alonso RM (2000) Determination of the pKa values of beta-blockers by automated potentiometric titrations. *J Pharm Biomed Anal* **23:**459-468.

Martinez-Guerrero LJ and Wright SH (2013) Substrate-dependent inhibition of human MATE1 by cationic ionic liquids. *J Pharmacol Exp Ther* **346:**495-503.

Masereeuw R and Russel FG (2001) Mechanisms and clinical implications of renal drug excretion. *Drug Metab Rev* **33:**299-351.

Mason JN, Farmer H, Tomlinson ID, Schwartz JW, Savchenko V, DeFelice LJ, Rosenthal SJ, and Blakely RD (2005) Novel fluorescence-based approaches for the study of biogenic amine transporter localization, activity, and regulation. *J Neurosci Methods* **143:**3-25.

Mason WD, Winer N, Kochak G, Cohen I, and Bell R (1979) Kinetics and absolute bioavailability of atenolol. *Clin Pharmacol Ther* **25:**408-415.

Masuda S, Terada T, Yonezawa A, Tanihara Y, Kishimoto K, Katsura T, Ogawa O, and Inui K (2006) Identification and functional characterization of a new human kidney-specific H+/organic cation antiporter, kidney-specific multidrug and toxin extrusion 2. *J Am Soc Nephrol* **17:**2127-2135.

Matsushima S, Maeda K, Inoue K, Ohta KY, Yuasa H, Kondo T, Nakayama H, Horita S, Kusuhara H, and Sugiyama Y (2009) The inhibition of human multidrug and toxin extrusion 1 is involved in the drug-drug interaction caused by cimetidine. *Drug Metab Dispos* **37:**555-559.

McLean MJ (1994) Clinical pharmacokinetics of gabapentin. *Neurology* **44:**S17-22; discussion S31-12.

Mehvar R, Gross ME, and Kreamer RN (1990) Pharmacokinetics of atenolol enantiomers in humans and rats. *J Pharm Sci* **79:**881-885.

Melin K (2014) Antihypertensives, in: *Lippincott Illustrated Reviews: Pharmacology* (Whalen K, Finkel R, and Panavelil T eds), Lippincott Williams & Wilkins, New York.

Meyer zu Schwabedissen HE, Verstuyft C, Kroemer HK, Becquemont L, and Kim RB (2010) Human multidrug and toxin extrusion 1 (MATE1/SLC47A1) transporter: functional characterization, interaction with OCT2 (SLC22A2), and single nucleotide polymorphisms. *Am J Physiol Renal Physiol* **298:**F997-F1005.

Mikkaichi T, Suzuki T, Onogawa T, Tanemoto M, Mizutamari H, Okada M, Chaki T, Masuda S, Tokui T, Eto N, Abe M, Satoh F, Unno M, Hishinuma T, Inui K, Ito S, Goto J, and Abe T (2004) Isolation and characterization of a digoxin transporter and its rat homologue expressed in the kidney. *Proc Natl Acad Sci U S A* **101:**3569-3574.

Minzi OM, Gupta A, Haule AF, Kagashe GA, Massele AY, and Gustafsson LL (2007) Lack of impact of artesunate on the disposition kinetics of sulfadoxine/pyrimethamine when the two drugs are concomitantly administered. *Eur J Clin Pharmacol* **63:**457-462.

Mitchell DY, Barr WH, Eusebio RA, Stevens KA, Duke FP, Russell DA, Nesbitt JD, Powell JH, and Thompson GA (2001) Risedronate pharmacokinetics and intra- and inter-subject variability upon single-dose intravenous and oral administration. *Pharm Res* **18:**166-170.

Mooradian AD (1988) Digitalis. An update of clinical pharmacokinetics, therapeutic monitoring techniques and treatment recommendations. *Clin Pharmacokinet* **15:**165-179.

Morgan DJ, Paull JD, Richmond BH, Wilson-Evered E, and Ziccone SP (1986) Pharmacokinetics of intravenous and oral salbutamol and its sulphate conjugate. *Br J Clin Pharmacol* **22:**587-593.

Morrissey KM, Stocker SL, Wittwer MB, Xu L, and Giacomini KM (2012) Renal transporters in drug development. *Annu Rev Pharmacol Toxicol* **53:**503-529.

Motohashi H and Inui K (2013) Organic cation transporter OCTs (SLC22) and MATEs (SLC47) in the human kidney. *AAPS J* **15:**581-588.

Motohashi H, Sakurai Y, Saito H, Masuda S, Urakami Y, Goto M, Fukatsu A, Ogawa O, and Inui K (2002) Gene expression levels and immunolocalization of organic ion transporters in the human kidney. *J Am Soc Nephrol* **13:**866-874.

Motohashi H, Uwai Y, Hiramoto K, Okuda M, and Inui K (2004) Different transport properties between famotidine and cimetidine by human renal organic ion transporters (SLC22A). *Eur J Pharmacol* **503:**25-30.

Muller F, Konig J, Glaeser H, Schmidt I, Zolk O, Fromm MF, and Maas R (2011) Molecular mechanism of renal tubular secretion of the antimalarial drug chloroquine. *Antimicrob Agents Chemother* **55:**3091-3098.

Muller F, Konig J, Hoier E, Mandery K, and Fromm MF (2013) Role of organic cation transporter OCT2 and multidrug and toxin extrusion proteins MATE1 and MATE2-K for transport and drug interactions of the antiviral lamivudine. *Biochem Pharmacol* **86:**808-815.

Mutschler E, Spahn H, and Kirch W (1984) The interaction between H2-receptor antagonists and beta-adrenoceptor blockers. *Br J Clin Pharmacol* **17 Suppl 1:**51S-57S.

Nakagomi-Hagihara R, Nakai D, Kawai K, Yoshigae Y, Tokui T, Abe T, and Ikeda T (2006) OATP1B1, OATP1B3, and mrp2 are involved in hepatobiliary transport of olmesartan, a novel angiotensin II blocker. *Drug Metab Dispos* **34:**862-869.

Nakagomi-Hagihara R, Nakai D, and Tokui T (2007a) Inhibition of human organic anion transporter 3 mediated pravastatin transport by gemfibrozil and the metabolites in humans. *Xenobiotica* **37:**416-426.

Nakagomi-Hagihara R, Nakai D, Tokui T, Abe T, and Ikeda T (2007b) Gemfibrozil and its glucuronide inhibit the hepatic uptake of pravastatin mediated by OATP1B1. *Xenobiotica* **37:**474-486.

Nakano M, Fujii K, and Goto S (1979) Binding of diuretics to human serum albumin and to human serum from healthy adults and patients with renal failure. *Chem Pharm Bull (Tokyo)* **27:**101-108.

Neuvonen PJ, Niemi M, and Backman JT (2006) Drug interactions with lipid-lowering drugs: mechanisms and clinical relevance. *Clin Pharmacol Ther* **80:**565-581.

Niemeyer C, Hasenfuss G, Wais U, Knauf H, Schafer-Korting M, and Mutschler E (1983) Pharmacokinetics of hydrochlorothiazide in relation to renal function. *Eur J Clin Pharmacol* **24:**661-665.

Nies AT, Koepsell H, Damme K, and Schwab M (2011) Organic cation transporters (OCTs, MATEs), in vitro and in vivo evidence for the importance in drug therapy. *Handb Exp Pharmacol***:**105-167.

Nozaki Y, Kusuhara H, Kondo T, Iwaki M, Shiroyanagi Y, Nakayama H, Horita S, Nakazawa H, Okano T, and Sugiyama Y (2007) Species difference in the inhibitory effect of nonsteroidal anti-inflammatory drugs on the uptake of methotrexate by human kidney slices. *J Pharmacol Exp Ther* **322:**1162-1170.

Ochs HR, Bodem G, and Greenblatt DJ (1981) Impairment of digoxin clearance by coadministration of quinidine. *J Clin Pharmacol* **21:**396-400.

Ohashi R, Kamikozawa Y, Sugiura M, Fukuda H, Yabuuchi H, and Tamai I (2006) Effect of P-glycoprotein on intestinal absorption and brain penetration of antiallergic agent bepotastine besilate. *Drug Metab Dispos* **34:**793-799.

Otsuka M, Matsumoto T, Morimoto R, Arioka S, Omote H, and Moriyama Y (2005) A human transporter protein that mediates the final excretion step for toxic organic cations. *Proc Natl Acad Sci U S A* **102:**17923-17928.

Overbosch D, Mattie H, and van Furth R (1985) Comparative pharmacodynamics and clinical pharmacokinetics of phenoxymethylpenicillin and pheneticillin. *Br J Clin Pharmacol* **19:**657-668.

Pabla N, Gibson AA, Buege M, Ong SS, Li L, Hu S, Du G, Sprowl JA, Vasilyeva A, Janke LJ, Schlatter E, Chen T, Ciarimboli G, and Sparreboom A (2015) Mitigation of acute kidney injury by cell-cycle inhibitors that suppress both CDK4/6 and OCT2 functions. *Proc Natl Acad Sci U S A* **112:**5231-5236.

Park MS, Okochi H, and Benet LZ (2011) Is Ciprofloxacin a Substrate of P-glycoprotein? *Arch Drug Inf* **4:**1-9.

Paterson CA, Jacobs D, Rasmussen S, Youngberg SP, and McGuinness N (2011) Randomized, open-label, 5-way crossover study to evaluate the pharmacokinetic/pharmacodynamic interaction between furosemide and the non-steroidal anti-inflammatory drugs diclofenac and ibuprofen in healthy volunteers. *Int J Clin Pharmacol Ther* **49:**477-490.

Peng KC, Cluzeaud F, Bens M, Duong Van Huyen JP, Wioland MA, Lacave R, and Vandewalle A (1999) Tissue and cell distribution of the multidrug resistance-associated protein (MRP) in mouse intestine and kidney. *J Histochem Cytochem* **47:**757-768.

Pentikainen PJ, Neuvonen PJ, and Penttila A (1979) Pharmacokinetics of metformin after intravenous and oral administration to man. *Eur J Clin Pharmacol* **16:**195-202.

Periclou A, Ventura D, Rao N, and Abramowitz W (2006) Pharmacokinetic study of memantine in healthy and renally impaired subjects. *Clin Pharmacol Ther* **79:**134-143.

Perry JL, Dembla-Rajpal N, Hall LA, and Pritchard JB (2006) A three-dimensional model of human organic anion transporter 1: aromatic amino acids required for substrate transport. *J Biol Chem* **281:**38071-38079.

Poirier L and Lacourciere Y (2012) The evolving role of beta-adrenergic receptor blockers in managing hypertension. *Can J Cardiol* **28:**334-340.

Porras AG, Holland SD, and Gertz BJ (1999) Pharmacokinetics of alendronate. *Clin Pharmacokinet* **36:**315-328.

Prasad B and Unadkat JD (2014) Optimized approaches for quantification of drug transporters in tissues and cells by MRM proteomics. *AAPS J* **16:**634-648.

Raghuram TC and Krishnaswamy K (1982) Pharmacokinetics and plasma steady state levels of doxycycline in undernutrition. *Br J Clin Pharmacol* **14:**785-789.

Randinitis EJ, Posvar EL, Alvey CW, Sedman AJ, Cook JA, and Bockbrader HN (2003) Pharmacokinetics of pregabalin in subjects with various degrees of renal function. *J Clin Pharmacol* **43:**277-283.

Regazzi MB, Iacona I, Campana C, Raddato V, Lesi C, Perani G, Gavazzi A, and Vigano M (1993) Altered disposition of pravastatin following concomitant drug therapy with cyclosporin A in transplant recipients. *Transplant Proc* **25:**2732-2734.

Reid G, Wolff NA, Dautzenberg FM, and Burckhardt G (1998) Cloning of a human renal p-aminohippurate transporter, hROAT1. *Kidney Blood Press Res* **21:**233-237.

Richer M, Allard S, Manseau L, Vallee F, Pak R, and LeBel M (1995) Suction-induced blister fluid penetration of cefdinir in healthy volunteers following ascending oral doses. *Antimicrob Agents Chemother* **39:**1082-1086.

Rizwan AN and Burckhardt G (2007) Organic anion transporters of the SLC22 family: biopharmaceutical, physiological, and pathological roles. *Pharm Res* **24:**450-470.

Roberts CJ (1984) Clinical pharmacokinetics of ranitidine. *Clin Pharmacokinet* **9:**211-221.

Roland M and Tozer TN (2010) *Clinical Pharmacokinetics and Pharmacodynamics: Concepts and Applications*. LWW, Philadelphia., Baltimore.

Roth M, Obaidat A, and Hagenbuch B (2012) OATPs, OATs and OCTs: the organic anion and cation transporters of the SLCO and SLC22A gene superfamilies. *Br J Pharmacol* **165:**1260-1287.

Roush GC and Sica DA (2016) Diuretics for Hypertension: A Review and Update. *Am J Hypertens*.

Rowland M and Tozer TN (2011) *Clinical Pharmacokinetics and Pharmacodynamics*. LWW, Baltimore.

Rudy AC and Poynor WJ (1990) Binding of pyrimethamine to human plasma proteins and erythrocytes. *Pharm Res* **7:**1055-1060.

Salvetti A and Ghiadoni L (2006) Thiazide diuretics in the treatment of hypertension: an update. *J Am Soc Nephrol* **17:**S25-29.

Sato T, Masuda S, Yonezawa A, Tanihara Y, Katsura T, and Inui K (2008) Transcellular transport of organic cations in double-transfected MDCK cells expressing human organic cation transporters hOCT1/hMATE1 and hOCT2/hMATE1. *Biochem Pharmacol* **76:**894-903.

Schachter M (2005) Chemical, pharmacokinetic and pharmacodynamic properties of statins: an update. *Fundam Clin Pharmacol* **19:**117-125.

Schaub TP, Kartenbeck J, Konig J, Spring H, Dorsam J, Staehler G, Storkel S, Thon WF, and Keppler D (1999) Expression of the MRP2 gene-encoded conjugate export pump in human kidney proximal tubules and in renal cell carcinoma. *J Am Soc Nephrol* **10:**1159-1169.

Scheen AJ (1996) Clinical pharmacokinetics of metformin. *Clin Pharmacokinet* **30:**359-371.

Scheffer GL, Kool M, de Haas M, de Vree JM, Pijnenborg AC, Bosman DK, Elferink RP, van der Valk P, Borst P, and Scheper RJ (2002) Tissue distribution and induction of human multidrug resistant protein 3. *Lab Invest* **82:**193-201.

Schenck-Gustafsson K and Dahlqvist R (1981) Pharmacokinetics of digoxin in patients subjected to the quinidine-digoxin interaction. *Br J Clin Pharmacol* **11:**181-186.

Schinkel AH and Jonker JW (2003) Mammalian drug efflux transporters of the ATP binding cassette (ABC) family: an overview. *Adv Drug Deliv Rev* **55:**3-29.

Schwartz MS, Frank MS, Yanoff A, and Morecki R (1989) Atenolol-associated cholestasis. *Am J Gastroenterol* **84:**1084-1086.

Seithel A, Eberl S, Singer K, Auge D, Heinkele G, Wolf NB, Dorje F, Fromm MF, and Konig J (2007) The influence of macrolide antibiotics on the uptake of organic anions and drugs mediated by OATP1B1 and OATP1B3. *Drug Metab Dispos* **35:**779-786.

Sekine T, Watanabe N, Hosoyamada M, Kanai Y, and Endou H (1997) Expression cloning and characterization of a novel multispecific organic anion transporter. *J Biol Chem* **272:**18526-18529.

Selen A, Amidon GL, and Welling PG (1982) Pharmacokinetics of probenecid following oral doses to human volunteers. *J Pharm Sci* **71:**1238-1242.

Sharma P, Butters CJ, Smith V, Elsby R, and Surry D (2012) Prediction of the in vivo OATP1B1-mediated drug-drug interaction potential of an investigational drug against a range of statins. *Eur J Pharm Sci* **47:**244-255.

Shiba K, Saito A, and Miyahara T (1990) Safety and pharmacokinetics of single oral and intravenous doses of fluconazole in healthy subjects. *Clin Ther* **12:**206-215.

Shin HJ, Anzai N, Enomoto A, He X, Kim do K, Endou H, and Kanai Y (2007) Novel liver-specific organic anion transporter OAT7 that operates the exchange of sulfate conjugates for short chain fatty acid butyrate. *Hepatology* **45:**1046-1055.

Shu Y, Bello CL, Mangravite LM, Feng B, and Giacomini KM (2001) Functional characteristics and steroid hormone-mediated regulation of an organic cation transporter in Madin-Darby canine kidney cells. *J Pharmacol Exp Ther* **299:**392-398.

Sica DA, Carter B, Cushman W, and Hamm L (2011) Thiazide and loop diuretics. *J Clin Hypertens (Greenwich)* **13:**639-643.

Singhvi SM, Pan HY, Morrison RA, and Willard DA (1990) Disposition of pravastatin sodium, a tissue-selective HMG-CoA reductase inhibitor, in healthy subjects. *Br J Clin Pharmacol* **29:**239-243.

Sjovall J, Alvan G, and Huitfeldt B (1986) Intra- and inter-individual variation in pharmacokinetics of intravenously infused amoxycillin and ampicillin to elderly volunteers. *Br J Clin Pharmacol* **21:**171-181.

Smith DA, Di L, and Kerns EH (2010) The effect of plasma protein binding on in vivo efficacy: misconceptions in drug discovery. *Nat Rev Drug Discov* **9:**929-939.

Smith DE, Gee WL, Brater DC, Lin ET, and Benet LZ (1980) Preliminary evaluation of furosemide-probenecid interaction in humans. *J Pharm Sci* **69:**571-575.

Somogyi A, Rohner HG, and Gugler R (1980) Pharmacokinetics and bioavailability of cimetidine in gastric and duodenal ulcer patients. *Clin Pharmacokinet* **5:**84-94.

Somogyi A, Stockley C, Keal J, Rolan P, and Bochner F (1987) Reduction of metformin renal tubular secretion by cimetidine in man. *Br J Clin Pharmacol* **23:**545-551.

Somogyi AA, Hovens CM, Muirhead MR, and Bochner F (1989) Renal tubular secretion of amiloride and its inhibition by cimetidine in humans and in an animal model. *Drug Metab Dispos* **17:**190-196.

Song IH, Zong J, Borland J, Jerva F, Wynne B, Zamek-Gliszczynski MJ, Humphreys JE, Bowers GD, and Choukour M (2016) The Effect of Dolutegravir on the Pharmacokinetics of Metformin in Healthy Subjects. *J Acquir Immune Defic Syndr*.

Song IS, Shin HJ, Shim EJ, Jung IS, Kim WY, Shon JH, and Shin JG (2008a) Genetic variants of the organic cation transporter 2 influence the disposition of metformin. *Clin Pharmacol Ther* **84:**559-562.

Song IS, Shin HJ, and Shin JG (2008b) Genetic variants of organic cation transporter 2 (OCT2) significantly reduce metformin uptake in oocytes. *Xenobiotica* **38:**1252-1262.

Sprowl JA, van Doorn L, Hu S, van Gerven L, de Bruijn P, Li L, Gibson AA, Mathijssen RH, and Sparreboom A (2013) Conjunctive therapy of cisplatin with the OCT2 inhibitor cimetidine: influence on antitumor efficacy and systemic clearance. *Clin Pharmacol Ther* **94:**585-592.

Srimaroeng C, Perry JL, and Pritchard JB (2008) Physiology, structure, and regulation of the cloned organic anion transporters. *Xenobiotica* **38:**889-935.

Sturgill MG, Seibold JR, Boruchoff SE, Yeh KC, Haddix H, and Deutsch P (1999) Trimethoprim/sulfamethoxazole does not affect the steady-state disposition of indinavir. *J Clin Pharmacol* **39:**1077-1084.

Sutherland R and Rolinson GN (1970) -amino-p-hydroxybenzylpenicillin (BRL 2333), a new semisynthetic penicillin: in vitro evaluation. *Antimicrob Agents Chemother (Bethesda)* **10:**411-415.

Suwannakul S, Ieiri I, Kimura M, Kawabata K, Kusuhara H, Hirota T, Irie S, Sugiyama Y, and Higuchi S (2008) Pharmacokinetic interaction between pravastatin and olmesartan in relation to SLCO1B1 polymorphism. *J Hum Genet* **53:**899-904.

Sweet DH, Wolff NA, and Pritchard JB (1997) Expression cloning and characterization of ROAT1. The basolateral organic anion transporter in rat kidney. *J Biol Chem* **272:**30088-30095.

Tabacova SA and Kimmel CA (2002) Atenolol: pharmacokinetic/dynamic aspects of comparative developmental toxicity. *Reprod Toxicol* **16:**1-7.

Tahara H, Kusuhara H, Endou H, Koepsell H, Imaoka T, Fuse E, and Sugiyama Y (2005) A species difference in the transport activities of H2 receptor antagonists by rat and human renal organic anion and cation transporters. *J Pharmacol Exp Ther* **315:**337-345.

Takabatake T, Ohta H, Maekawa M, Yamamoto Y, Ishida Y, Hara H, Nakamura S, Ushiogi Y, Kawabata M, Hashimoto N, and et al. (1985) Pharmacokinetics of famotidine, a new H2-receptor antagonist, in relation to renal function. *Eur J Clin Pharmacol* **28:**327-331.

Takashima T, Kitamura S, Wada Y, Tanaka M, Shigihara Y, Ishii H, Ijuin R, Shiomi S, Nakae T, Watanabe Y, Cui Y, Doi H, Suzuki M, Maeda K, Kusuhara H, Sugiyama Y, and Watanabe Y (2012) PET imaging-based evaluation of hepatobiliary transport in humans with (15R)-11C-TIC-Me. *J Nucl Med* **53:**741-748.

Takeda M, Khamdang S, Narikawa S, Kimura H, Hosoyamada M, Cha SH, Sekine T, and Endou H (2002a) Characterization of methotrexate transport and its drug interactions with human organic anion transporters. *J Pharmacol Exp Ther* **302:**666-671.

Takeda M, Khamdang S, Narikawa S, Kimura H, Kobayashi Y, Yamamoto T, Cha SH, Sekine T, and Endou H (2002b) Human organic anion transporters and human organic cation transporters mediate renal antiviral transport. *J Pharmacol Exp Ther* **300:**918-924.

Takeda M, Noshiro R, Onozato ML, Tojo A, Hasannejad H, Huang XL, Narikawa S, and Endou H (2004) Evidence for a role of human organic anion transporters in the muscular side effects of HMG-CoA reductase inhibitors. *Eur J Pharmacol* **483:**133-138.

Takeuchi K, Sugiura T, Umeda S, Matsubara K, Horikawa M, Nakamichi N, Silver DL, Ishiwata N, and Kato Y (2011) Pharmacokinetics and hepatic uptake of eltrombopag, a novel platelet-increasing agent. *Drug Metab Dispos* **39:**1088-1096.

Tamai I, China K, Sai Y, Kobayashi D, Nezu J, Kawahara E, and Tsuji A (2001) Na(+)-coupled transport of L-carnitine via high-affinity carnitine transporter OCTN2 and its subcellular localization in kidney. *Biochim Biophys Acta* **1512:**273-284.

Tamai I, Nakanishi T, Kobayashi D, China K, Kosugi Y, Nezu J, Sai Y, and Tsuji A (2004) Involvement of OCTN1 (SLC22A4) in pH-dependent transport of organic cations. *Mol Pharm* **1:**57-66.

Tamai I, Ohashi R, Nezu J, Yabuuchi H, Oku A, Shimane M, Sai Y, and Tsuji A (1998) Molecular and functional identification of sodium ion-dependent, high affinity human carnitine transporter OCTN2. *J Biol Chem* **273:**20378-20382.

Tamai I, Yabuuchi H, Nezu J, Sai Y, Oku A, Shimane M, and Tsuji A (1997) Cloning and characterization of a novel human pH-dependent organic cation transporter, OCTN1. *FEBS Lett* **419:**107-111.

Tamargo J, Segura J, and Ruilope LM (2014) Diuretics in the treatment of hypertension. Part 1: thiazide and thiazide-like diuretics. *Expert Opin Pharmacother* **15:**527-547.

Tamraz B, Fukushima H, Wolfe AR, Kaspera R, Totah RA, Floyd JS, Ma B, Chu C, Marciante KD, Heckbert SR, Psaty BM, Kroetz DL, and Kwok PY (2013) OATP1B1-related drug-drug and drug-gene interactions as potential risk factors for cerivastatin-induced rhabdomyolysis. *Pharmacogenet Genomics* **23:**355-364.

Tanihara Y, Masuda S, Sato T, Katsura T, Ogawa O, and Inui K (2007) Substrate specificity of MATE1 and MATE2-K, human multidrug and toxin extrusions/H(+)-organic cation antiporters. *Biochem Pharmacol* **74:**359-371.

Terada T and Inui K (2008) Physiological and pharmacokinetic roles of H+/organic cation antiporters (MATE/SLC47A). *Biochem Pharmacol* **75:**1689-1696.

Thevenod F, Ciarimboli G, Leistner M, Wolff NA, Lee WK, Schatz I, Keller T, Al-Monajjed R, Gorboulev V, and Koepsell H (2013) Substrate- and cell contact-dependent inhibitor affinity of human organic cation transporter 2: studies with two classical organic cation substrates and the novel substrate cd2+. *Mol Pharm* **10:**3045-3056.

Thiebaut F, Tsuruo T, Hamada H, Gottesman MM, Pastan I, and Willingham MC (1987) Cellular localization of the multidrug-resistance gene product P-glycoprotein in normal human tissues. *Proc Natl Acad Sci U S A* **84:**7735-7738.

Thyss A, Milano G, Kubar J, Namer M, and Schneider M (1986) Clinical and pharmacokinetic evidence of a life-threatening interaction between methotrexate and ketoprofen. *Lancet* **1:**256-258.

Tomino Y, Fukui M, Hamada C, Inoue S, and Osada S (1998) Pharmacokinetics of cefdinir and its transfer to dialysate in patients with chronic renal failure undergoing continuous ambulatory peritoneal dialysis. *Arzneimittelforschung* **48:**862-867.

Tsuda M, Terada T, Ueba M, Sato T, Masuda S, Katsura T, and Inui K (2009) Involvement of human multidrug and toxin extrusion 1 in the drug interaction between cimetidine and metformin in renal epithelial cells. *J Pharmacol Exp Ther* **329:**185-191.

Turck D, Weber W, Sigmund R, Budde K, Neumayer HH, Fritsche L, Rominger KL, Feifel U, and Slowinski T (2004) Pharmacokinetics of intravenous, single-dose tiotropium in subjects with different degrees of renal impairment. *J Clin Pharmacol* **44:**163-172.

Tweedie D, Polli JW, Berglund EG, Huang SM, Zhang L, Poirier A, Chu X, Feng B, and International Transporter C (2013) Transporter studies in drug development: experience to date and follow-up on decision trees from the International Transporter Consortium. *Clin Pharmacol Ther* **94:**113-125.

Ueo H, Motohashi H, Katsura T, and Inui K (2005) Human organic anion transporter hOAT3 is a potent transporter of cephalosporin antibiotics, in comparison with hOAT1. *Biochem Pharmacol* **70:**1104-1113.

Ullrich KJ, Fritzsch G, Rumrich G, and David C (1994) Polysubstrates: substances that interact with renal contraluminal PAH, sulfate, and NMeN transport: sulfamoyl-, sulfonylurea-, thiazide- and benzeneamino-carboxylate (nicotinate) compounds. *J Pharmacol Exp Ther* **269:**684-692.

Ulm EH, Hichens M, Gomez HJ, Till AE, Hand E, Vassil TC, Biollaz J, Brunner HR, and Schelling JL (1982) Enalapril maleate and a lysine analogue (MK-521): disposition in man. *Br J Clin Pharmacol* **14:**357-362.

Urban TJ, Brown C, Castro RA, Shah N, Mercer R, Huang Y, Brett CM, Burchard EG, and Giacomini KM (2008) Effects of genetic variation in the novel organic cation transporter, OCTN1, on the renal clearance of gabapentin. *Clin Pharmacol Ther* **83:**416-421.

Uwai Y, Saito H, Hashimoto Y, and Inui KI (2000) Interaction and transport of thiazide diuretics, loop diuretics, and acetazolamide via rat renal organic anion transporter rOAT1. *J Pharmacol Exp Ther* **295:**261-265.

Vaidyanathan S, Valencia J, Kemp C, Zhao C, Yeh CM, Bizot MN, Denouel J, Dieterich HA, and Dole WP (2006) Lack of pharmacokinetic interactions of aliskiren, a novel direct renin inhibitor for the treatment of hypertension, with the antihypertensives amlodipine, valsartan, hydrochlorothiazide (HCTZ) and ramipril in healthy volunteers. *Int J Clin Pract* **60:**1343-1356.

van Aubel RA, Smeets PH, Peters JG, Bindels RJ, and Russel FG (2002) The MRP4/ABCC4 gene encodes a novel apical organic anion transporter in human kidney proximal tubules: putative efflux pump for urinary cAMP and cGMP. *J Am Soc Nephrol* **13:**595-603.

van Crugten J, Bochner F, Keal J, and Somogyi A (1986) Selectivity of the cimetidine-induced alterations in the renal handling of organic substrates in humans. Studies with anionic, cationic and zwitterionic drugs. *J Pharmacol Exp Ther* **236:**481-487.

VandenBrink BM, Foti RS, Rock DA, Wienkers LC, and Wahlstrom JL (2012) Prediction of CYP2D6 drug interactions from in vitro data: evidence for substrate-dependent inhibition. *Drug Metab Dispos* **40:**47-53.

Varma MV, Feng B, Obach RS, Troutman MD, Chupka J, Miller HR, and El-Kattan A (2009) Physicochemical determinants of human renal clearance. *J Med Chem* **52:**4844-4852.

Vollmer KO, von Hodenberg A, and Kolle EU (1986) Pharmacokinetics and metabolism of gabapentin in rat, dog and man. *Arzneimittelforschung* **36:**830-839.

von Bergmann K, Laeis P, Puchler K, Sudhop T, Schwocho LR, and Gonzalez L (2001) Olmesartan medoxomil: influence of age, renal and hepatic function on the pharmacokinetics of olmesartan medoxomil. *J Hypertens Suppl* **19:**S33-40.

Vree TB, Van den Biggelaar-Martea M, Van Ewijk-Beneken Kolmer EW, and Hekster YA (1993) Probenecid inhibits the renal clearance and renal glucuronidation of nalidixic acid. A pilot experiment. *Pharm World Sci* **15:**165-170.

Vree TB, van den Biggelaar-Martea M, and Verwey-van Wissen CP (1995) Probenecid inhibits the renal clearance of frusemide and its acyl glucuronide. *Br J Clin Pharmacol* **39:**692-695.

Vujic Z, Mulavdic N, Smajic M, Brboric J, and Stankovic P (2012) Simultaneous analysis of irbesartan and hydrochlorothiazide: an improved HPLC method with the aid of a chemometric protocol. *Molecules* **17:**3461-3474.

Wadworth AN, Murdoch D, and Brogden RN (1991) Atenolol. A reappraisal of its pharmacological properties and therapeutic use in cardiovascular disorders. *Drugs* **42:**468-510.

Waller ES, Hamilton SF, Massarella JW, Sharanevych MA, Smith RV, Yakatan GJ, and Doluisio JT (1982) Disposition and absolute bioavailability of furosemide in healthy males. *J Pharm Sci* **71:**1105-1108.

Wang Q, Rager JD, Weinstein K, Kardos PS, Dobson GL, Li J, and Hidalgo IJ (2005) Evaluation of the MDR-MDCK cell line as a permeability screen for the blood-brain barrier. *Int J Pharm* **288:**349-359.

Wang ZJ, Yin OQ, Tomlinson B, and Chow MS (2008) OCT2 polymorphisms and in-vivo renal functional consequence: studies with metformin and cimetidine. *Pharmacogenet Genomics* **18:**637-645.

Watanabe S, Tsuda M, Terada T, Katsura T, and Inui K (2010) Reduced renal clearance of a zwitterionic substrate cephalexin in MATE1-deficient mice. *J Pharmacol Exp Ther* **334:**651-656.

WHO (2011) Causes of Death 2008, WHO, Geneva.

William M. M. Kirby and Regamey C (1973) Pharmacokinetics of cefazolin compared with four other cephalosporins. *The Journal of Infectious Diseases*.

Wittwer MB, Zur AA, Khuri N, Kido Y, Kosaka A, Zhang X, Morrissey KM, Sali A, Huang Y, and Giacomini KM (2013) Discovery of potent, selective multidrug and toxin extrusion transporter 1 (MATE1, SLC47A1) inhibitors through prescription drug profiling and computational modeling. *J Med Chem* **56:**781-795.

Wolff NA, Werner A, Burkhardt S, and Burckhardt G (1997) Expression cloning and characterization of a renal organic anion transporter from winter flounder. *FEBS Lett* **417:**287-291.

Wright SH and Dantzler WH (2004) Molecular and Cellular Physiology of Renal Organic Cation and Anion Transport. *Physiological Reviews* **84:**987-1049.

Wu X, Huang W, Prasad PD, Seth P, Rajan DP, Leibach FH, Chen J, Conway SJ, and Ganapathy V (1999) Functional characteristics and tissue distribution pattern of organic cation transporter 2 (OCTN2), an organic cation/carnitine transporter. *J Pharmacol Exp Ther* **290:**1482-1492.

Yabuuchi H, Tamai I, Nezu J, Sakamoto K, Oku A, Shimane M, Sai Y, and Tsuji A (1999) Novel membrane transporter OCTN1 mediates multispecific, bidirectional, and pH-dependent transport of organic cations. *J Pharmacol Exp Ther* **289:**768-773.

Yagi T, Naito T, Mino Y, Umemura K, and Kawakami J (2012) Impact of concomitant antacid administration on gabapentin plasma exposure and oral bioavailability in healthy adult subjects. *Drug Metab Pharmacokinet* **27:**248-254.

Yamada A, Maeda K, Kamiyama E, Sugiyama D, Kondo T, Shiroyanagi Y, Nakazawa H, Okano T, Adachi M, Schuetz JD, Adachi Y, Hu Z, Kusuhara H, and Sugiyama Y (2007) Multiple human isoforms of drug transporters contribute to the hepatic and renal transport of olmesartan, a selective antagonist of the angiotensin II AT1-receptor. *Drug Metab Dispos* **35:**2166-2176.

Yamashiro W, Maeda K, Hirouchi M, Adachi Y, Hu Z, and Sugiyama Y (2006) Involvement of transporters in the hepatic uptake and biliary excretion of valsartan, a selective antagonist of the angiotensin II AT1-receptor, in humans. *Drug Metab Dispos* **34:**1247-1254.

Yasui-Furukori N, Uno T, Sugawara K, and Tateishi T (2005) Different effects of three transporting inhibitors, verapamil, cimetidine, and probenecid, on fexofenadine pharmacokinetics. *Clin Pharmacol Ther* **77:**17-23.

Yin J, Duan H, Shirasaka Y, Prasad B, and Wang J (2015a) Atenolol Renal Secretion Is Mediated by Human Organic Cation Transporter 2 (hOCT2) and Multidrug and Toxin Extrusion Proteins (hMATEs). *Drug Metab Dispos*.

Yin J, Duan H, Shirasaka Y, Prasad B, and Wang J (2015b) Atenolol Renal Secretion Is Mediated by Human Organic Cation Transporter 2 and Multidrug and Toxin Extrusion Proteins. *Drug Metab Dispos* **43:**1872-1881.

Yonezawa A and Inui K (2011) Importance of the multidrug and toxin extrusion MATE/SLC47A family to pharmacokinetics, pharmacodynamics/toxicodynamics and pharmacogenomics. *Br J Pharmacol* **164:**1817-1825.

Yoshida K, Maeda K, and Sugiyama Y (2012) Transporter-mediated drug--drug interactions involving OATP substrates: predictions based on in vitro inhibition studies. *Clin Pharmacol Ther* **91:**1053-1064.

You G (2004) The role of organic ion transporters in drug disposition: an update. *Curr Drug Metab* **5:**55-62.

Yu J, Ritchie TK, Zhou Z, and Ragueneau-Majlessi I (2016) Key Findings from Preclinical and Clinical Drug Interaction Studies Presented in New Drug and Biological License Applications Approved by the Food and Drug Administration in 2014. *Drug Metab Dispos* **44:**83-101.

Yuan R, Madani S, Wei XX, Reynolds K, and Huang SM (2002) Evaluation of cytochrome P450 probe substrates commonly used by the pharmaceutical industry to study in vitro drug interactions. *Drug Metab Dispos* **30:**1311-1319.

Yusuf SW and Mishra RM (1995) Hepatic dysfunction associated with atenolol. *Lancet* **346:**192.

Zhang J, Wang C, Liu Q, Meng Q, Cang J, Sun H, Gao Y, Kaku T, and Liu K (2010) Pharmacokinetic interaction between JBP485 and cephalexin in rats. *Drug Metab Dispos* **38:**930-938.

Zhang L, Huang SM, and Lesko LJ (2011) Transporter-mediated drug-drug interactions. *Clin Pharmacol Ther* **89:**481-484.

Zhang X, Cherrington NJ, and Wright SH (2007) Molecular identification and functional characterization of rabbit MATE1 and MATE2-K. *Am J Physiol Renal Physiol* **293:**F360-370.

Zhang X and Wright SH (2009) MATE1 has an external COOH terminus, consistent with a 13-helix topology. *Am J Physiol Renal Physiol* **297:**F263-271.

Zhang Y, Zhang L, Abraham S, Apparaju S, Wu TC, Strong JM, Xiao S, Atkinson AJ, Jr., Thummel KE, Leeder JS, Lee C, Burckart GJ, Lesko LJ, and Huang SM (2009) Assessment of the impact of renal impairment on systemic exposure of new molecular entities: evaluation of recent new drug applications. *Clin Pharmacol Ther* **85:**305-311.

Zhou Q, Yu LS, and Zeng S (2014) Stereoselectivity of chiral drug transport: a focus on enantiomer-transporter interaction. *Drug Metab Rev* **46:**283-290.

Zolk O, Solbach TF, Konig J, and Fromm MF (2009a) Functional characterization of the human organic cation transporter 2 variant p.270Ala>Ser. *Drug Metab Dispos* **37:**1312-1318.

Zolk O, Solbach TF, Konig J, and Fromm MF (2009b) Structural determinants of inhibitor interaction with the human organic cation transporter OCT2 (SLC22A2). *Naunyn Schmiedebergs Arch Pharmacol* **379:**337-348.